Functionalised transition metal clusters of Cobalt and Osmium

by Alisdair James Brown

A thesis submitted for the Degree of Doctor of Philosophy

The University of Edinburgh.

1995

Declaration

The research described herein was conducted by the author at The Department of Chemistry, The University of Edinburgh, between the dates of October 1992 and July 1995. It is the author's original work unless specific reference is made to the contrary. None of the work described herein has been submitted for a degree at any other institution.

Acknowledgements

This thesis would never have been completed had it not been for a large number of people who, over the years, have given me their support, encouragement, help, and friendship.

First and foremost I wish to express my thanks to my supervisor, Professor Brian Johnson, for his seemingly endless supply of enthusiasm, humour and love for the subject, and also for giving me the chance to undertake a Ph.D. My thanks also go to my industrial supervisors, Dr. Phil Taylor and Dr. Ian Abrahams, and all the people at I. C. I. Paints, for their help, expertise and warm welcome.

I am forever indebted to all the talented people at The University of Edinburgh whose expertise I have called upon over the last 3 years; particular mention must be made of the NMR service- John Millar and Wesley Kerr were always willing to run my sometimes dubious and often sensitive samples at a moments notice. My thanks also go to Dr. David Reed for his help and interest with the nOe experiments. I was lucky enough to be able to call upon the crystallographic talents of Dr. Sandy Blake, Dr. Simon Parsons, and especially, Dr. Scott Ingham; thank you all for your help and time. I am also indebted to Dr. Steve Henderson for his prompt and objective proof reading of this thesis, as well as help with all things computerate.

Three years can be a long time, but thanks to the people I have worked with, it has gone all too quickly. For all the good times, I thank all those I worked alongside in *Laborotoires Johnson* over the last 3 years: Dr. Ros Gash, Dr. Justin Goldberg, Dr. Jane Haggitt, Dr. Scott Ingham, Gideon, Tom, Garry, Dave, Ruth P., Ruth M., Jackie, Nick, Lesley, Ash, and especially Mrs. Janet Hayes for fitting me in to Brian's schedule. Also thanks to Dr. Malcolm Banks for his continued friendship and interest.

I must also thank all of my friends and partners in crime, both in and out of the Chemistry Department, who are always there whenever sanity threatens; Bally, Nick, Chris & Jenny, Cammy, Andy, Ally & Kathy, Linda at M. I. T., Alex, and (of course) my brother, Stuart. My apologies to anyone I may have inadvertently missed out...

I am grateful to the EPSRC and I. C. I. Paints for financial assistance.

Last, but by no means least, I wish to thank my family for all the help, encouragement and support they have always given me.

For Mum and Dad, for all they have done for me.

"the days run away like wild horses over the hills..."

-Charles Bukowski, 1920 - 1994

Abstract

In Chapter One, a review of the chemistry of the tricobalt nonacarbonyl methylidyne cluster is presented. The concept of organic polymeric species containing inorganic moieties is introduced and methods of synthesis and characterisation are discussed. The importance of these compounds as potentially homogenised heterogeneous catalysis is highlighted, and some examples of these species are given. Finally, the catalytic cross linking of alkyd polymers is considered

In the second chapter, the synthesis and characterisation of some tricobalt clusters and their derivatives is presented. Reaction of $[(CO)_9Co_3(\mu_3\text{-}CCO)]^+$ $[AlCl_4]^-$ with nucleophiles ROH produced the compounds $[(CO)_9Co_3(\mu_3\text{-}CCOOR)]$, where R= $CH_2CH=CH_2$ (1) and $CH_2CH_2O(CO)CH=CH_2$ (2). The crystal structure of (1) is presented, and whilst it does not undergo polymerisation, compound (2) is readily polymerised by free radical initiation in both solution and emulsion systems with acrylic comonomers. The polymeric systems were characterised by infrared and ultra violet spectroscopy, as well as by gel permeation chromatography. However, neither the polymeric or monomeric cluster systems were found to catalyse the cross linking of alkyd polymers as they exhibit no redox properties under the ambient conditions studied.

Chapter Three describes the synthesis and characterisation of triosmium clusters which contain functionalised alkynes. The crystal structure of $[Os_3(CO)_8(\mu\text{-}CO)(HOCH_2C=CCHOCCHCCH_2)]$ is reported. Attempts to make polymeric and multicluster derivatives of these functionalised compounds are described.

Chapter Four details the synthesis and characterisation of a novel amide linked di-cluster. Reaction of $[(CO)_9Co_3(\mu_3\text{-}CCO^+)][PF6^-]$ with $[(CO)_9Co_3(\mu_3\text{-}C)(p\text{-}C_6H_4NH_2)]$ produced the species $[(CO)_9Co_3(\mu_3\text{-}CCON(H)\text{-}p\text{-}C_6H_4(\mu_3\text{-}CCo_3(CO)_9]$, which has been characterised by X Ray crystallography, as well as by IR, NMR, FABMS and electrochemical techniques.

Finally, Chapter Five presents details of the equipment and experimental procedures used in this research.

Glossary of Abbreviations

IR	Infra Red
$\nu(CO)$	carbonyl stretching frequency
v	very
w	weak
m	medium
s	strong
br	broad
sh	shoulder
cm^{-1}	wavenumbers
MS	mass spectrum
amu	atomic mass units
NMR	Nuclear Magnetic Resonance
nOe	nuclear Overhauser effect
s	singlet
d	doublet
t	triplet
m	multiplet
δ	chemical shift
ppm	parts per million
J	coupling constant
Hz	hertz
UV/VIS	Ultra Violet / Visible
tlc	thin layer chromatography
GPC	Gel Permeation Chromatography
TBA	tertiary butyl ammonium
HEA	hydroxyethylacrylate
Å	Angstrom $(\times 10^{-10} m)$
	Polymer backbone

Numbering of Compounds

$[(CO)_9Co_3(\mu_3\text{-CCl})]$ **(1)**

$[(CO)_9Co_3(\mu_3\text{-CCO}_2C_2H_5)]$ **(2)**

$[(CO)_9Co_3(\mu_3\text{-CCOOCH2CH=CH2})]$ **(3)**

$[(CO)_9Co_3(\mu_3\text{-CCOOCH}_2C\equiv CH)]$ **(4)**

$[(CO)_9Co_3(\mu_3\text{-CCOOCH}_2CH_2OCOCH=CH_2)]$ **(5)**

solution polymer of (5)   **(6)**

emulsion polymer of (5)   **(7)**

$[(CO)_9Co_3(\mu_3\text{-CH})]$ **(8)**

alkyd polymer   **(9)**

acrylic polymers of HEA   **(10a), (10b) and (10c)**

$[(CO)_9Co_3(\mu_3\text{-CCO})]^+\ PF_6^-$ **(11)**

modified polymers   **(12a), (12b) and (12c)**

$Os_3(CO)_{10}(MeCN)_2$ **(13)**

$Os_3(CO)_9(\mu\text{-CO})(\mu_3\text{-}\eta^2\text{-HCC}\equiv CH_2OH)$ **(14)**

$[Os_3(CO)_8(\mu\text{-CO})\{(HOCH_2C_2H)_2(CO)\}]$ **(15)**

$[p\text{-NH}_2C_6H_4HgCl]$ **(16)**

$[(CO)_9Co_3\{\mu_3\text{-C}[(p\text{-C}_6H_4NH_2)]\}]$ **(17)**

$[(CO)_9Co_3(\mu_3\text{-CCON(H)-}p\text{-C}_6H_4(\mu_3\text{-CCo}_3(CO)_9]$ **(18)**

$[(CO)_9Co_3CC_6H_4N\{COCCo_3(CO)_9\}_2]$ **(19)**

Table of Contents

Chapter 3:   **Synthesis and reactivity of hydrox functionalised clusters**

Chapter 4:   **Tricobalt nonacarbonyl alkylidyne as a ligand**

Chapter 5:   **Experimental**

Chapter 1: Introduction

In this chapter are discussed the following topics : Metal Containing Polymer Systems, Polymer Supported Catalysts and the catalytic cross linking of alkyd polymers in the paint industry, with particular attention to tricobalt nonacarbonyl alkylidyne clusters.

One of the principal justifications for much of the research carried out into cluster chemistry is the expectation that metal clusters will have applications in catalysis, both directly in the form of novel homogeneous catalysts (or catalyst precursors) and indirectly by serving as models for chemisorption processes in heterogeneous catalysis. Muetterties[1] argued that metal clusters have different reactivities from those of complexes with single metal atoms because they have neighbouring metal centres, and the unique metal-ligand bonding patterns in clusters could be expected to facilitate reactions similar to those occurring on metal surfaces. If metal cluster – metal surface analogies are to be found, they are expected to be closest when the metals are dispersed in the form of small particles ("clusters") on solid supports, as recognised by Basset and Ugo[2]. This is precisely the form of many industrial metal catalysts. Relatively robust carbonyl metal clusters such as $[H_3Os_4(CO)_{12}]^-$ have been observed on surfaces during catalysis of CO hydrogenation[3], but their role in catalysis remains uncertain. In the last three decades, considerable efforts have been made to combine the advantages of homogeneous catalysis (selectivity, mild operating conditions) with those of heterogeneous catalysis (duration, ease of separation of products and reactants). This may be made possible by attaching homogeneous catalysts to either inorganic supports or organic polymers in such a way that the ligand sphere is preserved around the metal and the complex is kept in contact with the solvents and reactants[4]. Therefore the attachment of a metal cluster to either an inorganic support or an organic polymer is of fundamental importance.

The chemistry of bridging hydrocarbyl ligands is also of interest because of the analogy to the chemistry of hydrocarbyl ligands adsorbed on metal surfaces. The alkylidyne ligand has an extensive chemistry for monometallic complexes and is implied in acetylene metathesis[5]. Furthermore, alkylidynes have been identified in numerous studies of surface adsorbed hydrocarbons, although little is known of the reactivity of these surface bound species[6]. Metal clusters containing the alkylidyne moiety have been known for many years; one of the best known clusters containing a bridging alkylidyne group has the general formula $Co_3(\mu_3-CR)(CO)_9$. The chemistry of these compounds has been mainly found to involve either modification of the alkylidyne substituent or ligand substitution on the metal atoms[7].

The chemistry reported in this work has centred on this family of tricobalt nonacarbonyl alkylidynes, the general structure of which is shown in Figure 1.1.
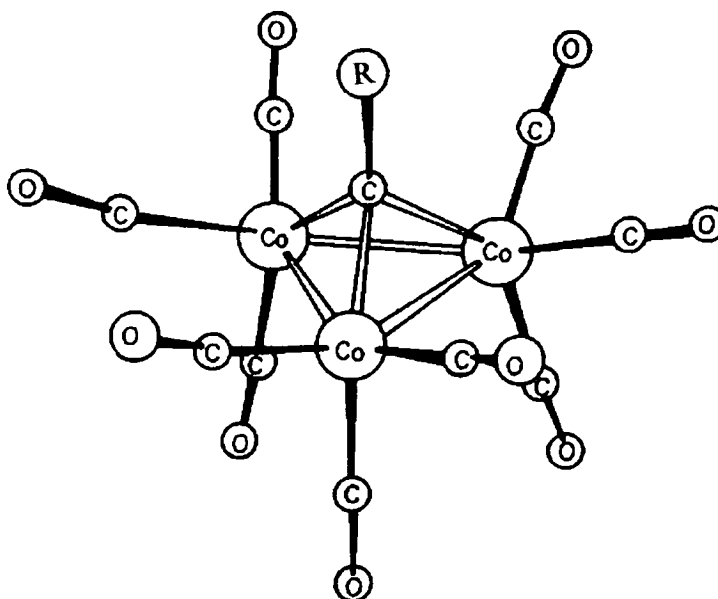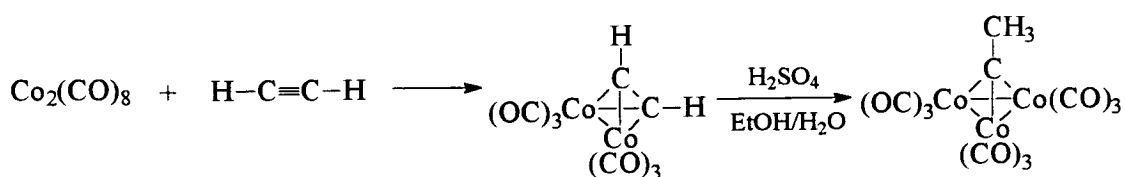

Figure 1.1: General structure of tricobaltnonacarbonyl alkylidynes

2

At the outset of these studies, it was hoped that the incorporation of these cobalt clusters onto a polymeric support may exhibit homogeneous catalytic activity. In the paint industry, cobalt (II) is used as a catalyst for the crosslinking of polymers. During the process, cobalt becomes entrained in the crosslinked product. Once applied to a substrate, the cobalt is leached out by weathering *etc.*, and thus causes an environmental problem. It was hoped that by attaching a cobalt species to a polymeric support, any catalytic activity could be investigated and hopefully problems associated with entrained cobalt would be alleviated. Therefore, one of the major aims of this project was to synthesise polymers containing the tricobalt alkylidyne moiety and evaluate their catalytic ability.

1.1 General properties of tricobalt nonacarbonyl complexes

The serendipitous preparation of the first member of this class of compounds was reported by workers at the Bureau of Mines laboratory in Brucetown, Pennsylvania, USA in 1958[8], as shown in Scheme 1.1.

$$Co_2(CO)_8 \ + \ H-C\equiv C-H \ \longrightarrow \ (OC)_3Co\overset{\overset{\displaystyle H}{|}{\underset{\displaystyle C}{\underset{|}{C}}}}{\underset{\underset{\displaystyle (CO)_3}{Co}}{}} C-H \ \xrightarrow[\text{EtOH/H}_2\text{O}]{\text{H}_2\text{SO}_4} \ (OC)_3Co\overset{\overset{\displaystyle CH_3}{|}{\underset{\displaystyle C}{}}}{\underset{\underset{\displaystyle (CO)_3}{Co}}{}} Co(CO)_3$$

Scheme 1.1: Preparation of methylidyne tricobalt nonacarbonyl

The X-ray crystal structure of methylmethylidyne tricobalt nonacarbonyl is reproduced in Figure 1.2.
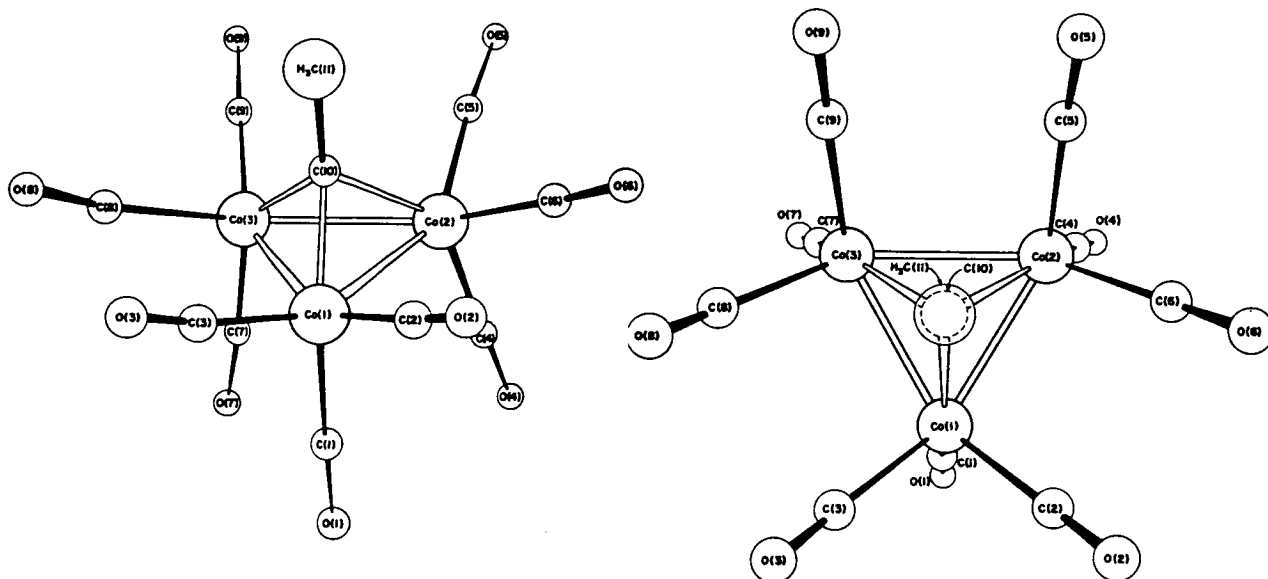
3

Figure 1.2 : Methylmethylidyne tricobalt nonacarbonyl[9]

The apical carbon atom is co-ordinated symmetrically, apparently *via* sigma bonds to three cobalt atoms. Each cobalt atom may be regarded as achieving a closed shell configuration by sigma bonding to two other cobalt atoms, the apical carbon atom and three terminal carbon monoxide ligands. The C-CH$_3$ distance is 1.53Å; a normal C$_{sp}$3-C$_{sp}$3 distance. The Co-C(apical)-Co bond angles average 81.1°, the H$_3$C-C-Co angles average 131.3°[9]. The arrangement of the carbon monoxide ligands in this complex merits special notice because it has important consequences with regard to the chemistry of this class of compounds. Six of the nine CO ligands are disposed upward in the general direction of the apical carbon atom and its substituent. As a result, any reactions at the apical carbon atom or at its substituent group will be subject to substantial steric hinderance. Not only is the backside of the apical carbon atom well shielded, but attack from other directions will also be hindered by steric interference of these six CO groups. Thus, steric factors play an important role in the chemistry of alkylidynetricobalt nonacarbonyls.

4

The alkylidynetricobalt nonacarbonyl complexes are all highly coloured, with colours ranging from red to purple to brown to black, depending on the apical substituent. Their thermal stability also depends on the apical substituent; some survive heating to 100°C, whereas others survive to 185°C, and many may be sublimed in vacuo at 50-80°C. Unlike their pyrophoric parent- dicobalt octacarbonyl- most (but not all) are air stable both in the solid state and in solution. Most of the compounds worked with are crystalline solids; however, the longer the apical substituent chain, the lower the melting point. In view of their colour, stability and solubility properties, thin layer and column chromatography are ideal for their detection, purification and isolation.
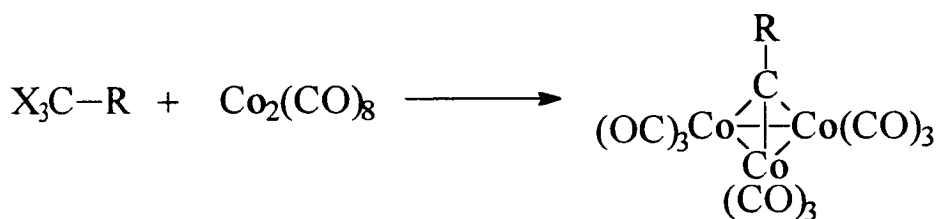
The general chemical reactivity of the alkylidynetricobalt nonacarbonyls includes instability towards attack by oxidizing agents and many bases and nucleophiles. However, many are stable towards protonic and Lewis acids. This property provides the basis for much of the chemistry developed since 1970 by several groups.

1.2 Synthesis of alkylidynetricobalt carbonyl complexes

Procedures are available for the preparation of $Co_3(\mu_3\text{-}CR)(CO)_{9-x}L_x$ complexes with a wide range of substituents, R, and ligands L. The original preparation of $CH_3CCo_3(CO)_9$ via acetylenedicobalt hexacarbonyl[8] (Scheme 1.1) can be extended to dicobalt hexacarbonyl complexes of terminal acetylenes, $(RC_2H)Co_2(CO)_6$, but the effect of R on the success or failure of this reaction has not been explored with a systematic variation of R. In any case, the $(RC_2H)Co_2(CO)_6$ to $RCH_2CCo_3(CO)_9$ conversion is not always successful. Furthermore, it is limited in scope to the synthesis of complexes with the CH_2 group attached to the apical carbon atom. Complexes of the type $(OC)_9Co_3CCH_2R$ have been prepared by this route with

5

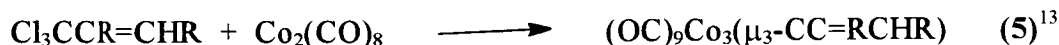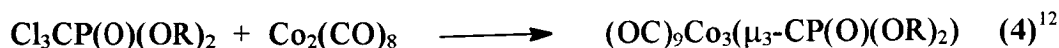R= H, CH$_3$, MeO$_2$C, C$_2$H$_5$, HO(CH$_2$)$_2$, n-C$_3$H$_7$, Me$_2$CH, PhCH$_2$, Me$_3$C, C$_6$H$_5$, p-BrC$_6$H$_4$, C$_6$F$_5$ [10].

Another more general preparative route to such complexes was developed by Shaw *et al* [11] ,involving reaction of dicobalt octacarbonyl with trihalo compounds Cl$_3$CR:

$$X_3C-R \ + \ Co_2(CO)_8 \longrightarrow \ (OC)_3Co \overset{\overset{\displaystyle R}{\overset{|}{C}}}{\underset{\underset{(CO)_3}{Co}}{\diagup | \diagdown}} Co(CO)_3$$

Scheme 1.2: Tricobalt cluster synthesis from trihalo compounds

This procedure may be used to prepare a great diversity of alkylidynetricobalt nonacarbonyl complexes, including RCCo$_3$(CO)$_9$ compounds where R= H, halogen, alkyl or aryl. Of particular use are those reactions which introduce reactive organic functional groups at the apical carbon:

$$Cl_3CCO_2R \ + \ Co_2(CO)_8 \longrightarrow \ (OC)_9Co_3(\mu_3\text{-}CCO_2R) \qquad \textbf{(1)}^{11}$$

$$Cl_3CCOR \ + \ Co_2(CO)_8 \longrightarrow \ (OC)_9Co_3(\mu_3\text{-}CCOR) \qquad \textbf{(2)}^{11}$$

$$Cl_3CCONR_2 \ + \ Co_2(CO)_8 \longrightarrow \ (OC)_9Co_3(\mu_3\text{-}CCONR_2) \qquad \textbf{(3)}^{12}$$

$$Cl_3CP(O)(OR)_2 \ + \ Co_2(CO)_8 \longrightarrow \ (OC)_9Co_3(\mu_3\text{-}CP(O)(OR)_2) \qquad \textbf{(4)}^{12}$$

$$Cl_3CCR{=}CHR \ + \ Co_2(CO)_8 \longrightarrow \ (OC)_9Co_3(\mu_3\text{-}CC{=}RCHR) \qquad \textbf{(5)}^{13}$$

The product yields are, in general, only low to moderate. Some attempted RCX$_3$ / Co$_2$(CO)$_8$ reactions are unsuccessful not because of difficulties with the

6

reactions *per se*, but because of the instability of the product to the reaction and/or work-up conditions; this is especially true for reaction (5) above, which is of most interest to this study, as it introduces a potentially polymerisable group to the molecule. Work up of such unsaturated species requires rigorously aprotic conditions and chromatography using pH7 silicic acid for separations. Even with these precautions, many derivatives have never been fully resolved and in many cases, instead of the unsaturated compound, the fully saturated species is isolated [13, 14]. Furthermore, a suitable trihalo compound is not always available.

Another method of preparing substituted tricobalt alkylidyne nonacarbonyls from dicobalt octacarbonyl is by reaction with a suitable organic dithioester[15] (Scheme 1.3).
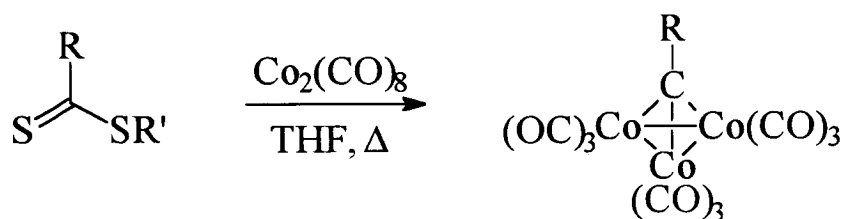
Scheme 1.3 : Alkylidyne formation from dithioesters

This method of preparation has been reported for the synthesis of the derivatives in Table 1 [16], as well as the styryl derivative shown in Figure 1.3 [17].

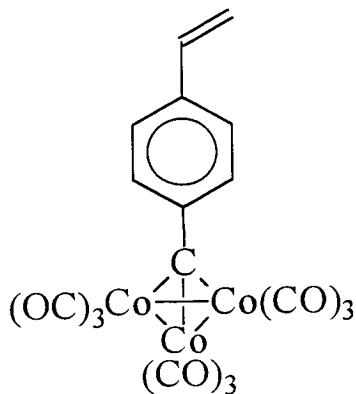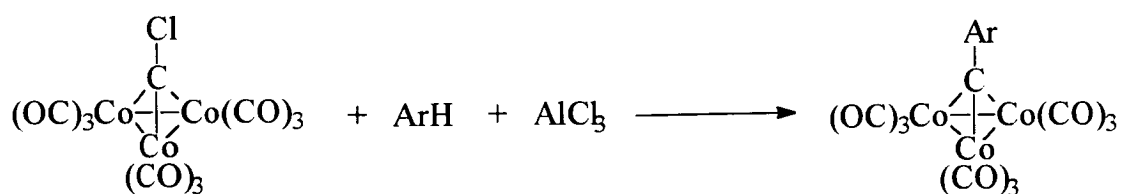| R in RCCo$_3$(CO)$_9$	% yield
CH$_3$-	44
C$_2$H$_5$-	47
^{i}Pr-	35
CH$_3$(CH$_2$)$_3$-	42
cyclohexyl	33
C$_6$H$_5$-	68
p-Me-C$_6$H$_4$-	53
p-MeO-C$_6$H$_4$-	74
(Me)$_2$-3,4-C$_6$H$_3$-	49
p-(CH$_3$)$_2$N-C$_6$H$_4$-	51
2-thiophenyl	65
a-napthyl	45

Table 1 : Species prepared from dithioesters

Figure 1.3 : *para*-styrylmethylidyne tricobalt nonacarbonyl

Interconversion of one alkylidynetricobalt nonacarbonyl complex to another is possible, but rather limited in scope. As already mentioned, many strong bases and nucleophiles ultimately destroy the RCCo$_3$(CO)$_9$ cluster. In a halogen derivative,

XCCo$_3$(CO)$_9$, any nucleophilic attack in which the halogen atom is displaced must occur by way of nucleophilic attack at the halogen or by an electron transfer mechanism, since, as noted previously, the backside of the apical carbon atom is very effectively shielded. Nucleophilic attack at the carbon atoms of coordinated CO ligands is also possible. However, this is usually nonproductive because of cluster decomposition.

Bromo- and chloromethylidynetricobalt nonacarbonyl are arylated in moderate yield by action of an aryl Grignard reagent in ten-fold excess[18]. Primary and secondary alkyl Grignard reagents, on the other hand, destroy rather than alkylate these clusters[18]. Organolithium reagents react initially with Co$_3$(CO)$_9$(μ_3-CCl) to form [ClCCo$_3$(CO)$_9$]$^{\bullet}$, a radical anion of some stability, which is detectable by ESR[7]. Unfortunately subsequent reaction results in cluster decomposition rather than the desired alkylated product.
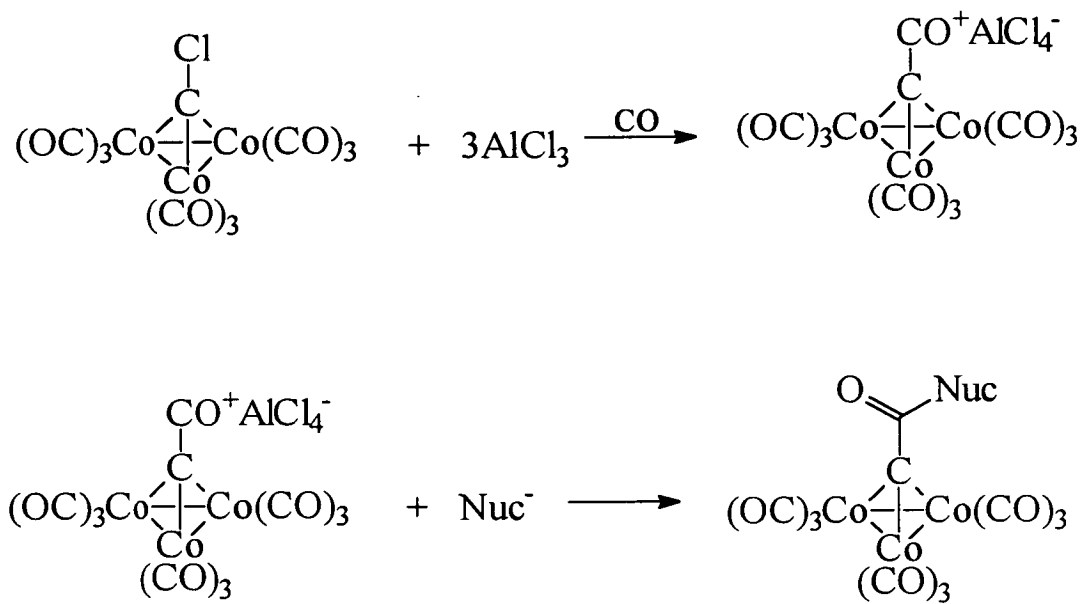
Another successful method for the arylation of alkylidynetricobalt nonacarbonyls was developed by Dolby and Robinson[19], who found that chloromethylidynetricobalt nonacarbonyl alkylates aromatic compounds in a Friedel-Crafts type reaction (Scheme 1.4). High product yields were obtained when equimolar amounts of ClCCo$_3$(CO)$_9$ and aluminium trichloride were stirred with an excess of arene at 60-70°C for 2 hours.

$$\underset{\substack{(CO)_3}}{(OC)_3Co\overset{\overset{\overset{\displaystyle Cl}{|}}{C}}{\diagdown}Co(CO)_3} \quad + \quad ArH \quad + \quad AlCl_3 \quad \longrightarrow \quad \underset{\substack{(CO)_3}}{(OC)_3Co\overset{\overset{\overset{\displaystyle Ar}{|}}{C}}{\diagdown}Co(CO)_3}$$

Scheme 1.4: Friedel-Crafts type reactions

Treatment of (CO)$_9$Co$_3$CCl with a three-fold excess of aluminium trichloride[20] induces sacrificial donation of carbon monoxide to produce the acylium salt

$[(OC)_9Co_3CCO]^+ [AlCl_4]^-$. This versatile derivative can then be further reacted with a number of nucleophiles, *viz.*: (i) alcohols to give the respective esters; (ii) thiols to give the respective thio-esters; and (iii) reactions with ammonia and primary and secondary amines, to produce the expected amides. The general reaction is shown in Scheme 1.5.

$$(OC)_3Co\overset{\overset{\displaystyle Cl}{|}}{\underset{\underset{\displaystyle (CO)_3}{Co}}{C}}Co(CO)_3 \quad + \quad 3AlCl_3 \quad \xrightarrow{\quad CO \quad} \quad (OC)_3Co\overset{\overset{\displaystyle CO^+AlCl_4^-}{|}}{\underset{\underset{\displaystyle (CO)_3}{Co}}{C}}Co(CO)_3$$

$$(OC)_3Co\overset{\overset{\displaystyle CO^+AlCl_4^-}{|}}{\underset{\underset{\displaystyle (CO)_3}{Co}}{C}}Co(CO)_3 \quad + \quad Nuc^- \quad \longrightarrow \quad (OC)_3Co\overset{\overset{\displaystyle O\diagdown\diagup Nuc}{C}}{\underset{\underset{\displaystyle (CO)_3}{Co}}{C}}Co(CO)_3$$

Scheme 1.5: Acylium ion production and reaction with nucleophiles .

The production of this cation *via* sacrificial cluster degradation suggested the involvement of a transfer of a carbon monoxide ligand from a cobalt atom to the apical carbon atom of the cluster [20, 21] (*vide infra*).

The tricobalt decacarbonyl cation has been used in numerous studies, one of the most recent and perhaps the most elegant was published in 1994; Deschenaux *et al* [22] employed the chemistry of the acylium decacarbonyl salt to attach cholesterol to the carbon apex of the cluster framework. By subsequently substituting one CO ligand for an isocyanide derivative bearing a hydrophilic functional group, a polar head was introduced to the molecule, allowing assemblies of Langmuir Blodgett films to be constructed on various substrates. Hence the tricobalt decacarbonyl cation is

probably the most versatile of all the tricobalt nonacarbonyl species, allowing a rich and varied number of derivatives to be produced.

The $[Co_3(CO)_9(\mu_3\text{-}CCO)]^+$ ion however, is a relatively poor carbon electrophile in that it will acylate only the most reactive aromatic nucleophiles but not benzene or toluene. This suggests that the positive charge is delocalised away from the carbonyl on the apical carbon atom. In the cluster acylium ion salt the shift of the group of terminal carbonyl absorptions to higher energy, compared to neutral cluster derivatives, indicates that a greater amount of positive charge accumulates on the cobalt atoms when the cation is formed. This raises the question of the structure and bonding of the $[Co_3(CO)_9(\mu_3\text{-}CCO)]^+$ ion. A structure with gross geometry unchanged from that of neutral $Co_3(CO)_9(\mu_3\text{-}CR)$ complexes (Figure 1.4) would provide means for transfer of electron density to the electron-deficient carbonyl group attached to the apical carbon atom. In this structure the three cobalt-carbon framework orbitals of the cluster possess a C_{3v} symmetry and transform as a_1 + e. The two π-antibonding orbitals of the apical acylium carbonyl are of e symmetry and are appropriate for interaction with one of the filled e framework orbitals [20].
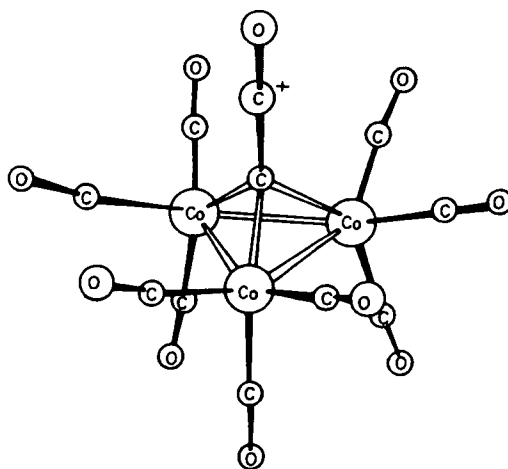

Figure 1.4: Proposed structure of the Tricobalt decacarbonyl cation.

However, other structures with a more complete electron transfer from cobalt to carbon involving a change of geometry are possible, for example the complex ketene shown in Figure 1.5[20]. Further experimental information regarding this species has never been reported, so further speculation is not justified.
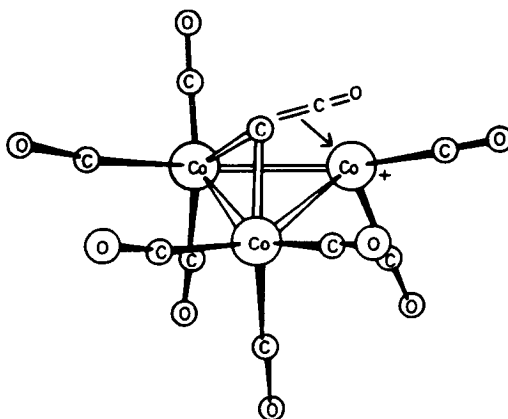

Figure 1.5: Another possible structure of the tricobalt decacarbonyl cation.

Other interconversions of the apical substituents are possible, albeit rather limited in scope. Interconversion of $Co_3(CO)_9(\mu_3\text{-CH})$ to $Co_3(CO)_9(\mu_3\text{-CAr})$ can be achieved by refluxing diarylmercurials with methylidynetricobaltnonacarbonyl[23]. Excellent yields, often in the range 90-98%, have been obtained in some cases. The general reaction is summarised in Scheme 1.6, below.
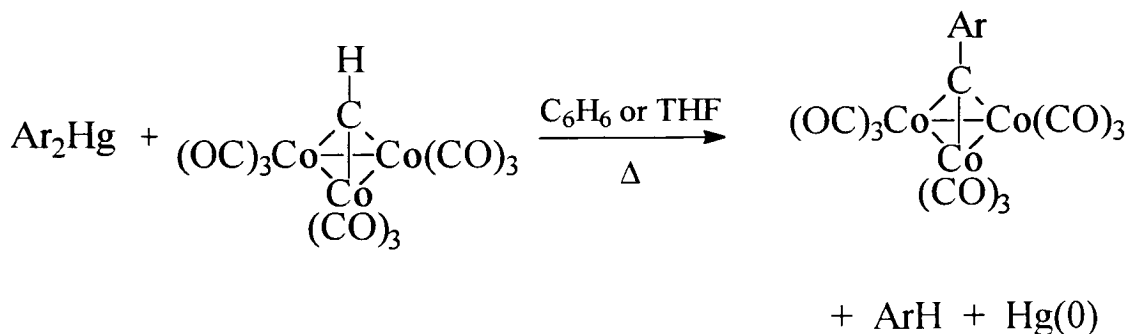
Scheme 1.6 : Apical interconversion *via* organomercury compounds

12

Arylmercuric halides may be used in place of diarylmercurials. Table 1.2 lists some examples of the species prepared by these reactions.

organomercurial[a]	R in RCCo$_3$(CO)$_9$	% Yield
$(C_6H_5)_2Hg$	C_6H_5	93
$(p\text{-}CH_3OC_6H_4)_2Hg$	$p\text{-}CH_3OC_6H_4$	64
$(p\text{-}CH_3C_6H_4)_2Hg$	$p\text{-}CH_3C_6H_4Hg$	92
$(m\text{-}CH_3C_6H_4)_2Hg$	$m\text{-}CH_3C_6H_4$	96
$(o\text{-}CH_3C_6H_4)_2Hg$	$o\text{-}CH_3C_6H_4$	49
$(p\text{-}ClC_6H_4)_2Hg$	$p\text{-}ClC_6H_4$	83
$(m\text{-}ClC_6H_4)_2Hg$	$m\text{-}ClC_6H_4$	93
$(o\text{-}ClC_6H_4)_2Hg$	$o\text{-}ClC_6H_4$	57
$(m\text{-}FC_6H_4)_2Hg$	$m\text{-}FC_6H_4$	85
$(p\text{-}BrC_6H_4)_2Hg$	$p\text{-}BrC_6H_4$	86
$(p\text{-}IC_6H_4)_2Hg$	$p\text{-}IC_6H_4$	51
$(C_6F_5)_2Hg$	C_6F_5	63
$(C_6H_5CH_2)_2Hg$	$C_6H_5CH_2$	75
C_6H_5HgBr	C_6H_5	58
$p\text{-}FC_6H_4HgBr$	$p\text{-}FC_6H_4$	57
$(p\text{-}H_2NC_6H_4)HgCl$	$H_2NC_6H_4$	26
$p\text{-}ClC_6H_4HgBr$[b]	$p\text{-}ClC_6H_4$	54
$\alpha\text{-}C_{10}H_7HgBr$[b]	$\alpha\text{-}C_{10}H_7$	11
$FcHgCl$[b]	Fc	14
$[(OC)_3CrPh]_2Hg$	$(OC)_3CrPh$	37
$CH_3OCH_2CH_2HgCl$	$CH_3OCH_2CH_2$	32
$(n\text{-}C_5H_{11})_2Hg$	$n\text{-}C_5H_{11}$	32

[a] reactions were carried out under an atmosphere of carbon monoxide unless stated otherwise
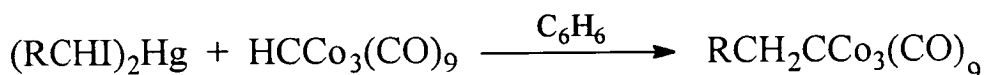[b] reaction carried out under dry nitrogen

Table 1.2: Preparation of RCCo$_3$(CO)$_9$ complexes by reactions of organomercurials with HCCo$_3$(CO)$_9$ [23]

Oxidative degradation studies of selected products showed that the aryl carbon originally attached to mercury was the one that became bonded to the apical carbon of the cluster. This reaction was much less successful for the preparation of alkyl derivatives, because of much longer reaction times (2-3 weeks) giving at best only moderate yields (Table 2, above). The reaction of α-haloalkylmercurials with $Co_3(CO)_9(\mu_3\text{-CH})$ occurred with concomitant reduction of the carbon-halogen bond but proved to be an unexpectedly effective synthesis of alkyl-substituted cluster complexes, as shown in Scheme 1.7.

$$R\text{-}\underset{\underset{X}{|}}{C}H\text{-}HgX \ + \ HCCo_3(CO)_9 \ \xrightarrow{C_6H_6} \ RCH_2CCo_3(CO)_9$$
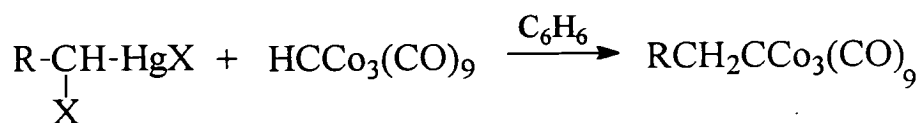
R=H, X=Br: yield = 59%

R= Me$_3$Si, X=Br: yield = 70%

$$(RCHI)_2Hg \ + \ HCCo_3(CO)_9 \ \xrightarrow{C_6H_6} \ RCH_2CCo_3(CO)_9$$
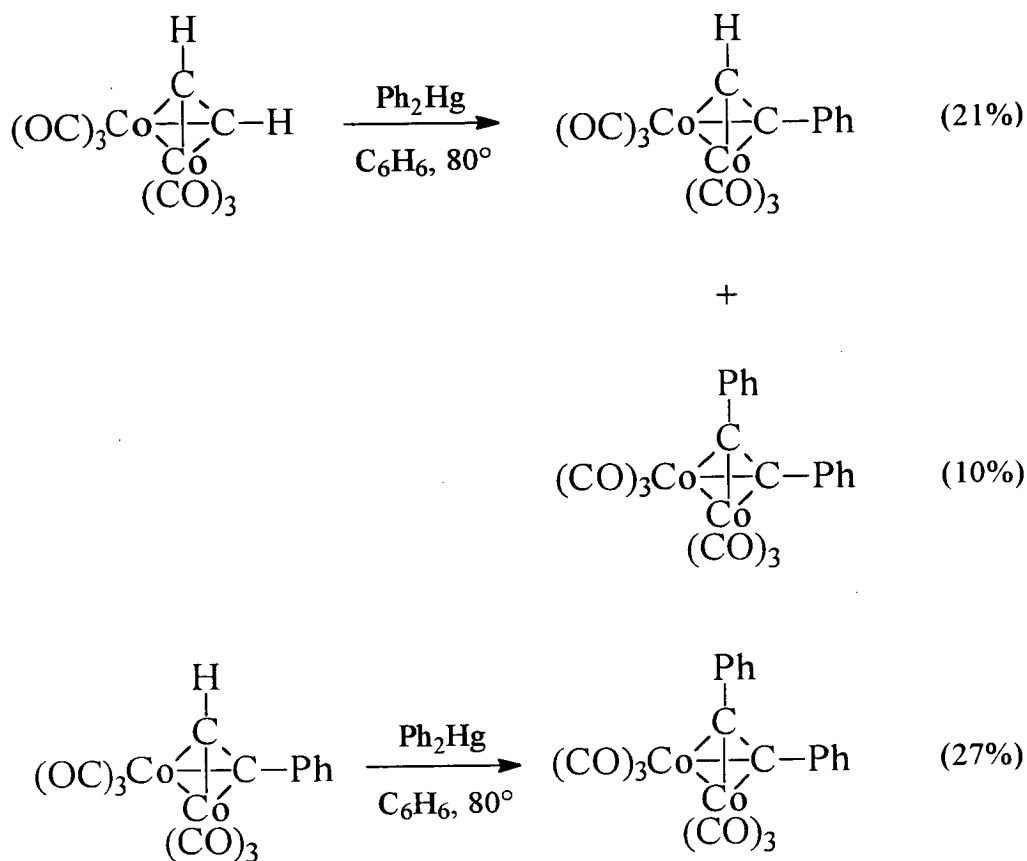
R= H: yield = 77%

R= CH$_3$: yield = 88%

Scheme 1.7: Cluster alkylation by α-haloalkylmercury compounds

As with all tricobalt nonacarbonyl species, reactions of organomercurials with $Co_3(CO)_9(\mu_3\text{-CH})$ are subject to steric hindrance. As seen in Table 2, *ortho*-substituted arylmercury compounds usually give lower product yields than those with substituents in *meta* or *para* positions. The presence of two *ortho* substituents larger than fluorine causes such reactions to fail completely. Thus, no organocobalt cluster

product was obtained in the reactions of $Co_3(CO)_9(\mu_3\text{-CH})$ with bis(pentachlorophenyl)mercury and dimesitylmercury [23].

Acetylenedicobalt hexacarbonyl complexes are related structurally to the alkylidyne tricobalt nonacarbonyls in that they contain a pseudotetrahedral array of two carbon and two cobalt atoms. In such complexes also, C-H bonds can be phenylated with diphenylmercury, (Scheme 1.8) but the product yields are rather low[23].

$$(OC)_3Co\overset{\displaystyle \overset{\text{H}}{|}\overset{\text{C}}{\diagup\diagdown}}{\underset{\text{Co}}{|}}C-H \xrightarrow[C_6H_6,\ 80°]{Ph_2Hg} (OC)_3Co\overset{\displaystyle \overset{\text{H}}{|}\overset{\text{C}}{\diagup\diagdown}}{\underset{\text{Co}}{|}}C-Ph \quad (21\%)$$

$$+$$

$$(CO)_3Co\overset{\displaystyle \overset{\text{Ph}}{|}\overset{\text{C}}{\diagup\diagdown}}{\underset{\text{Co}}{|}}C-Ph \quad (10\%)$$

$$(OC)_3Co\overset{\displaystyle \overset{\text{H}}{|}\overset{\text{C}}{\diagup\diagdown}}{\underset{\text{Co}}{|}}C-Ph \xrightarrow[C_6H_6,\ 80°]{Ph_2Hg} (CO)_3Co\overset{\displaystyle \overset{\text{Ph}}{|}\overset{\text{C}}{\diagup\diagdown}}{\underset{\text{Co}}{|}}C-Ph \quad (27\%)$$

Scheme 1.8 : Arylation of acetylenedicobalt hexacarbonyls

While organomercurials appear to be the most effective alkylating agents for $Co_3(CO)_9(\mu_3\text{-CH})$, organic derivatives of tin and lead can also be used to effect organic group transfer to the $Co_3(CO)_9(\mu_3\text{-C})$ cluster. Thus, a reaction of tetraphenyl

15

tin with $Co_3(CO)_9(\mu_3\text{-CH})$ in refluxing benzene for 48 hours gave $Co_3(CO)_9(\mu_3\text{-CPh})$ in 27% yield, while a similar reaction carried out for 12 hours with tetraphenyllead as the phenyl source gave the product in 18% yield [23].

Unfortunately, nothing is known about the mechanism of these alkylation and arylation reactions, and the reduction processes accompanying the reactions of α-halo alkylmercurials with $Co_3(CO)_9(\mu_3\text{-CH})$ still remain a mystery.

1.3 Clusters as ligands

The use of transition metals to modify the reactivity of organic ligands[24, 25] and to act as ligand assembly points[26] are approaches that continue to be exploited. Fehlner[27] has described how transition metal clusters can be viewed as bulky π-donating ligands co-ordinated to main group atom centres. A logical extension of these observations is the use of a derivatised transition metal cluster as a ligand bound to other transition metal clusters, and to thus construct large metallic structures. This could have interesting consequences regarding the physical and chemical properties of the resulting compounds, especially regarding electron transfer between metal centres in different clusters.

1.4 Electrochemistry of tricobalt alkylidynes

The capping carbyne atom of the tricobaltcarbonyl cluster is, as already mentioned, susceptible to both electrophilic and nucleophilic attack. This is a reflection on not only the aforementioned steric interactions, but is also a consequence of specific electronic interactions within the cluster.

Electron density can be transmitted within the Co_3C core by inductive and mesomeric mechanisms, but Chesky and Hall[28] have suggested that the carbyne carbon is electron rich. The delocalized cluster bonding is sufficiently flexible for the Co_3C
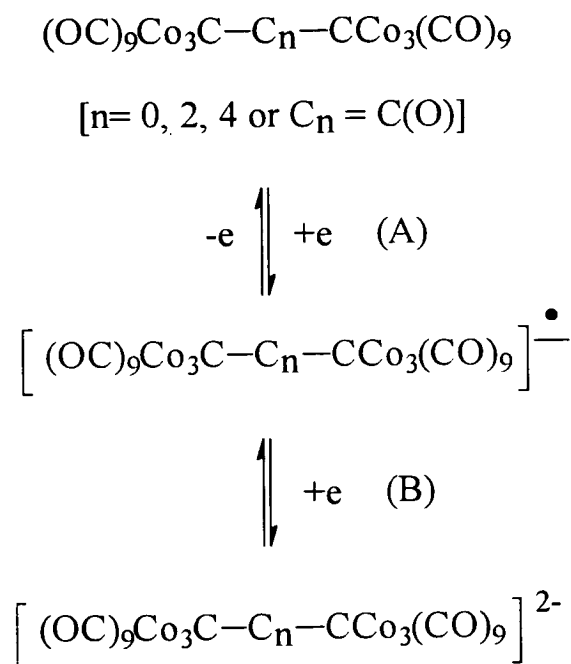
16

core to act as either a donor or an acceptor towards the apical substituent. Spectroscopic data[28] from UPS spectra and MO calculations support these ideas

Electronic interactions between adjacent organometallic moieties which are readily oxidised or reduced can lead to a range of electron transfer responses[29]. These responses are normally classified according to the degree to which the interaction brings about a change in physical properties[30, 31]. Redox studies[29, 32] on many transition metal clusters have shown that they are structurally flexible electron reservoirs with "tunable" redox properties dependent on the coordination sphere of the metal framework

Extension of this work to systems where the cluster is linked to other redox centres, such as ferrocene, demonstrate that transition metal clusters can participate in electronic interactions which lead to classical mixed-valence molecules[33]. However interpolation of an electronically saturated system such as CH_2 or SiR_2 between the ferrocene and cluster removes the possibility of electronic communication between the two redox centres[34]. This raised the question of whether intracluster communication could be established if two cluster moieties were directly linked, for instance by an unsaturated carbon-carbon bridge, a communication well established in ferrocene chemistry[35, 36]. The CCo_3 cluster displays several attractive features as redox centres. It has an upper occupied molecular orbital which has contributions from the metal, capping carbon atom and ligands, conferring tunable electron reservoir character[25, 28, 29]. An all CO configuration for a CCo_3 cluster gives a reducible centre[38], but successive replacement of CO by electron donors ultimately results in an oxidisable centre[39, 40, 41]. Molecules with CCo_3 clusters linked by conducting bridges could therefore provide a variety of redox responses. Furthermore, the apical carbon atom provides a reaction site for the development of cluster multiplicity[7].

Robinson and coworkers[42] found that the clusters $[CCo_3(CO)_9]_2$, $OC[CCo_3(CO)_9]_2$, and $C_n[CCo_3(CO)_9]_2$ (n= 2, 4), linked by formal single and/or triple

carbon-carbon bonds, displayed electrochemical processes indicative of interacting redox centres. After the formation of a radical anion (in which the electron is delocalised via the Co_3C-C_n-CCo_3 link), a CE mechanism gives a new species with a reversible redox couple. IR evidence suggests that the species produced is a bridged carbonyl isomer of the initial radical anion; the bridging carbonyls being a result of electron delocalisation through the carbyne link and the steric influence of the equatorial CO groups. If the Co_3C-C_n-CCo_3 entity is stabilised by electron delocalisation along the chain, the addition of an electron to the cluster could create a situation where the clusters revert to a bridged-carbonyl configuration to relieve the excess charge and the nonbonded repulsions between the equatorial carbonyl groups. The electron transfer reactions for molecules containing two $CCo_3(CO)_9$ clusters linked by direct C-C, C-C-C, or $C\equiv C$ bonds are shown in Scheme 1.9.

$$(OC)_9Co_3C-C_n-CCo_3(CO)_9$$

$$[n = 0, 2, 4 \text{ or } C_n = C(O)]$$

$$-e \Updownarrow +e \quad (A)$$

$$\left[(OC)_9Co_3C-C_n-CCo_3(CO)_9 \right]^{\bullet -}$$

$$\Updownarrow +e \quad (B)$$

$$\left[(OC)_9Co_3C-C_n-CCo_3(CO)_9 \right]^{2-}$$

Scheme 1.9 : Electrochemical processes for linked clusters

18

1.5 Clusters as catalysts

Metal cluster catalysis is difficult to study because the clusters often fragment in solution to give mononuclear complexes (which may be responsible for the catalysis); alternatively they also have potential to aggregate to form colloids which may also be responsible for catalysis. Most reported examples of catalysis by metal clusters are viewed with scepticism since the catalyst characterisation is incomplete. Experiments are needed which include the characterisation of the metal structures *during catalysis*. However, this is equally true for all hetero- and homogeneous catalytic systems.

In 1976 Deeming[43] and Keister[44] independently published details of one of the most thorough studies of catalysis by a metal cluster. They found that a triosmium cluster catalysed olefin isomerisation and hydrogenation, and elucidated the catalytic cycle reproduced in Scheme 1.10. Carbon monoxide ligands have been omitted for clarity, and to highlight the the interactions of the reactive hydride and hydrocarbon ligands.
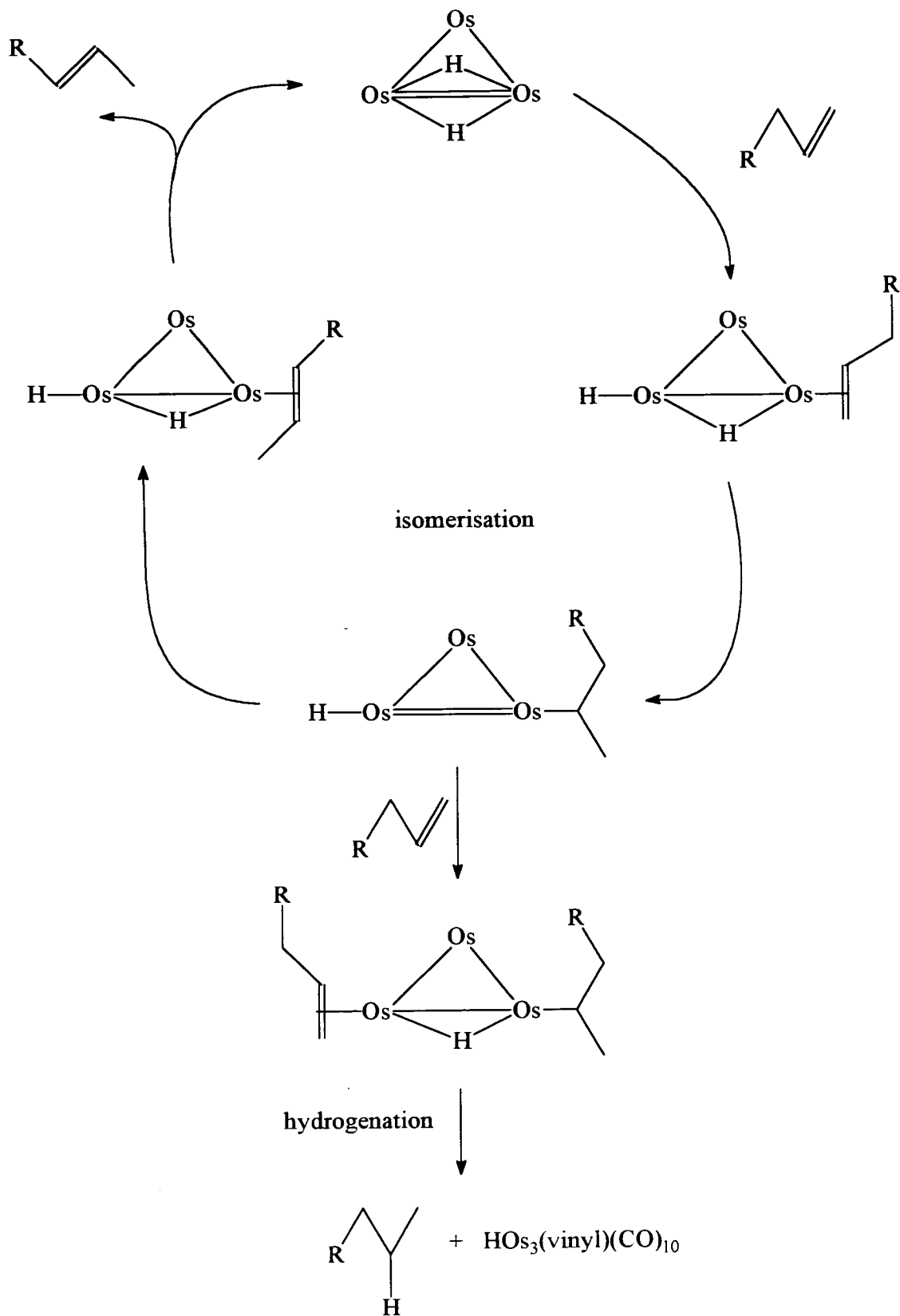
Scheme 1.10: Catalytic alkene isomerisation and hydrogenation by Os₃

20

An essential feature of the triosmium species entering the cycle, $[H_2Os_3(CO)_{10}]$, is coordinative unsaturation. This species has an Os-Os double bond where the alkene coordinates to cluster at the start of the catalytic cycle. Coordinative unsaturation to allow bonding of reactants to the metal centre is a general requirement for metal catalysis. Metal clusters may become coordinatively unsaturated by simple dissociation of a ligand like CO or a bridging hydride. Since both CO and H are common ligands on clusters, there are good prospects for cluster catalysis for synthesis gas $(CO + H_2)$.

We must now consider how to attach a metal species, cluster or otherwise, to a polymeric organic support.

1.6 Metal Containing Polymer Systems

Traditionally, polymers have been thought of as macromolecules containing only about 9 elements, namely C, H, N, O, S, P, Cl, Br and Si, whereas there are over 44 metals, many of which can be present in several oxidation states. A number of nonmetal-containing polymers are often included as organometallic polymers since they exhibit metal-like behaviour, particularly with regard to electrical conductivity. These polymers include sulphur nitrides, polyphosphazenes, boron nitrides and polyphosphinates. These polymers will not be covered here.

Upon the discovery of vinylferrocene[45] (Figure 1.6) in 1955, research into polymers containing transition metals began. It was soon found that vinylferrocene and other vinylic transition metal π-complexes could undergo polymerization[46] in much the same way as conventional organic monomers, under free radical, cationic and Zeigler Natta conditions
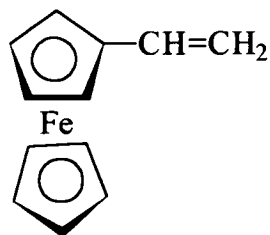
Figure 1.6 : Vinylferrocene

The resulting high polymers were of particular interest as they contained a potentially reactive metal as an integral part of the polymer's structure. Some of these polymeric materials could act as semiconductors and possessed one or two dimensional conductivity- thus, applications in the electronics industry could be visualised immediately. As interest in homogeneous catalysis developed in the late 1960s and early 1970s, parallel to the growth of research into solid inorganic supports (*e.g.* silica, alumina) for catalysts, interest in polymer supported catalysts grew, with the driving force being the homogenisation of heterogeneous catalysts.

Homogenous catalysts have the advantage of being highly selective under relatively mild operating conditions[2, 47]. In addition their activity and selectivity can often be tailored by varying the ligands attached to the metal centre and by varying the solvent. Furthermore, every molecule of the catalytic complex is available to catalyse the reaction, unlike the situation in heterogeneous catalysis where only the surface atoms or molecules may contribute. Heterogeneous catalysts, such as metals or metal oxide surfaces, are often less active and less selective; however they are generally very durable and are readily separated from the reactants and products. They may be used in fixed bed gas-solid and liquid-solid contact reactors. It would therefore be ideal to combine the advantages and simultaneously avoid the disadvantages of each class of catalyst.

One approach is therefore to attach homogeneous catalysts to either an inorganic support (*e.g.* alumina, silica, zeolites), or to an organic polymer support, in

such a way that the ligand sphere of the metal is essentially unchanged and the attached complex is bathed in solvents and reactants. Thus the heterogenised homogeneous catalyst could function mechanistically as if it were in solution, but it would operate as a separate immobile phase.

Polymer supports of three major types have been employed[48] . Firstly, highly crosslinked resin beads of large surface area called macroreticular or macroporous resins[49]. An example of such a support is a styrene-divinylbenzene resin, where the divinylbenzene resin content may be varied to tailor the crosslinking and hence the surface area of the resin. The attached catalysts lie mainly in a thin layer at the internal surface, where they are wet by solvents. The high cross link density prevents rapid diffusion into the particles' core below the internal surface. Usually the surface is not as highly cross linked as the core. Common ion- exchange resins are an example of this class of support.

Swellable, lightly cross linked microporous resins constitute the second class of support. These resins swell in solvents and all of their internal volume is accessible to solvent and reagents. Therefore they may be functionalised with catalyst sites, giving them the advantage of high capacity. Unlike macroreticular resins, they must be used with a swelling solvent to permit access to this internal volume. Examples include styrene resins crosslinked with 1 or 2% divinylbenzene. Finally, soluble polymers may be used as supports. Reaction products may be continuously separated from catalysts supported by such polymers using membrane filtration[50, 51] or by the addition of a non-solvent which precipitates the polymer[52, 53].

The question still remains though, of how to synthesise a polymer which supports either a metal, a catalyst, or, better still, a metal species that exhibits catalytic activity. There are two routes available to the synthetic chemist: (i) Modification of an existing polymer network and (ii) Polymerisation of functionalised monomers

1.6.1 Modification of existing polymer networks

The simplest method of modifying an existing polymer network is to exploit the chemistry of a functionalised site on the polymer. Examples include preparation of chloromethylated styrene polymers followed by treatment with metal carbonyl anions to give σ-bonded transition metal to polymer linkages[54] (see Scheme 1.11).
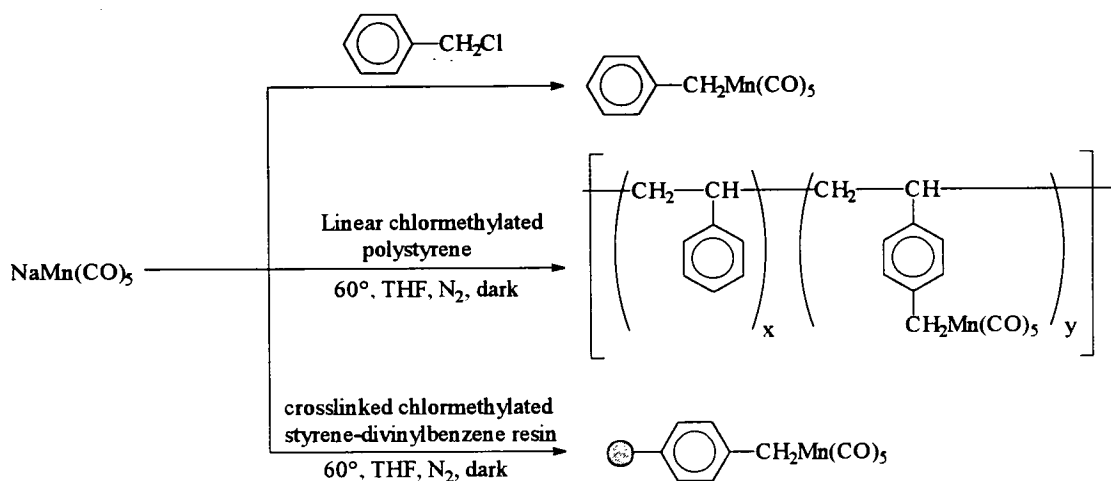
Scheme 1.11 : Reaction with metal carbonyl anions

Cyclopentadienyl ligands may also be introduced in a similar fashion, and have been used to attach titanium[55], cobalt[56, 57], and rhodium[56] (Scheme 1.12).
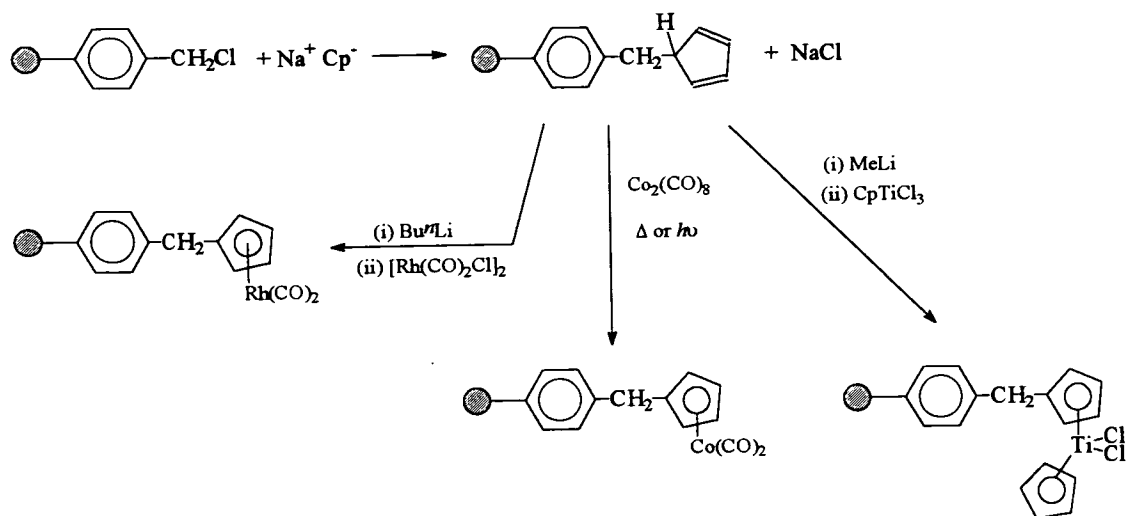
Scheme 1.12 : Cp complexes of Ti, Co, Rh

Phosphines may also be introduced by reacting chloromethylated polymers with $LiPR_2$ or KPR_2 (Scheme 1.13, below). Phosphines or Cp ligands have also been bound directly to aryl rings of the polymer support prior to attaching metal complexes. Diphenylphosphino-polystyrene resins have been the most widely used supports for attaching organometallic catalytic complexes[58-65]. The ready availability of polystyrene in varying cross link densities, molecular weights and types has facilitated this research: Scheme 1.13 shows several ligand replacement reactions used to prepare polymer anchored homogeneous catalysts[48]. Most commonly, carbonyl substitution or phosphine exchange reactions are employed.
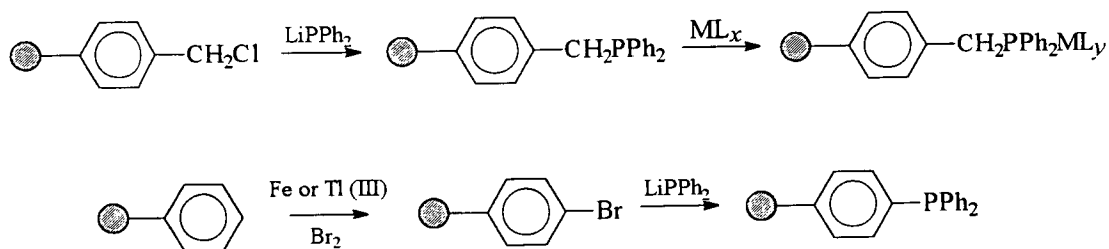
Scheme 1.13 : Ligand preparation for polymer anchored catalysts

25

Clusters have been attached to polymer backbones in several fashions. For example, styrene resins containing dimethylbenzylamino groups have been used to anchor $Rh_4(CO)_{12}$ [66] and $Rh_6(CO)_{16}$ [67]. These polymer bound rhodium cluster species catalyse alkene hydrogenation and the water gas shift reaction, respectively, and arylnitro group reduction[67] with H_2O / CO and H_2 / CO. Under the reaction conditions, it is thought that Rhodium cluster anions are produced which then undergo a variety of equilibria on the resin, depending on the reaction conditions. Polymers have also been used to support a variety of other metal clusters[68, 69]. Ligand exchange processes were used to attach the cluster to the polymer backbone. This was achieved by using a styrene-divinylbenzene polymer functionalised with phosphines to replace a carbonyl ligand. Multiple exchange may even occur, as in Scheme 1.14, and IR spectroscopy was used to characterise the substituted moieties. Multiple attachment of phosphine results from polymer internal mobility and is favoured, as expected, by higher phosphine loadings within the polymer.
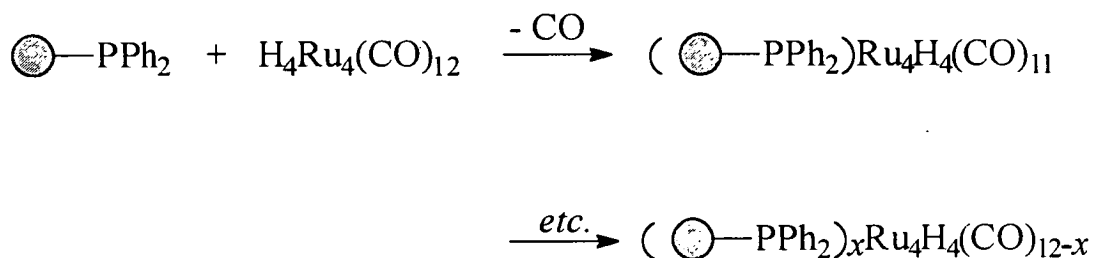
Scheme 1.14 : Multiple exchange with Ruthenium clusters

Table 1.3 lists some of these polymer bound clusters and the catalytic activity displayed.

26

Structure of supported cluster	Catalytic activity	Ref.
{O—PPh$_2$}Ir$_4$(CO)$_{11}$	alkene hydrogenation	70, 71, 72
{O—PPh$_2$}$_2$Ir$_4$(CO)$_{10}$	alkene hydrogenation	72
{O—PPh$_2$}$_3$Ir$_4$(CO)$_9$	alkene hydrogenation	72
{O—PPh$_2$}Ru$_4$H$_4$(CO)$_{11}$	alkene hydrogenation	73
{O—PPh$_2$}$_3$Ru$_4$H$_4$(CO)$_9$	alkene hydrogenation	73
{O—PPh$_2$}$_3$Ru$_4$H$_4$(CO)$_9$	alkene hydrogenation	74
{O—PPh$_2$}$_2$Fe$_2$Pt(CO)$_8$	alkene hydrogenation	74
{O—PPh$_2$}$_3$RuPt$_2$(CO)$_5$	alkene hydrogenation	74
{O—PPh$_2$}Os$_3$H$_2$(CO)$_9$	alkene isomerisation	69

Table 1.3 : Structures of some supported cluster catalysts

One final example of polymer modification, of particular interest to this project, is the chemical modification of polymers bearing either carboxydithiolate or thiocarboxamide functionalities[75]. These functions were utilised to attach carbonyl clusters of cobalt and iron to preformed polymer resins (Scheme 1.15). In the case of cobalt, copolymers of *para*-styryldithioformate, methyl methacrylate and [tri(hydroxymethyl)methl]acrylamide (tris A) were treated with dicobalt octacarbonyl in THF. A clusterisation yield of more than 80% was acheived, and a high content of cluster units on the polymer chain was easily obtained. However, similar chemical modifications on copolymers of vinylthiobenzamide and polythiocarboxamides did not lead to the expected cluster containing products, but to cross linked products. It

would appear that $Co_2(CO)_8$ does not react selectively with one function but acts as a cross linking reagent; a high proportion of cobalt in an undetermined form remains present in the polymer chain. Infra red spectroscopy shows no absorptions characteristic of cobalt carbonyl species. Scheme 1.15 summarises these findings.
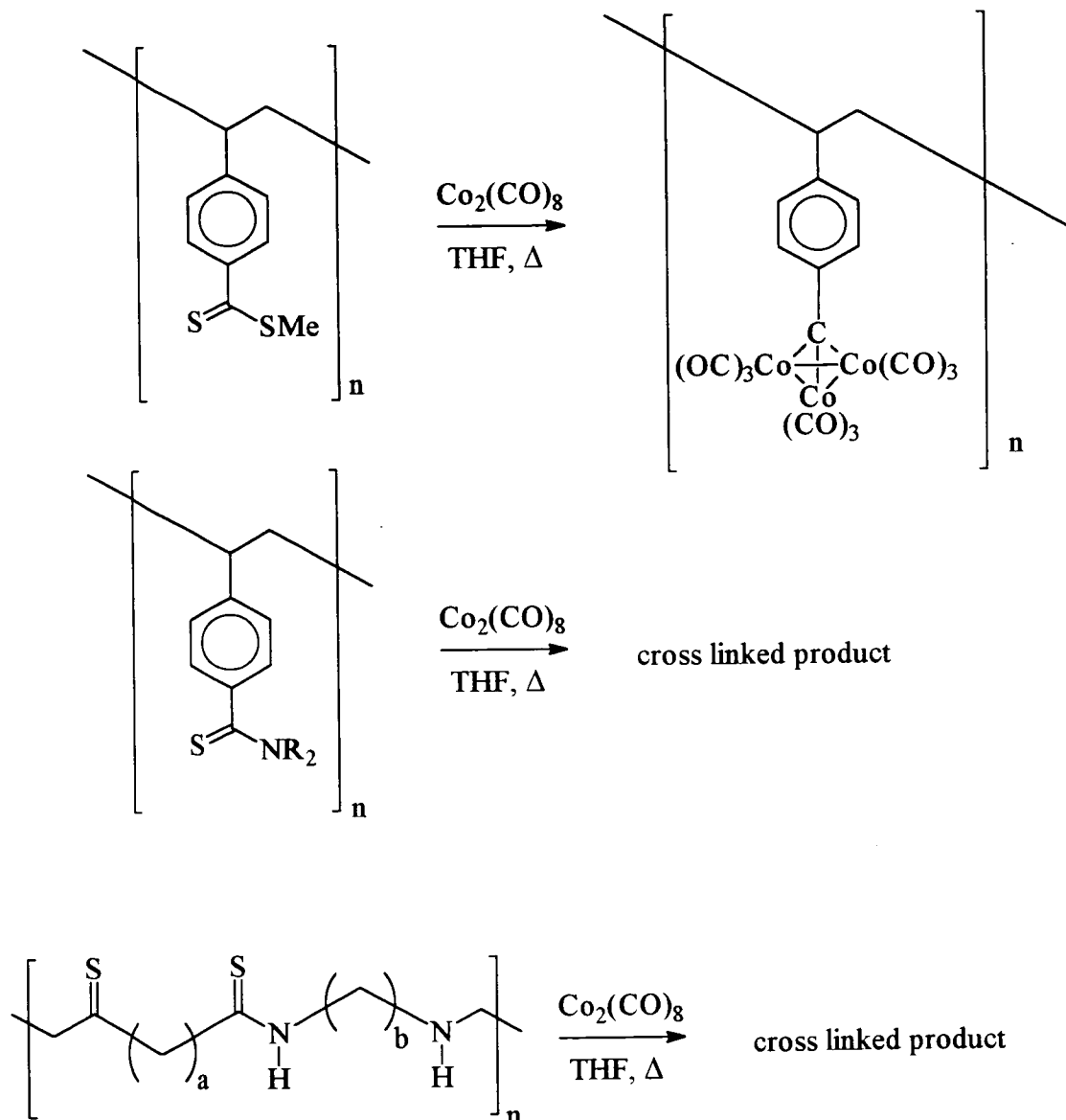
**Scheme 1.15 :** Polmer modifications with dicobalt octacarbonyl

Similar studies on these polymers using di-iron nonacarbonyl enabled analysis by Mössbauer Spectroscopy[75]. Analysis of the polymers formed by chemical

28

modification showed incorporation of 30 - 40% Fe as Fe_2O_3, presumably formed from the destruction of $Fe_2(CO)_9$ by free radicals.

Hence it can be clearly seen that preparation and subsequent polymerisation of suitable organometallic monomers is preferred to chemical modification of existing polymer networks. At first glance, chemical modification of polymers would appear to be the more convenient route to polymer supported species; the yields are high and separation of polymeric species is easy. However, it is more convenient to prepare such species by the copolymerisation of suitable organometallic monomers- a route which offers a higher degree of purity and preserves the integrity of the cluster units.

1.6.2 Polymerisation of organometallic monomers

As mention previously, the other method by which polymeric metal containing systems may be synthesised is by polymerisation (or copolymerisation) of suitable organometallic monomers. With few exceptions, the same parameters which affect chain growth, chain branching, etc. for nonmetal containing polymerisations, affect chain growth where metals are present. Figure 1.7 shows the structures of organometallic vinyl species incorporated into polymers up until the early 1980s[76].

R = H, CH₃ R = H, CH₃

R = H, CH₃

$$Me_3SiCH\!\!=\!\!CH_2 \qquad Me_3GeCH\!\!=\!\!CH_2 \qquad Me_3SnCH\!\!=\!\!CH_2$$
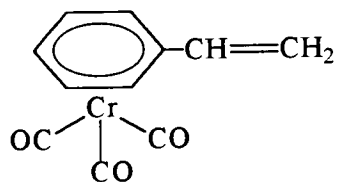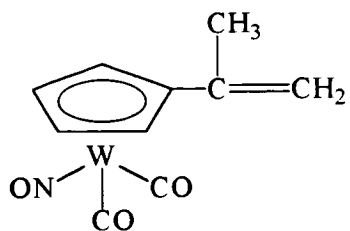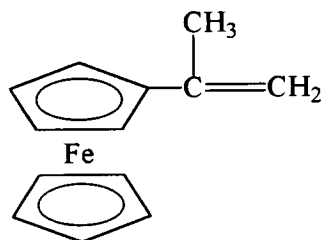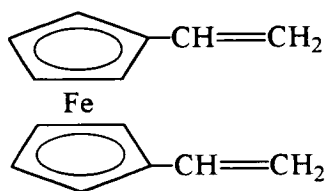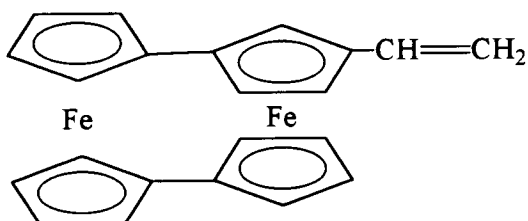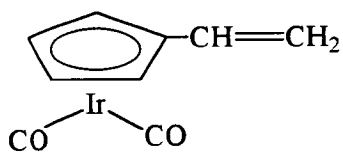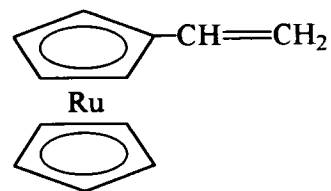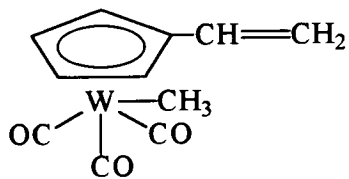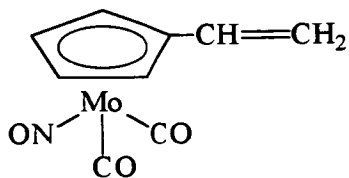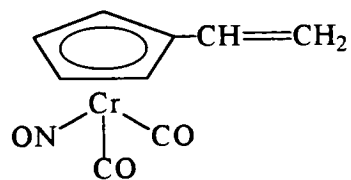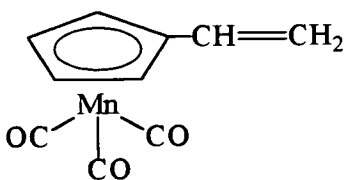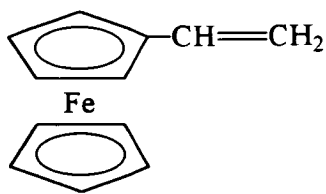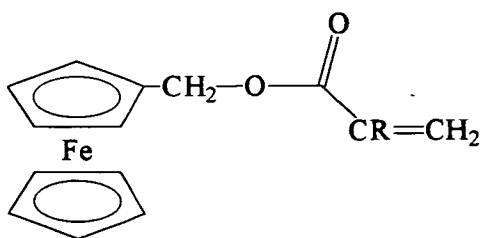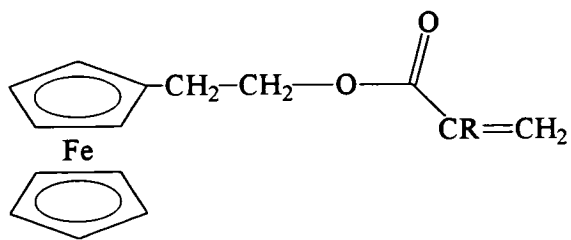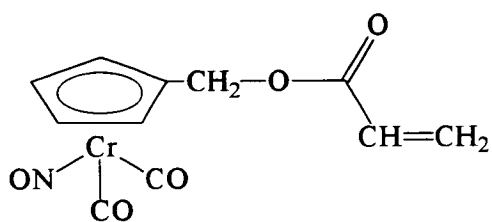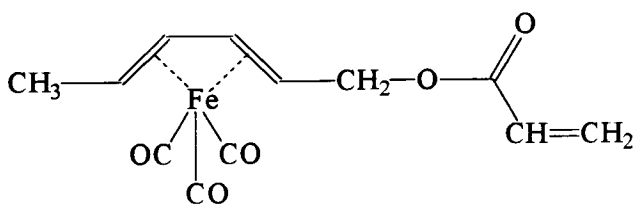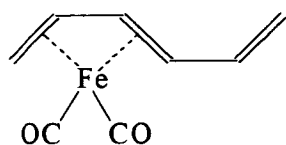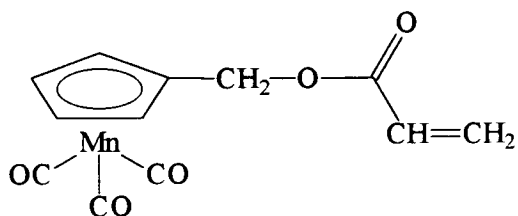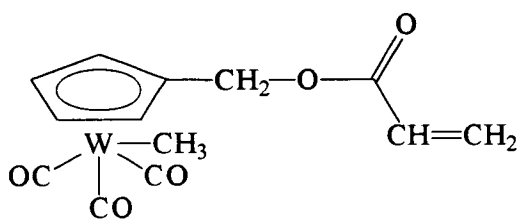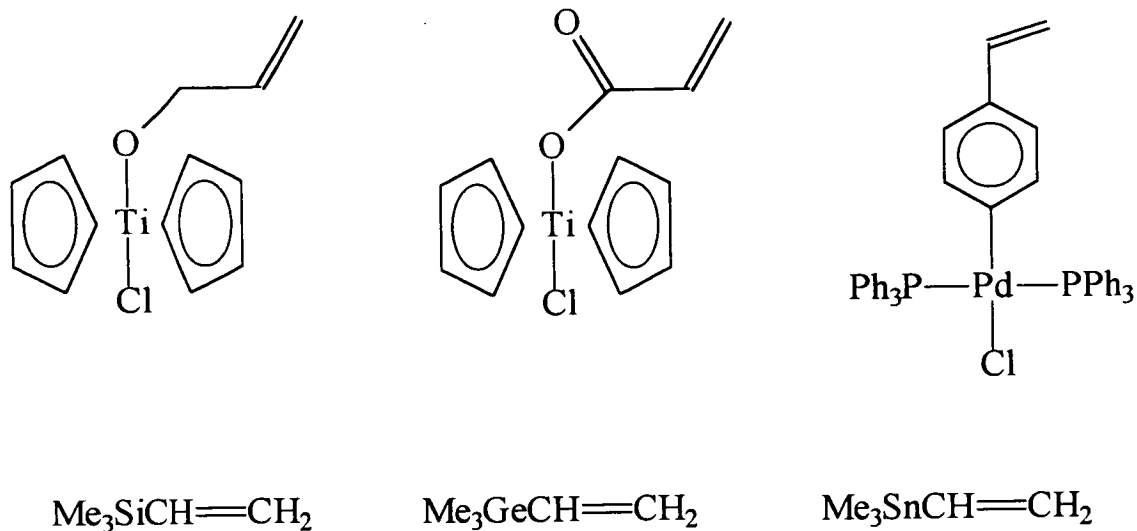
Figure 1.7: Organometallic vinyl monomers

The number of copolymers synthesised far outweighs the number of homopolymers synthesised, due to a hesitancy of many metal containing monomers to homopolymerise. The structures depicted in Figure 1.7 are electron rich systems which undergo either cationic or radical polymerisation, but typically not anionic polymerisation [77, 78, 79]. Cationic polymerisation 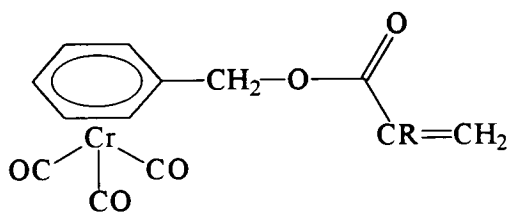may be initiated using Lewis acids such as $BF_3.OEt_2$, $Et_2AlCl/M(acac)_2$ (where M= Ni, Cu, VO, *etc.*) and H_2SO_4. Attack occurs preferentially on the vinyl group although electrophilic substitution on the ring is also possible. While a large number of free radical initiators have been used, some problems which are due to choice of initiator may be encountered. For instance, peroxide initiatiors can cause oxidation of the metal atom and extensive decomposition. Thus consideration must be given to the choice of initiator employed.

Branching and/or crosslinking is much more common with vinyl organometallic polymers than with classical (organic) vinyl polymers. Thus attack of the carbonium ion on a monomer such as vinyl ferrocene leads to branching and

crosslinking [80] (Scheme 1.16).   Internal hydride transfer would also lead to branching[81].
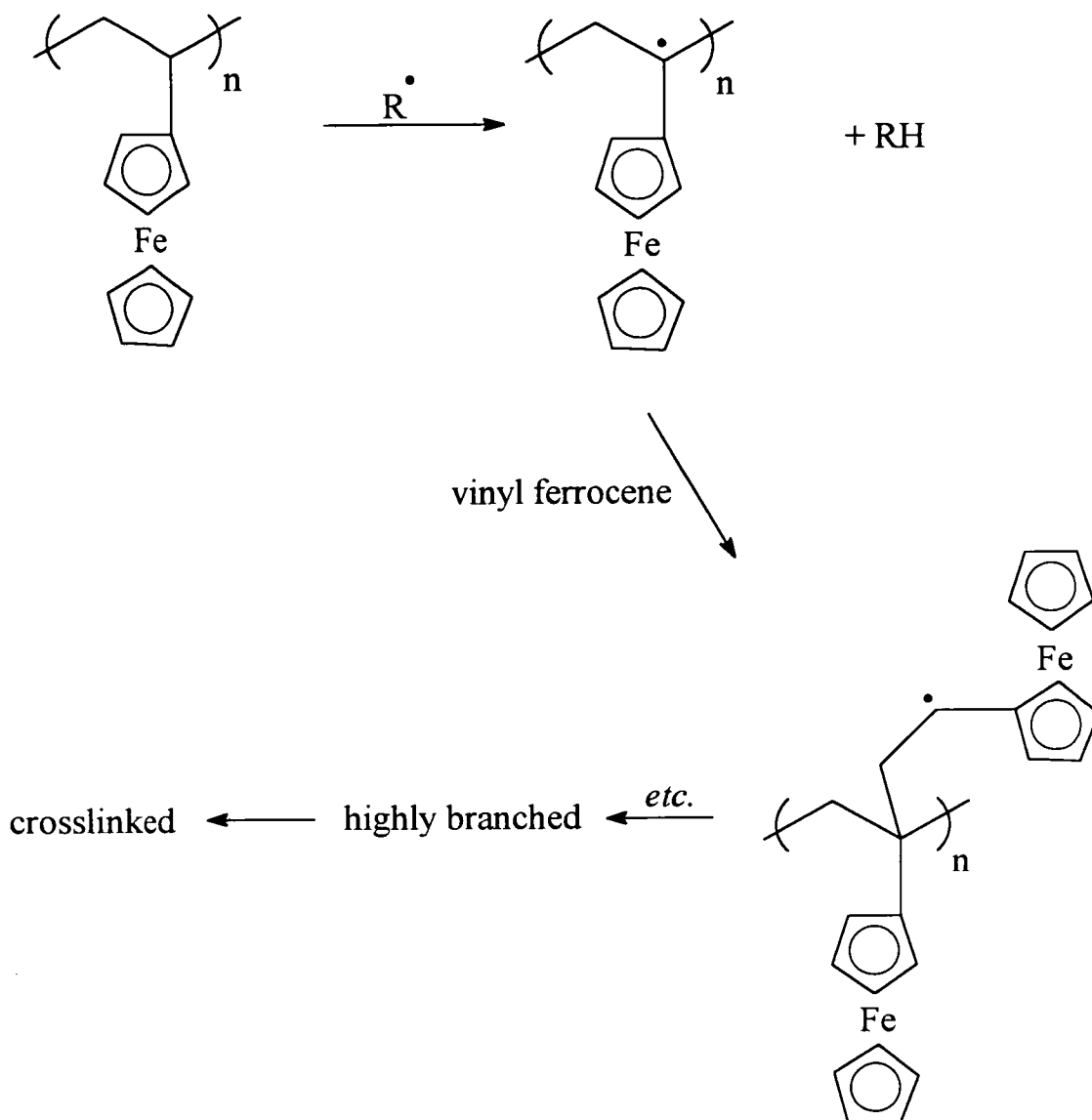
Scheme 1.16 : Branching and cross linking of poly(vinylferrocene)

Typically, the vinyl metal monomers are considered as "chain stiffening" units. Flexibility for copolymers is increased through the use of "flexible" comonomers and/or limiting the amount of metal containing moiety present in the copolymer. More flexible polymers may also be obtained if the organometallic group is moved away from the vinyl moiety. The flexibility can also be enhanced through the addition

33

of plasticisers. Typically there is a direct relationship between polymer flexibility and such thermal properties as the onset of whole chain mobility (melting point, T_m) and segmental chain mobility (glass transition, T_g) and softening range, and these in turn are important if a given material is to be used for certain applications.

The first example of the polymerisation of a vinyl organometallic monomer reported was the polymerisation of vinylferrocene by Arimoto and Haven [45] who found that pyrolysis of the carbinol of ferrocene (or its acetate, both prepared from acetylferrocene) produced a low melting red solid with a strong camphor like odour, characterised as vinylferrocene (see Scheme 1.17). Free radical homo- and copolymerisation initiated by azo-*bis*(isobutyronitrile) (AIBN) and other initiators produced a range of molecular weight polymers, from viscous oils to solids
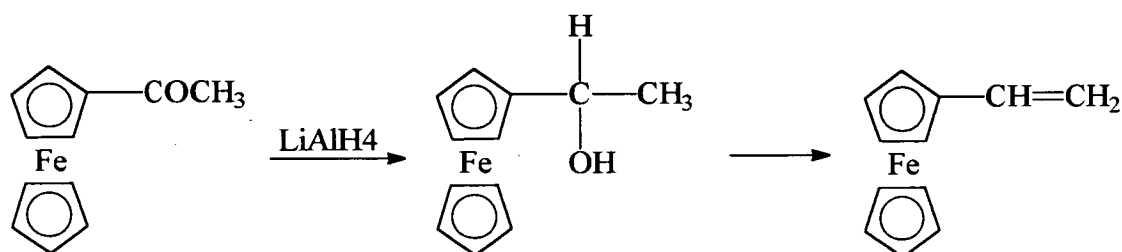
Scheme 1.17: Synthesis of vinylferrocene

More recently, and more appropriate to this study, Patin *et al* [17] synthesised two organovinyl cobalt cluster monomers, and produced a variety of organo and water soluble copolymers. Direct action of dicobalt octacarbonyl in THF on *para*-styryldithioformate produced the cluster monomer *para*-styryl methylidyne tricobaltnonacarbonyl, as shown in Scheme 1.18. The pure monomer was obtained in 40% yield after chromatography to remove byproducts (mainly cobalt sulphides).
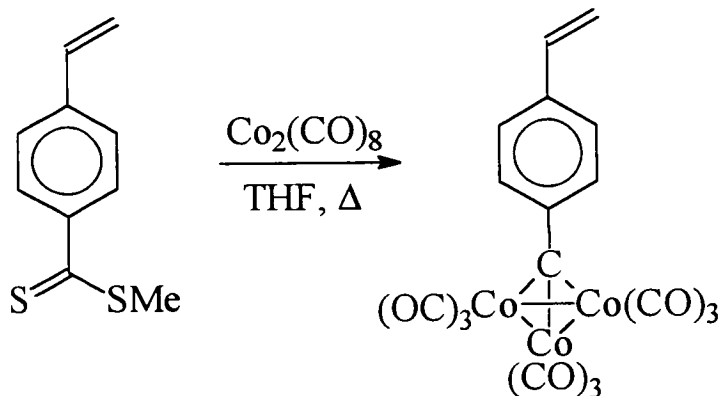
Scheme 1.18 : Preparation of *para*-styryl methylidyne tricobaltnonacarbonyl

Similarly, reaction of $Co_2(CO)_8$ in THF on the styrylthiocarboxamide produced the thioalkylidyne species shown in Scheme 1.19.
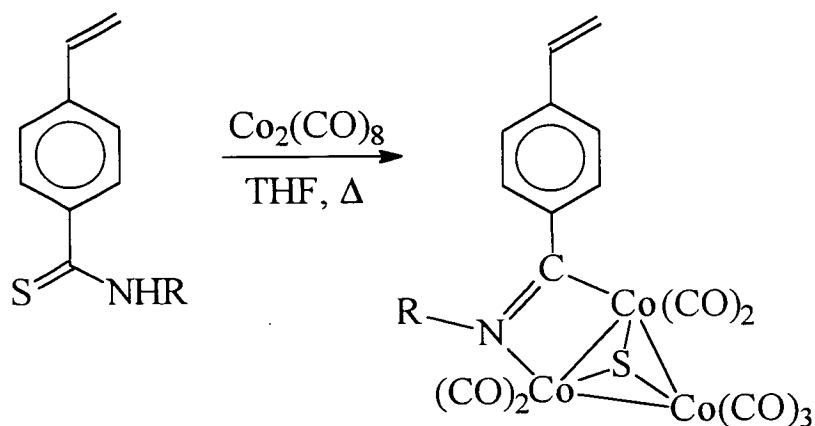
Scheme 1.19 : Thioalkylidyne monomer preparation

Free radical homopolymerisation of both these monomeric species was unsuccessful as ionic initiators destroyed them immediately. However, copolymerisation with styrene or methylmethacrylate and water soluble comonomers such as [tris(hydroxymethyl) methyl] acrylamide produced copolymers containing the clusters in 1 to 1.5 mol%.

Table 1.4 summarises the results obtained for polymers obtained by this route.

cluster unit in copolymer	starting material	cluster unit in copolymer (mol%)	Mn ; Mw (GPC)
stryryl	styrene, cluster, (99:1)	3.7	6400, 14720
styryl	MMA, cluster, (99:1)	1.0	21300, 44700
styryl	Tris A, cluster, (99:1)	1.6	-
thioalkylidyne	styrene, cluster, (99:1)	1.3	7200, 16800
thioalkylidyne	MMA, cluster, (99:1)	1.8	7200, 16800
thioalkylidyne	Tris A, cluster, (99:1)	1.6	-

MMA = methyl methacrylate

Tris A = N-[tris-1,1,1(hydroxymethyl) methyl] acrylamide

Table 1.4: Copolymers containing tricobalt clusters

1.7 Cobalt catalysed cross linking of alkyd polymers

Finally, let us consider the reaction we wish to catalyse. Commercially, one application of cobalt is as a catalyst for the cross linking of alkyd polymers, (derived from *alc*ohols and ac*ids*). Alkyd polymers are condensation polymers formed by the transetherification of phthalic anhydride, pentaerythritol and long chain fatty acids (Scheme 1.20).
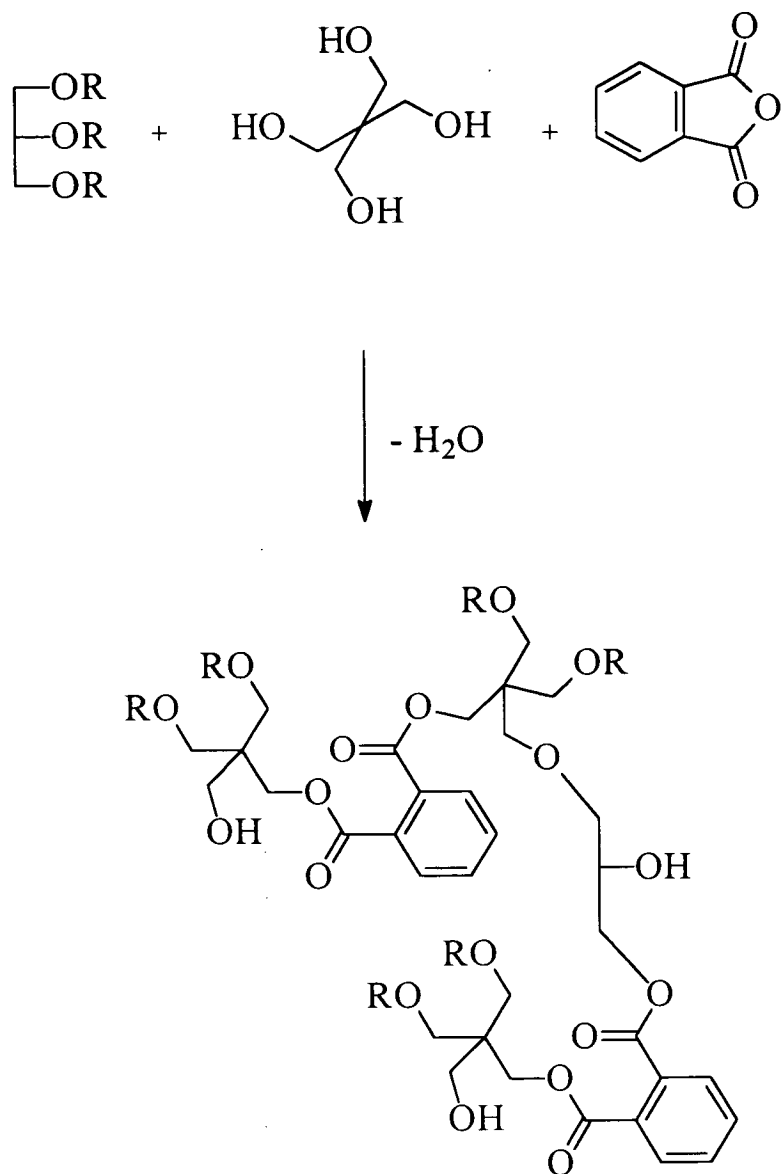
Scheme 1.20 : Preparation and general composition of alkyd polymers

The nature of the R group depends on the the time of harvest and the strain of bean used as the source of the triglyceride. Generally, though, linseed oil or soya bean oil is used, depending on economics. Soya bean oil has the general composition shown in Figure 1.8.

Soya bean oil:

```
      ┌──OR
      ├──OR      where R=
      └──OR
```

$$\underset{\text{O}}{\|} \quad \text{(oleic acid chain structure)}$$
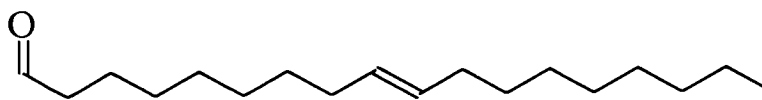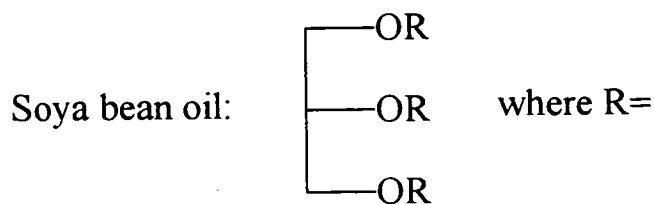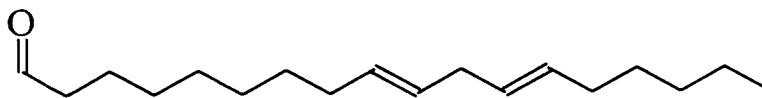
22-28% Oleic acid

52-55% 9,12 Linoleic acid
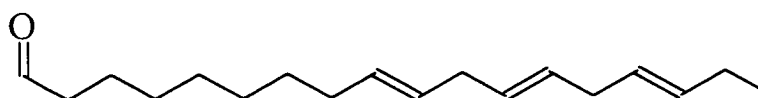
5-9% 9,12,15 Linolenic acid

plus 14% saturated acid

Figure 1.8 : Composition of soya bean oil

Hence the alkyd polymer produced has unsaturated side chains, which are exploited commercially in the formation of polymer films.

Alkyd polymers are the main component of gloss paints. However, for the polymer (paint) to form a suitable protective and/or decorative surface coating, the polymer must crosslink to form a bulk network. There are many ways in which it is possible to chemically crosslink polymers. However, as the bulk of such paint is for domestic use, a simple, foolproof and failsafe method of crosslinking is necessary. The crosslinking must also be effective at ambient temperatures and humidities prevalent from Siberia to India, and give consistent, satisfactory results. Common sense (and legislation) also dictate that the method of crosslinking must pose no threat

to the consumer or the environment, and must be so simple that no specialist knowledge or equipment is necessary. The solution to this problem lies in the unsaturated groups present in the alkyd, and their inherent instability, as with all unsaturated systems, to atmospheric exposure.

The resultant alkyd polymer contains unconjugated fatty acids- these unsaturated groups are susceptible to autoxidation which occurs in air on exposure to ultraviolet radiation and/or elevated temperatures. Bolland[83] has shown that the mechanism is free radical in nature. For the unconjugated fatty acids (*e.g.* linoleic acid), the initial reaction is the formation of a hydroperoxide, and the mechanism may be represented by the reaction shown below in Scheme 1.21.

$$H_3C(CH_2)_4 \diagup\!\!=\!\!\diagdown\!\!=\!\!\diagup (CH_2)_7COOH$$

$$\downarrow -H^\bullet$$

$$H_3C(CH_2)_4 \diagup\!\!=\!\!\overset{\bullet}{\diagdown}\!\!=\!\!\diagup (CH_2)_7COOH$$

$$\downarrow O_2, H^\bullet$$

$$H_3C(CH_2)_4 \diagup\!\!=\!\!\overset{OOH}{\diagdown}\!\!=\!\!\diagup (CH_2)_7COOH$$
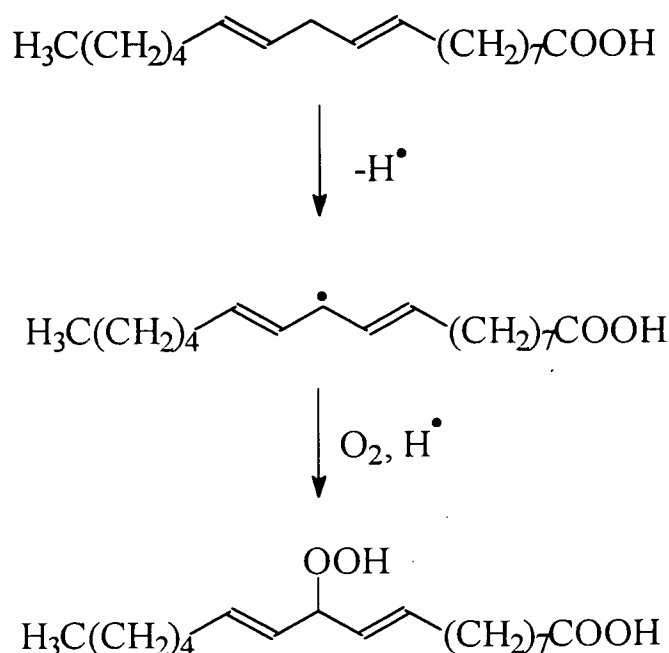
Scheme 1.21 : Hydroperoxide formation in unconjugated systems

In the case of polyesters such as these alkyd polymers, a methylene group adjacent to a double bond is particularly liable to lose a hydrogen atom, since the resulting radical is resonance stabilised. This radical can react with oxygen to produce a peroxidic radical which then abstracts hydrogen from a further α-methylene group to form a hydroperoxide and to propagate the reaction. The hydroperoxides of

the types shown above (ROOH) may decompose in the ways shown below in Scheme 1.22.

$$ROOH \longrightarrow RO^\bullet + HO^\bullet$$

$$2\,ROOH \longrightarrow RO^\bullet + ROO^\bullet + H_2O$$
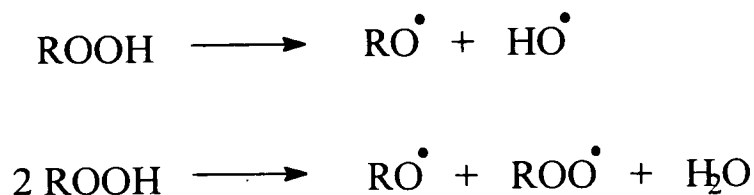
Scheme 1.22 : Primary hydroperoxide decomposition

Subsequent to the primary decomposition, induced decomposition may occur as shown in Scheme 1.23.

$$RO^\bullet + ROOH \longrightarrow ROO^\bullet + ROH$$

$$ROO^\bullet + ROOH \longrightarrow RO^\bullet + ROH + O_2$$

$$RO^\bullet + RH \longrightarrow ROH + R^\bullet$$

$$HO^\bullet + RH \longrightarrow H_2O + R^\bullet$$

$$R^\bullet + ROOH \longrightarrow ROH + RO^\bullet$$
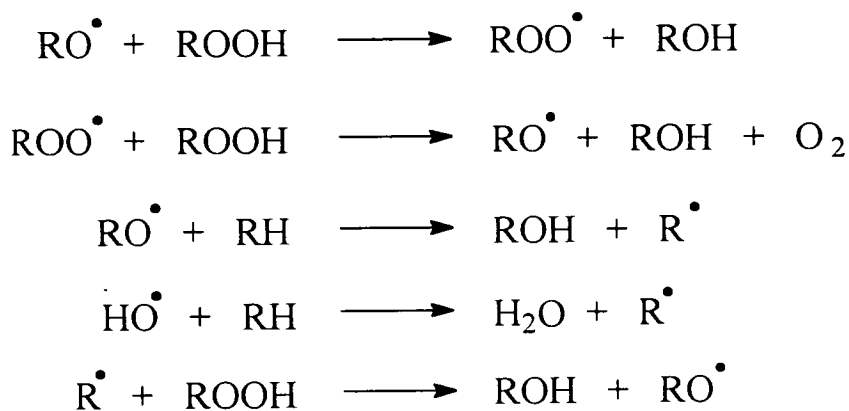
Scheme 1.23 : Induced peroxide decomposition

Termination of the above reaction chain may then occur by radical coupling reactions as in Scheme 1.24.

40

$$RO^\bullet + RO^\bullet \longrightarrow ROOR$$

$$ROO^\bullet + ROO^\bullet \longrightarrow ROOR + O_2$$

$$R^\bullet + R^\bullet \longrightarrow R\text{—}R$$

$$RO^\bullet + R^\bullet \longrightarrow ROR$$

$$R^\bullet + ROO^\bullet \longrightarrow ROOR$$
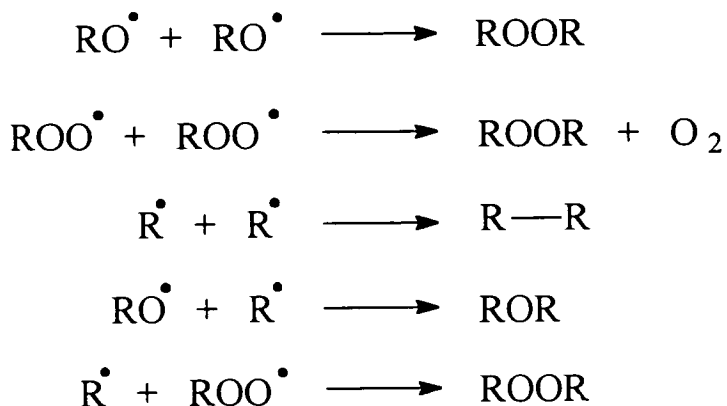
Scheme 1.24 : Radical coupling

Although the products shown above represent simple dimers, it will be appreciated that extension of the reaction sequence to non-conjugated saturated oils and corresponding alkyd resins would result in the formation of a network polymer.

The formation of cross linked films by the various reactions described above is not rapid enough for practical puroposes. Commercial surface coatings therefore contain catalysts or *driers* which speed up the drying process. The detailed mechanism by which driers operate has not been elucidated, although it is generally agreed that an important function of driers is to catalyse the decomposition of the hydroperoxides formed by the aerial oxidation of non conjugated fatty acids and esters. Cobalt Octoate is used commercially to catalse the drying of alkyd polymers (gloss paints), the redox system shown in Scheme 1.25 may be envisaged.

$$ROOH + Co^{2+} \longrightarrow RO^\bullet + OH^- + Co^{3+}$$

$$ROOH + Co^{3+} \longrightarrow ROO^\bullet + H^+ + Co^{2+}$$
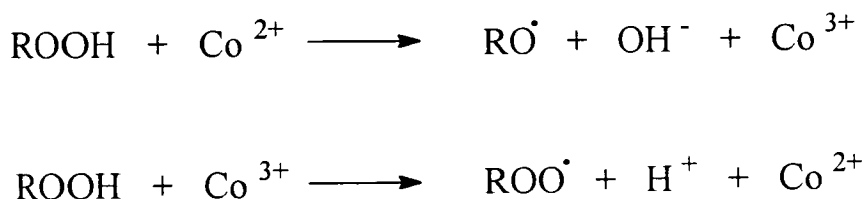
Scheme 1.25 : Catalytic decomposition of hydroperoxides

It has also been suggested that driers also initiate the oxidation sequence by direct interaction of the metal ion with the fatty acid or ester, *e.g.* Scheme 1.26

$$RH + Co^{3+} \longrightarrow R + Co^{2+} + H^{+}$$
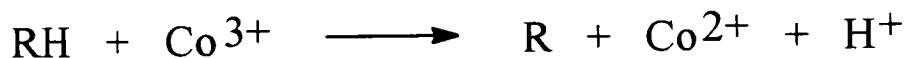
Scheme 1.26: Proposed initiation of oxidation

One problem for this system is that, when applied to exterior surfaces, weathering leaches cobalt from the coating and hence may pose an environmental problem. From a commercial point of view, it would also be advantageous to find a better catalyst for the drying process- *i.e.* find a catalytic species which speeded up the cross linking process more effectively than the catalyst used at present. If the paint can be made to dry (crosslink) in a shorter period of time, then the consumer would wait less time between applying coats of paint to the substrate, and would benefit from faster room reoccupancy.

It was therefore hoped that incorporating cobalt clusters into polymers would not only produce a better catalyst for alkyd cross linking, but would also enable the synthesis of some novel polymeric materials.

1.8 References

1. E. L. Muetterties, *Bull. Soc. Chim. Belg.* 1975, **84**, 959

2. J. -M. Basset and R. Ugo, in *"Aspects Of Homogeneous Catalysis, Vol III"* Ed. R. Ugo, Reidel, Dordrecht, 1977, 137

3. H. H. Lamb and B. C. Gates, *J. Am. Chem. Soc.* 1986, **108**, 81

4. C. U. Pittmann, in *"Polymer Supported Reactions in Organic Synthesis"*, Ed. P. Hodge and D.C. Sherrington, Wiley and Sons, New York, 1980

5. M. H. Chisholm, K. Folting, D. M. Hoffman and J. C. Huffman, *J. Am. Chem. Soc.* 1984, **106**, 6794

6. M. M. Hills, J. E. Parmeter and W. Weinberg, *J. Am. Chem. Soc.*, 1987, **109**, 4224

7. D. Seyferth, *Adv. Organomet. Chem.* 1976, **14**, 97

8. R. Markby, I. Wender, R. A. Friedel, F. A. Cotton and H. W. Sternberg, *J. Am. Chem. Soc.*, 1958, **80**, 6529

9. P. W. Sutton and L. F. Dahl, *J. Am. Chem. Soc.*, 1967, **89**, 261

10. R. S. Dickson and P. J. Fraser, *Adv. Organomet. Chem.* 1974, **12**, 323

11. W. T. Dent, L. A. Duncanson, R. G. Guy, H. W. B. Reed and B. L. Shaw, *Proc. Chem. Soc.* 1961, 169

12. D. Seyferth, J. E. Hallgren and P. L. K. Hung, *J. Organomet. Chem.*, 1973, **50**, 265

13. D. Seyferth, C. S. Eschbach, G. H. Williams, P. L. K. Hung and Y. M. Cheng, *J. Organomet. Chem.*, 1974, **78**, C13

14. D. Seyferth, C. S. Eschbach, G. H. Williams and P. L. K. Hung, *J. Organomet. Chem.*, 1977, **134**, 67

15. J. Meijer, P. Vermeer and L. Brandsma, *Rec. Trav. Chim.*, 1973, **92**, 601

16. H. Patin, G. Mignani and M-T.Van Hulle, *Tetrahedron Lett.* 1979, 2441

17. J. C. Gressier, G. Levesque and H. Patin, *Poly. Bull.*, 1982, 55

18. T. W. Matheson, B. M. Peake, B. H. Robinson, J. Simpson and D. J. Watson, *J. Chem. Soc. Chem. Comm.* 1973, 894

19. R. Dolby and B. H. Robinson, *J. Chem. Soc. Dalton Trans.* 1973, 1794

20. D. Seyferth, J. E. Hallgren and C. L. Nivert, *Inorg. Chem.*, 1977, **16**, 758

21. D. Seyferth, J. E. Hallgren and C. S. Eschbach, *J. Am. Chem. Soc.*, 1974, **96**, 1730

22. R. Deschenaux, C. Masoni, H. Stoecki-Evans, S. Vaucher, J. Ketterer, R. Steiger and A. L. Weisenhorn, *J. Chem. Soc. Dalton Trans.* 1994, 1051

23. D. Seyferth, J. E. Hallgren, R. J. Spohn, G. H. Williams, M. O. Nestle and P. L. K. Hung, *J. Organomet. Chem.*, 1974, **65**, 99

24. S. G. Davies, *"Organotransitionmetal Chemistry : Applications to Organic Synthesis. "*, Pergamon Press, Oxford, UK, 1982

25. L. Weber, K, Reizig, D. Bungdart and R. Boese, *Organometallics*, 1987, **6**, 110

26. L. T. Taylor, S. C. Vergez and D, H. Busch, *J. Am. Chem. Soc.*, 1966, **88**, 3170

26. D. C. Miller and T. B. Brill, *Inorg. Chem.*, 1978, **17**, 240

27. X. Meng, N. P. Rath and T. P. Fehlner, *Organometallics*, 1991, **10**, 1986

27. D. Seyferth, J. E. Hallgren and C. S. Eschbach, *J. Am .Chem. Soc.*, 1974, **96**, 1730

28. P. T. Chesky and M. B. Hall, *Inorg. Chem.*, 1981, **20**, 4419

29. W.E. Geiger and N. G. Connelly, *Adv. Organomet. Chem.* 1985, **24**, 87

30. M. B. Robin and P. Day, *Adv. Inorg. Chem. Radiochem.* 1980, **58**, 451

31. N. S. Hush, *Chem. Phys.*, 1975, **10**, 361

32. B. H. Robinson and J. Simpson, *"Paramagnetic Organometallic Species in Activation / Selectivity, Catalysis"*, Eds. M. Chanon, M. Juillard and J. C. Pointe, p. 357, Vol. 257, NATO ASI Series, Kluwer, Dordrecht, 1989

33. S.B. Colbram, B. H. Robinson and J. Simpson, *J. Chem. Soc., Chem. Commun.*, 1982, 1362

34. J. Borgdorff, E. J. Ditzel, N. W. Duffy, B. H. Robinson and J. Simpson, *J. Organomet. Chem.*, 1992, **437**, 323

35.   D. D. Cowan, C. LeVanda, J. Park and F. Kaufman, *Acc. Chem. Res.*, 1973, **6**, 1

36.   M. J. Powers and T. J. Meyer, *J. Am. Chem. Soc.*, 1978, **100**, 4393

37.   B. E. R. Schilling and R. J. Hoffmann, *J. Am. Chem. Soc.*, 1979, **101**, 3456

38.   A. M. Bond, B. M. Peake, B. H. Robinson, J. Simpson, D. J. Watson, *Inorg. Chem.*, 1977, **16**, 410

39.   A. J. Downard, B. H. Robinson, J. Simpson, *Organometallics*, 1986, **5**, 1122

40.   A. J. Downard, B. H. Robinson, J. Simpson, *Organometallics*, 1986, **5**, 1132

41.   A. M. Bond, P. A. Dawson, B. M. Peake, B. H. Robinson and J. Simpson, *Inorg. Chem.*, 1979, **18**, 1413

42.   G. H. Worth, B. H. Robinson and J. Simpson, *Organometallics*, 1992, **11**, 3863

43.   A. J. Deeming and S. Hasso, *J. Organomet. Chem.*, 1976, **114**, 313

44.   J. B. Keister and J. R. Shapely, *J. Am. Chem. Soc.*, 1976, **98**, 1056

45.   F.S. Arimoto and A. C. Haven Jr., *J. Am. Chem. Soc.*, 1955, **77**, 6295

46.   Y. Sasaki, L. L. Walker, E. L. Hurst and C. U. Pittman Jr., *J. Polym. Sci. Chem. Ed.*, 1973, **11**, 1213

47.   J. P. Collman, *Acc. Chem. Res.*, 1968, **1**, 136

48.   C. U. Pittman Jr., in *Comprehensive Organometallic Chemistry*, Ed. G. Wilkinson and F. G. A. Stone, Pergamon, 1982, Vol. 8, 553

49.   W. Heitz, *Adv. Polym. Sci.*, 1977, **23**, 1

50.   E. Bayer and V. Schurig, *Chem. Technol.*, 1976, 212

51.   E. Bayer and V. Schurig, *Angew. Chem. Intl. Ed. Engl.*, 1975, **14**, 493

52.   G. Bernard, Y. Chauvin and D. Commereuc, *Bull. Chim. Soc. Fr.*, 1976, 1163

53.   G. Bernard, Y. Chauvin and D. Commereuc, *Bull. Chim. Soc. Fr.*, 1976, 1168

54.   C. U. Pittmann Jr. and R. F. Felis, *J. Organomet. Chem.* 1974, **72**, 389

55.   R. H,. Grubbs, C. Gibbons, L. C. Kroll, W. D. Bonds and C. H. Brubaker Jr., *J. Am. Chem. Soc.*, 1973, **95**, 2373

56.   B. H. Chang, R. H. Grubbs, and C. H. Brubaker Jr., *J. Organomet. Chem.*, 1979, **172**, 81

57.   P. Perkins and K. P. C. Vollhardt, *J. Am. Chem. Soc.*, 1979, **101**, 3985

58.   M. Capka, P Svoboda, M. Corny and J. Hetflejs, *Tetrahedron. Lett.* 1971, 4787

59.   R. H. Grubbs and L. C. Kroll, *J. Am. Chem. Soc.*, 1971, **93**, 3062

60.   R. H. Grubbs and E. M. Sweet, *Macromolecules*, 1975, **8**, 241

61.   C. U. Pittman, Jr. and L. R. Smith, *J. Am. Chem. Soc.*, 1975, **97**, 1749

62.   C. U. Pittman, Jr., L. R. Smith and R. M. Hanes, *J. Am. Chem. Soc.*, 1975, **97**, 1742

63.   C. U. Pittman, Jr., S. E. Jacobsen and H. Hiramota, *J. Am. Chem. Soc.*, 1975, **97**, 4774

64.   G. O. Evans, C. U. Pittman, Jr., R. McMillan, R. T. Beach and R. Jones, *J. Organomet. Chem.*, 1974, **67**, 295

65.   L. D. Rollman, *Inorg. Chim. Acta*, 1972, **6**, 137

66.   T. Kitamura, T. Joh and N. Hagihara, *Chem. Lett.*, 1975, 203

67.   R. C. Ryan, G. M. Wilemon, M. P. DalSanto and C. U. Pittman, Jr., *J. Mol. Catal.*, 1979, **5**, 319

68.   B. C. Gates and J. Lieto, *Chem Technol.*, 1980, 195

69.   B. C. Gates and J. Lieto, *Chem Technol.*, 1980, 248

70.   J. Lieto, J. J. Minkiewicz, P. W. Rafalko and B. C. Gates, in *Fundamental Research in Homogeneous Catalysis*, Vol. 3, Ed. M. Tsutsui, Plenum, New York, 1979

71.   J Lieto, J. J. Rafalko and B. C. Gates, *J. Catal.*, 1980, **62**, 149

72.   J. J. Rafalko, J. Lieto, B. C. Gates and G. L. Schrader, Jr., *J. Chem. Soc. Chem. Commun.*, 1978, 540

73.   Badische Anilin und Soda-Fabrik A. G., *Fr. Pat.* 2 053 300

74.   R. Pierantozzi, K. J. McQuade, B. C. Gates, M. Wolf, H. Knözinger and W. Ruhmann, *J. Am. Chem. Soc.*, 1979, **101**, 5436

75.   J. C. Gressier, G. Levesque, H. Patin and F. Varret, in *Metal Containing Polymeric Systems*, Eds. J. E. Sheats, C. E. Carraher Jr., and C. U. Pittman, Jr., Plenum, New York, 1984, 291

76.   C. E. Carraher, Jr., *J. Chem. Ed.*, 58, 11, 1981

77. C. U. Pittman, Jr., in *Organometallic Reactions*, Eds. E. Becker and M. Tsutsui Plenum, New York, 1977, Vol 6

78. E. Neuse and H. Rosenberg, *Metallocene Polymers*, Marcel Decker, NY, 1970

79. C. Carraher, J. Sheats and C. Pittman, Jr., *Organometallic Polymers*, Academic Press, New York, 1978

80. T.C. Willis and J. E. Sheats, *J. Poly. Sci. Poly. Chem. Ed.*, 1984, **22**, 1077

81. J. Sheats, J. Macromol. Sci.-Chem., **A15**, 1173

82. J. L. Bolland and H. Hughs, *J. Chem. Soc.*, 1949, 492

83. C. Aso, T. Kunitake and T. Nakashima, *Makromol. Chem.*, 1969, 124, 232

Chapter 2

Preparation of polymers containing cobalt alkylidynes

2.1 Introductory remarks

There are many ways in which monomers combine to make polymers; the method used depending on the nature of the functional group(s) present in the monomer. For organic molecules containing carbon-carbon double bonds, the most common methods of polymerisation are (i) free radical induced polymerisation (ii) ionic polymerisation and (iii) coordination polymerisation (*i.e.* Ziegler Natta polymerisation). For molecules with other functionalities, several other methods of polymerisation exist; depending on the functionality present. Polymer formation through reaction of functional groups (*e.g.* condensation and addition polymerisations) will be considered later, in Chapter 3.

From the outset of this study it was clear that the easiest way to produce polymers was by the free radical induced polymerisation of unsaturated species. Other methods of polymerisation are possible but, given the limited chemistry of the tricobalt alkylidyne cluster, it was thought that an unsaturated functionality could be introduced with more ease and success than any other polymerisable functionality.

2.2 Free radical induced polymerisation

2.2.1 Solution polymerisation

Free radical polymerisation can be divided into two types: solution polymerisation and heterophase (dispersion) polymerisation. In solution

polymerisation, the monomers, polymers, solvents and initiators are chosen so that the reaction is carried out in one phase. The product is a solution of polymer in solvent.

The principle reactions of free radical polymerisation can be summarised as follows[1,2]:

Initiation: an initiator decomposes to form two primary radicals:

$$I \longrightarrow 2R^{\bullet}$$
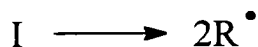
which then add monomer to yield a chain radical

$$R^{\bullet} + M \longrightarrow M_1^{\bullet}$$
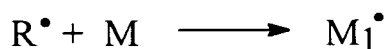
Propagation: chain growth continues, represented by the general equation

$$M_x^{\bullet} + M \longrightarrow M_{x+1}^{\bullet}$$
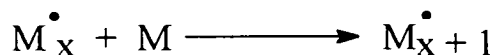
Termination: growing radicals may be terminated by disproportionation

$$R^1CH_2\overset{\bullet}{C}H_2 + R^2CH_2\overset{\bullet}{C}H_2 \longrightarrow R^1CH_2CH_3 + CH_2{=}CHR^2$$

or by combination

$$M_x^{\bullet} + M_y^{\bullet} \longrightarrow M_{x+y}^{\bullet}$$

overall

$$M_r^{\bullet} + M_s^{\bullet} \longrightarrow M_{r+s} \text{ or } M_r + M_s$$
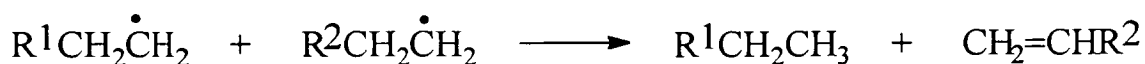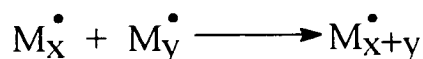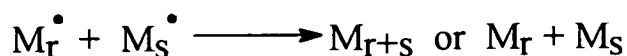
The growing radical may also be terminated by chain transfer to solvent or to a chain transfer agent (*e.g.* a thiol)- the transfer agent itself acquiring radical character:

$$M_x^{\bullet} + RSH \longrightarrow M_xH + RS^{\bullet}$$
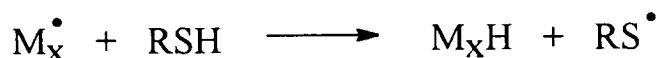
If the new radical is sufficiently active, a new chain may be initiated

At any stage of an addition polymerisation the reaction mixture will consist of high molecular weight polymer and unreacted monomer, *i.e.* a chain grows to completion and then another chain is initiated. Solution polymerisations may be carried out by a batch process -where all the ingredients are added to the reaction vessel- or by a feeding (semi-continuous) process- where the monomers and initiator are fed into the solvent in the reaction vessel over a period of 1 - 3 hours. The latter route is much preferred because of the highly exothermic nature of the polymerisation reaction- feeding gives much more control and safety. Some of the more commonly used initiators are: the peroxide initiators (benzoyl peroxide, *tert*-butyl peroxide, *tert*-butyl perbenzoate and di-*tert*-butyl peroxide), and the azo initiators, based on azo[bis(isobutyronitrile].

Molecular weight control of solution polymers may be achieved in several ways. The molecular weight can be decreased by

(1)   **Increasing the radical flux throughout the polymerisation**

This can be achieved by

- increasing the temperature (for initiators that decompose in a purely thermal manner),

- (in a feed process) by increasing the concentration of initiator relative to the monomer, or by increasing the initiator feed rate relative to the monomer feed rate.

(2) **Decreasing the monomer concentration (for the same initiator concentration)**

(3) **Increasing the extent of chain transfer.**

As already mentioned, chain transfer agents terminate the growth of the growing polymer chain by acquiring radical character. This can be achieved by the addition of Co^{2+} species. Industrially, cobalt porphyrins are used, e.g. *bis*(diglyoxamato) cobalt(II). The actual mechanism of chain transfer by such species was finally elucidated in 1981 by Morozova *et al* [3]. A hydride is transferred from the growing polymer chain to the cobalt porphyrin complex to form a cobaltoporphyrin hydride. The cobaltoporphyrin hydride complex then transfers the hydride to an unreacted monomer, hence initiating a new polymer chain, i.e. chain transfer has taken place. This process is illustrated in Scheme 2.1.
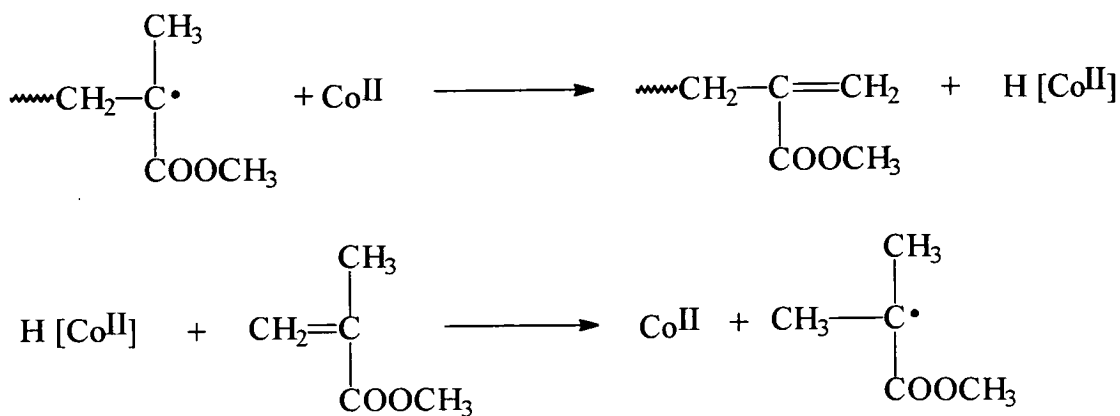
Scheme 2.1: Chain transfer

Pattenden and Bandaranayake[4] also demonstrated that such hydrocobaltoporphyrin species can reactivate oligomers of methyl methacrylate by the sequence of hydrocobaltation-dehydrocobaltation. Figure 2.3 shows hydrocobaltation of a dimer followed by conversion of the organocobalt species to an adduct of styrene, and demonstrates the possibilities for cobalt catalysed reactivation of saturated oligomers.
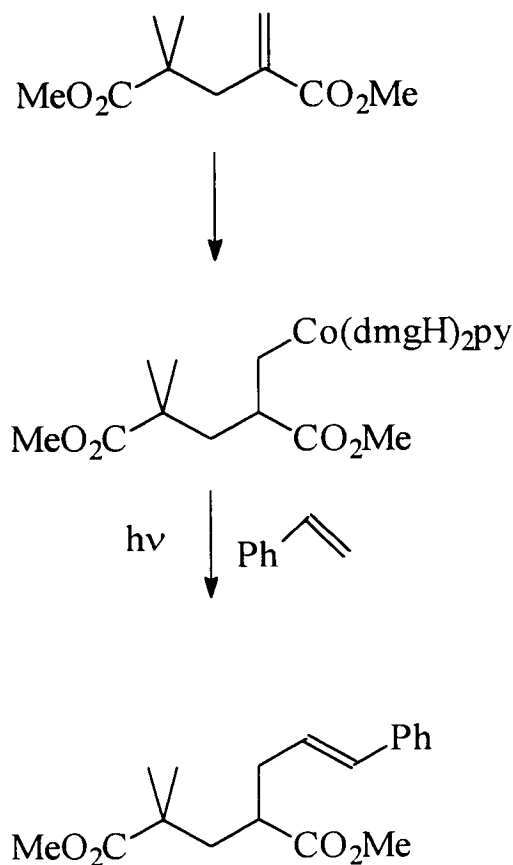

Figure 2.3: Reactivation of unsaturated species by hydrocobaltoporphyrins

Kijima *et al* [5] also reported that alkylcobaloximes catalyse the photoinduced dimerisation of olefins. Because of the role played by cobalt in chain transfer processes, we were also interested in investigating if cobalt alkylidynes would have any effect as chain transfer agents.

Other methods of molecular weight control include:

- introducing species with high chain transfer constants, e.g. mercaptans, chlorinated solvents, etc.

- using an increased level of chain transfer agent.

The solution polymerisations undertaken in this study all produced random copolymers, *i.e.* a polymer which has monomer units distributed in a random manner along the polymer chain; it is defined as a polymer which has properties that are an average of the properties of its constituent homopolymers. Long sequences of monomer units of the same type are not found.

2.2.2 Dispersion polymerisation

A number of processes can be classified under this heading of dispersion polymerisation. In each case the final product consists of a colloidally stable dispersion of polymer particles in a liquid, with particle sizes in the range 100 - 600nm. The polymer particles are referred to as the "disperse phase" and the liquid the "continuous phase". Particles are prevented from flocculating by attaching/adsorbing stabilising groups (such as surfactants) on their surfaces. In the case to be considered here, emulsion polymerisation, the continuous phase is water and the monomer-water mixture is a two-phase system. A surfactant is added to give an emulsion of monomer in water, rather then gross phase separation.

Figure 2.1 [6] shows this method of polymerisation diagramatically
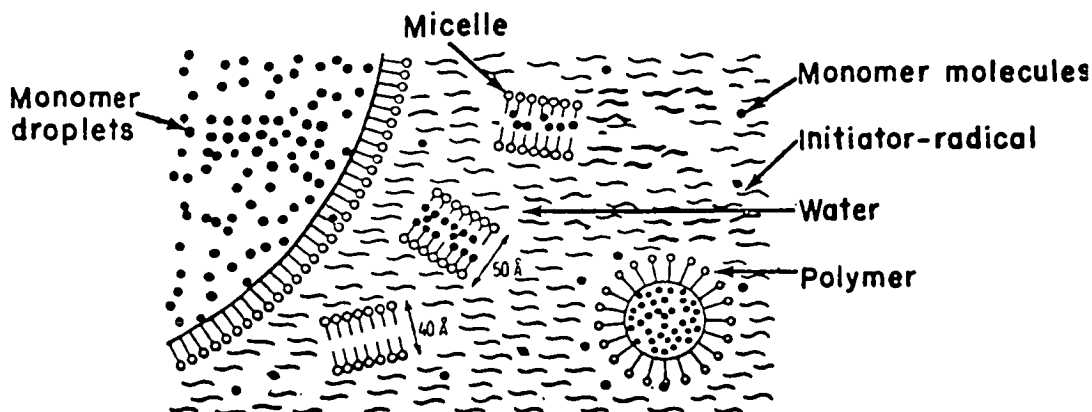
Figure 2.1: Emulsion polymerisation

Commercially, emulsion polymerisation is carried out by a "seed and feed" methodology. This allows high solids (50%) dispersions to be made without large exotherms resulting. In the seed and feed process, 5 - 10% of the monomers are polymerised to give a seed dispersion. The remaining monomers are fed into the seed dispersion over a period of 3 - 5 hours, and the seed particles are grown to large particles.

2.3 Monomer preparation and characterisation

The first problem was to decide which polymerisable functionality could be attached to the apical carbon and subsequently successfully isolated and characterised. This task proved difficult: although synthesis of some unsaturated tricobalt nonacarbonyl derivatives is possible, their isolation is made difficult by their reactivity. For instance, Seyferth *et al* [7, 8] prepared the unsaturated derivatives $HCR=CHCCo_3(CO)_9$, shown in Figure 2.2, by reaction of dicobalt octacarbonyl with the appropriate trihalo compound. However, synthesis of these species was only made possible by using rigorously anhydrous conditions. Due to the instability of many of these derivatives to acidic conditions it was necessary to employ pH 7 silicic

acid for chromatographic separations. Even with these precautions, many attempted unsaturated derivatives were never prepared.
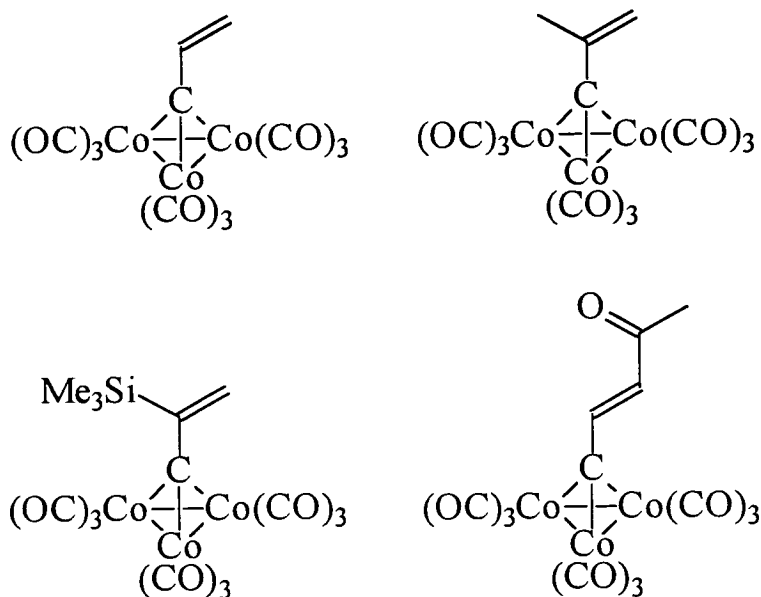
Figure 2.2: Unsaturated species from trihalo compounds

Secondly, the potential monomer would have to be polymerisable by routine methods, and readily form amenable, characterisable polymers. With the chemistry of the apical substituent being limited in scope, and the experimental difficulties encountered by other researchers when preparing unsaturated derivatives of the tricobalt cluster, it was decided that the chemistry of the tricobalt decacarbonyl cation would provide the best route to potential monomers. All that was needed was a suitable nucleophile *i.e.* a nucleophile that also contained a polymerisable functionality. The chemistry of the tricobalt decacarbonyl species is well documented [9], and it is easily prepared (in bulk if necessary) from readily available starting materials. As for a suitable functional group, allyl alcohol is readily available, and contains, in addition to the nucleophilic hydroxyl function, a carbon-carbon double bond. Hence, reaction of the tricobalt decacarbonyl cation with excess allyl alcohol produced μ_3-[(allyloxycarbonyl)methylidyne]tricobaltnonacarbonyl, **(3)**, the preparation of which is shown in Scheme 2.3. No difficulties in the synthesis of this

unsaturated compound were encountered, and it was readily isolated by column chromatography on silica.

$$C\text{-}Cl$$
$$\underset{(CO)_3}{(OC)_3Co\!-\!|\!-\!Co(CO)_3} \quad + \quad 3AlCl_3 \xrightarrow{\ -CO\ } \underset{(CO)_3}{(OC)_3Co\!-\!|\!-\!Co(CO)_3}$$

$C\text{-}CO^+AlCl_4^-$

$$\underset{(CO)_3}{(OC)_3Co\!-\!|\!-\!Co(CO)_3} \quad + \quad HO\diagup\!\!\diagdown\!\!\diagup\!\!/ \quad \longrightarrow \quad \underset{(CO)_3}{(OC)_3Co\!-\!|\!-\!Co(CO)_3}$$
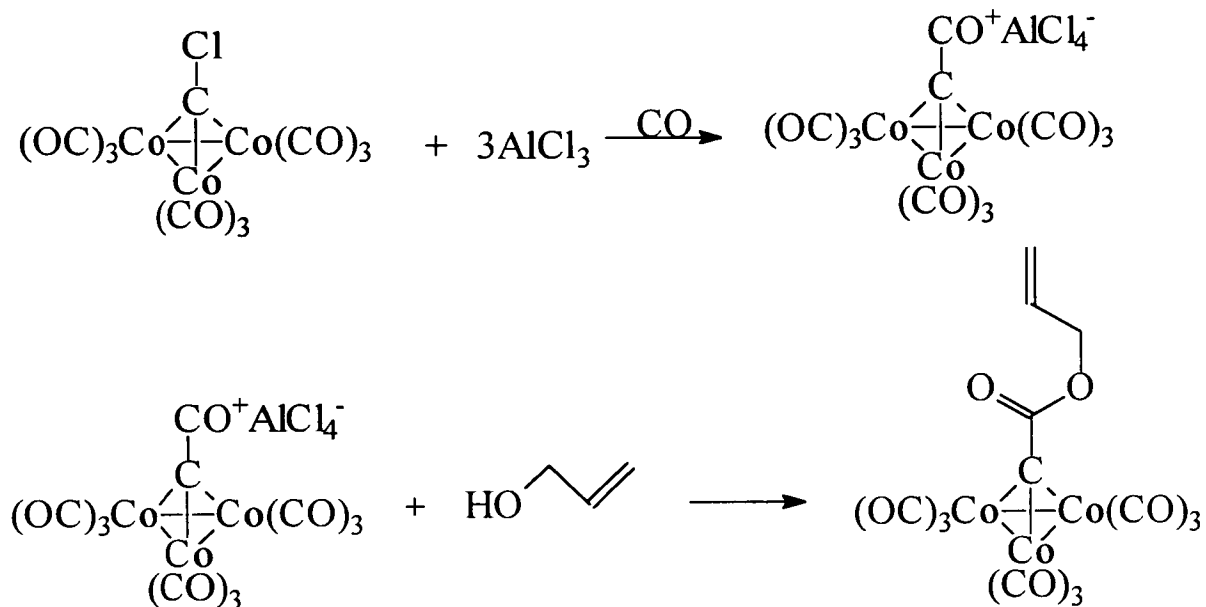
Scheme 2.3: Synthesis of [(allyloxycarbonyl)methylidyne]tricobaltnonacarbonyl, (3)

The corresponding propargyl derivative, (4), where the carbon-carbon double bond is replaced by a carbon-carbon triple bond (figure 2.3), was prepared by an analagous reaction. This derivative, however, was found to be unstable, decomposing to an insoluble brown material in a short time after isolation.
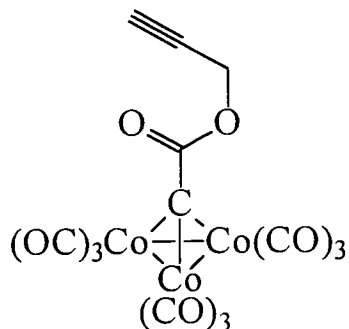
$$\underset{(CO)_3}{(OC)_3Co\!-\!|\!-\!Co(CO)_3}$$

Figure 2.3: [(propargyloxycarbonyl)methylidyne]tricobaltnonacarbonyl (4)

A single crystal of the allyl derivative **(3)** suitable for X ray diffraction was grown by vacuum sublimation. The structure, as determined by the X ray study, is shown in Figure 2.4.
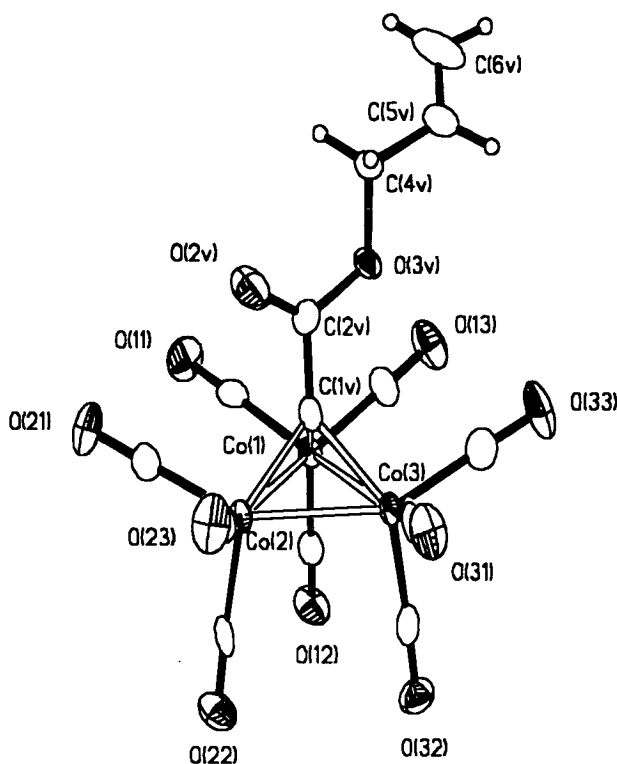
Figure 2.4: The Molecular Structure of [(OC)$_9$Co$_3$(μ_3-CCOOCH$_2$CHCH$_2$)] **(3)**

Significant molecular geometry parameters are Co(1)-Co(2) 2.475(2), Co(1)-Co(3) 2.473(2), Co(2)-Co(3) 2.469(2), Co(1)-C(1v) 1.897(4), Co(2)-C(1v) 1.873(4), Co(3)-C(1v) 1.904(4), C(1v)-C(2v) 1.479(5), C(2v)-O(2v) 1.203(5), C(2v)-O(3v) 1.337(4), O(3v)-C(4v) 1.456(4), C(4v)-C(5v) 1.471(5), C(5v)-C(6v) 1.305(6)Å; Co(1)-Co(2)-Co(3) 60.03(6), Co(2)-Co(1)-Co(3) 59.86(5), Co(1)-Co(3)-Co(2) 60.11(5), Co(1)-C(1v)-C(2v) 131.0(3), Co(2)-C(1v)-C(2v) 130.3(3), Co(3)-C(1v)-C(2v) 131.7(3), C(1v)-C(2v)-O(2v) 123.8(3), O(2v)-C(2v)-O(3v) 123.1(3), C(1v)-C(2v)-O(3v) 113.0(3), C(2v)-O(3v)-C(4v) 116.3(3), O(3v)-C(4v)-C(5v) 108.4(3), C(4v)-C(5v)-C(6v) 124.7(4)°.

The structure determination of the allyl derivative **(3)** (Figure 2.4) shows a Co$_3$(CO)$_9$C fragment similar to that observed in a large number of related derivatives with C_3 symmetry and bound symmetrically to C(1v), the first atom of the -C-C(=O)-O-CH$_2$-CH=CH$_2$ substituent chain. A search of the Cambridge Structural Database showed that the internal molecular geometry of this chain differs very little from that

found in the small number of organic compounds which contain the substituent. The most striking differences affect the C(1v)-C(2v) and C(5v)=C(6v) distances of 1.479(5) and 1.305(6) respectively. However, these values lie close to those found in bis[(μ_2-chloro)(allylacetato-O)trichlorotitanium(IV)] [10]. The chain adopts a *trans-trans-gauche* conformation about C(2v)-O(3v) and O(3v)-C(4v): the torsion about C(4v)-C(5v) is such that C(6v) eclipses one of the methylene H atoms on C(4v).

The established solid phase structure is entirely consistent with the spectroscopic data reproduced in Figure 2.5.
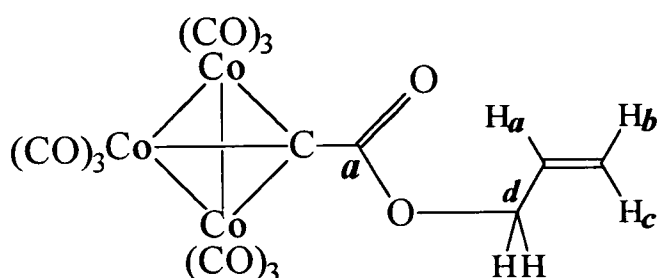
		$\delta\,^1H\,/\,ppm$
a		5.93 - 6.12, m, 1H
b		5.26, dd, 1H,
		J_{cis} = 18.8Hz
		J_{gem} = 1.27Hz
c		5.37, dd, 1H,
		J_{trans} = 10.3Hz,
		J_{gem} = 1.27Hz
d		4.77 - 4.81, m, 2H

Figure 2.5: ^{1}H NMR data for [(allyloxycarbonyl)methylidyne]tricobaltnonacarbonyl (3)

58

FAB mass spectroscopic data, and infra red data consistent with the solid phase structure were also obtained.

However, consultation with I. C. I. Paints revealed that allyl compounds are not as readily polymerised as acrylates due to the lower reactivity of the allyl double bond due to allylic stabilisation of the first formed radical. An alternative nucleophile which fitted the same criteria was sought. The corresponding vinyl derivative would have been ideal for such polymerisation, but as vinyl alcohol is not available, an alternative was needed. 2 -hydroxyethylacrylate (Figure 2.6) is readily available, and has the added advantage that, being an acrylate, free radical polymerisation should be relatively straight forward, unless the cluster was able to impart some steric or electronic effect on the acrylate group. This was not expected to be a problem however, given the distance of the cluster from the acrylate group and the nature of the chemical link between them.
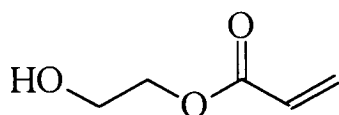
Figure 2.6: 2-hydroxyethylacrylate

The synthesis of μ_3-[(ethylacrylylcarboxy)methylidyne] tricobalt nonacarbonyl (5) proved to be straightforward- no problems were encountered with the synthesis (outlined in Scheme 2.4), nor in the isolation of the product.
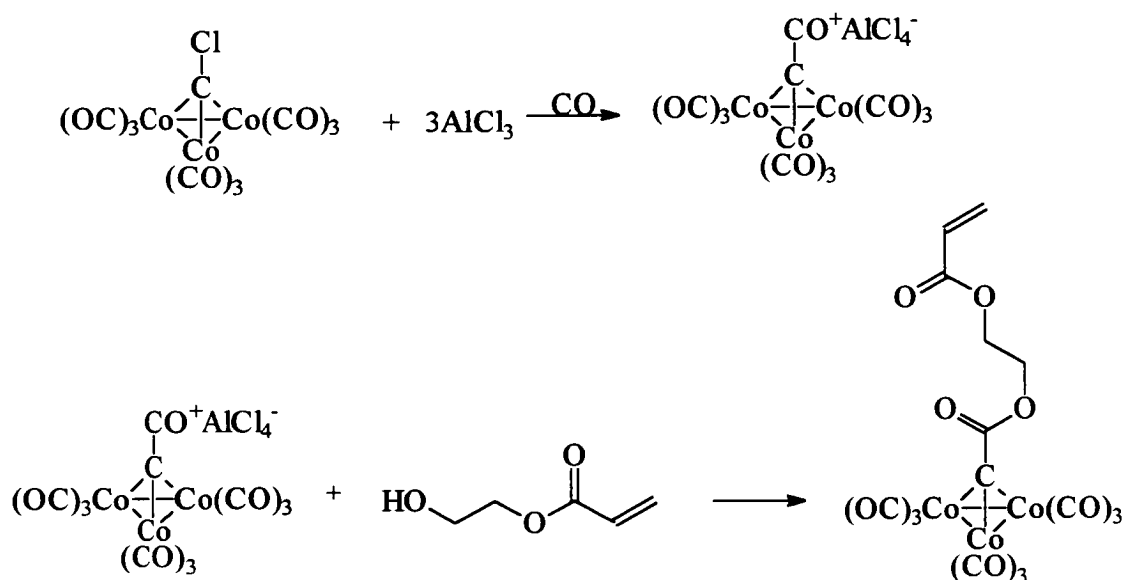
Scheme 2.4: Synthesis of

μ_3-[(ethylacrylylcarboxy)methylidyne]tricobaltnonacarbonyl (5)

Separation by column chromatography on silica, eluting with hexane and dichloromethane, proved to be ideal, with no saturated by-products detected. However, the monomer was found to undergo decomposition, to products as yet unidentified, when stored under argon or nitrogen in the freezer for extended periods. Also, samples in solution were found to decompose rapidly. However, this did not preclude studies involving solutions of the compound; infrared and excellent ^{1}H and ^{13}C NMR spectra were obtained. As anticipated, due to the long, flexible nature of the ethyl acrylate apical substituent, the acrylic compound (5) is a purple liquid, hence characterisation by X ray diffraction was not possible. The ^{1}H and ^{13}C data from these experiments is reproduced below in Figure 2.7.

60

Figure 2.7: ^{1}H and ^{13}C NMR data for cluster monomer (5)
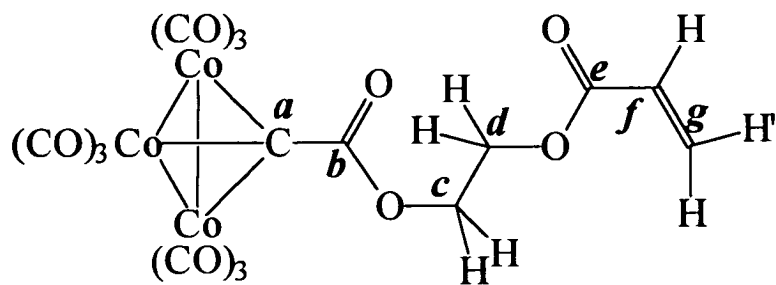
	$\delta\,^1H\,/\,ppm$	$\delta\,^{13}C\,/\,ppm$
a	-	178.5
b	-	170.0
c	4.54, m, 2H	63.5
d	4.44, m, 2H	62.6
e	-	165.8
f	6.05, dd, 1H	
	J_{cis}=17.2 Hz	128.2
	J_{trans}=10.4 Hz	
g	H: 6.38, dd, 1H	
	J_{trans}=10.4 Hz	
	J_{gem}=1.6 Hz	130.9
	H': 5.80, dd, 1H	
	J_{cis}=17.2 Hz	
	J_{gem}=1.6 Hz	
Co(*C*O)	-	199.0

2.4 Homopolymerisation

Initial reactions of the monomer using free radical homopolymerisation induced by azo[*bis*(isobutyronitrile)] (AIBN) led to insoluble purple solids. Due to the insolubility of the sample, analysis of the solid proved inconclusive. All that could be determined *via* infrared spectroscopy (as a nujol mull) was that the species did

contain terminal metal carbonyl species. Difficulties have been encountered before during homopolymerisation of organometallic vinyl monomers [11]. This may have been due to the choice of radical initiator, the conditions employed (in particular the radical flux), or the nature of the homopolymer formed. Therefore it was decided to copolymerise the monomer with other acrylic monomers.

2.5 Free radical initiator choice

Historically, textbooks on polymer science have almost always quoted AIBN as the source of free radicals for radical induced polymerisation (Scheme 2.5). One molecule of AIBN decomposes thermally to produce two primary radicals and dinitrogen.
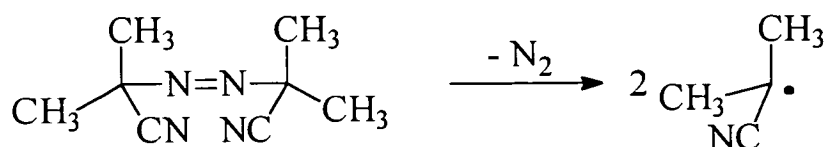
Scheme 2.5: AIBN initiation

However, AIBN is only sparingly soluble in organic solvents, and this leads to problems, as it is preferable to add the initiator to the reaction as a solution over the course of the reaction, to maintain a steady radical flux. As radical flux is one of the factors which governs molecular weight of the polymer produced, it is important that the rate of addition is controllable. Also, in the case of organometallic monomers, it is essential to ensure that the monomer is not destroyed by excess radicals reacting with the metal centre, oxidising the metal atom and therefore decomposing the monomer.

Dow Chemical Company supply variants of AIBN which are made more soluble by altering the length and branching of the alkyl side chain. This also affects the radical flux and half life, but the benefits gained from solubility far outweigh any

reduced flux or half life. It was therefore decided to employ Vazo67, [2,2'-azo *bis*(methylbutyronitrile] (Figure 2.8), as the initiator, which is soluble in methoxypropanol which was used as the solvent. Vazo is the Dow Chemical Company's trade name for this family of azo compounds, and the number refers to the Celsius temperature at which the half life in solution is ten hours.
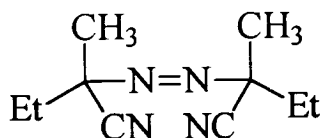
Figure 2.8: VAZO67, azo initiator

2.6 Solution polymerisation of monomer

Solution polymerisation reactions were carried out by the continuous feed method: monomers and a solution of initiator were fed into a stirred, heated reaction flask charged with solvent, purged with nitrogen and fitted with a double surface condenser and a temperature probe. Due to the previously described instability of the cluster monomer, samples were stored under argon at -78°C and purified by column chromatography immediately prior to use. The feedstocks were added to the reaction flask at known rates of addition by peristaltic pumps, over a period of 2 hours. The temperature of the reaction was controlled *via* a thermocouple attached to the heating mantle, hence the exotherm from the polymerisation reaction was safely controlled.

Initial experiments under reflux (at 120°C) led to cluster decomposition- the characteristic purple colour of the cluster being replaced with a murky grey solution of unidentified cobalt species, with no characteristic metal-carbonyl bands in the infrared spectrum. The reaction was repeated at a lower temperature, despite the effect this would have on the radical flux and hence the rate of reaction and overall yield of polymer.

63

By carrying out the reaction at 60°C, thermal decomposition of the metal carbonyl was avoided, and a purple solution resulted. Infra red spectroscopy showed that the metal carbonyl unit was intact . However, infrared evidence on its own does not prove conclusively that the cluster is covalently attached to the polymer backbone. There remained the possibility, however remote, that the cluster species was merely present, unattached to the polymer, in a solution of polymer and solvent. Therefore, it was necessary to devise an experiment that would prove that the cluster was covalently attached to the polymer molecule. This was achieved by Gel Permeation Chromatography (GPC) with UV/VIS detection. GPC is a form of chromatography which separates molecules (in particular macromolecules) by molecular size- the heaviest components of the mixture being eluted from the column first. Small molecules are able to diffuse through the pores of the column packing more efficiently, and hence they travel through the column more slowly. Higher molecular weight species are thus eluted first [12]. Detection of polymer fractions in the eluant is most commonly accomplished with refractive index or spectroscopic (ultra violet and infrared) detectors. The major problem with calibrating a GPC column for a particular polymer is that few standard samples of narrow molecular weight distribution are available commercially. Narrow molecular weight distribution polystyrene standards are used to calibrate the column. However, when dealing with a polymer other than polystyrene, the molecular weights thus obtained are at best approximate. For the purpose of this study though, more important was the information gained from the refactive index and the UV-VIS chromatograms.

Hence by using GPC, it was possible to separate the individual molecular weight polymer chains and simultaneously obtain a molecular weight profile of the polymer mixture. By allowing the eluting solution to pass through a UV-VIS detector, it was also possible to check for the presence or absence of the cobalt cluster unit in the polymer molecules eluted. Using this technique, it was possible to determine that the polymer (6), produced by copolymerising the cluster monomer, $^{n\text{-}}$butyl acrylate and methyl methacrylate in the ratio 10 : 72 : 118 (by weight) had an average molecular weight of 28931 daltons, and a peak molecular weight of 24180

daltons (relative to a polystyrene standard). The GPC data for this polymer is reproduced below in Figure 2.9. The molecular weight profile can be clearly seen
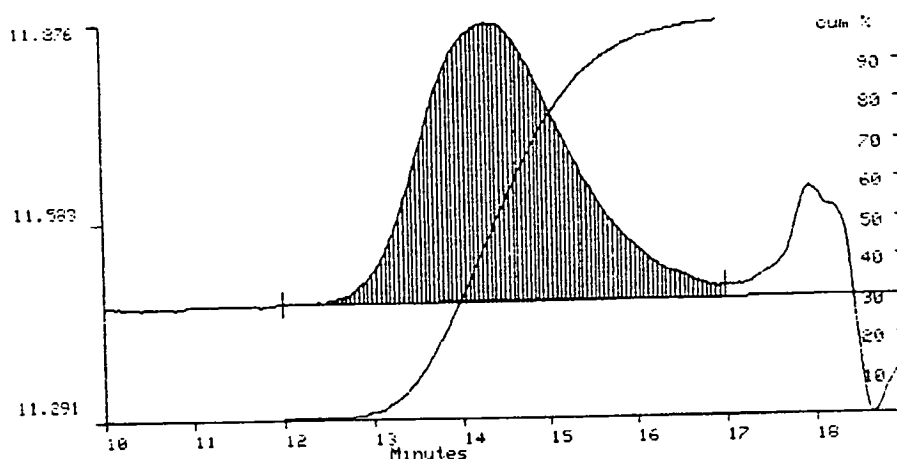
Molecular Weight Distribution Averages

Weight Average	28391	Number Average	11315
Z Average	53070	Dispersivity	2.509
Viscosity Average	28391	Intrinsic Viscosity	0.000
Z + 1 Average	86892	Peak Mol Weight	24180
Mz / Mw	1.869	Mz+1 / Mw	3.061

Figure 2.9: GPC for solution polymer **(6)** containing cobalt alkylidyne

The peak eluting between 12 and 17 minutes is polymeric and it was hoped that a UV-VIS chromatogram obtained at 500 nm would confirm the presence of the cobalt species. However, this signal at 500 nm was very noisy. For this reason, 300 nm, a wavelength no quite as specific as 500 nm, was monitored. As can be seen in Figure 2.10, the overlay of the chromatogram at 230 nm with that obtained at 300 nm confirms that the signal due to the cobalt species is in line with the bulk polymer distribution. The peak eluting at retention time 19 minutes shows no absorbance above 240nm and is thought to be solvent. The retention time and the UV spectrum of the peak at 17.4 minutes confirm this to be a non polymeric cobalt alkylidyne containing species.

Figure 2.10: UV-VIS chromatogram for solution polymer (6)

Hence the random copolymer formed contained the tricobalt nonacarbonyl group, and has the general structure as depicted in Figure 2.11.
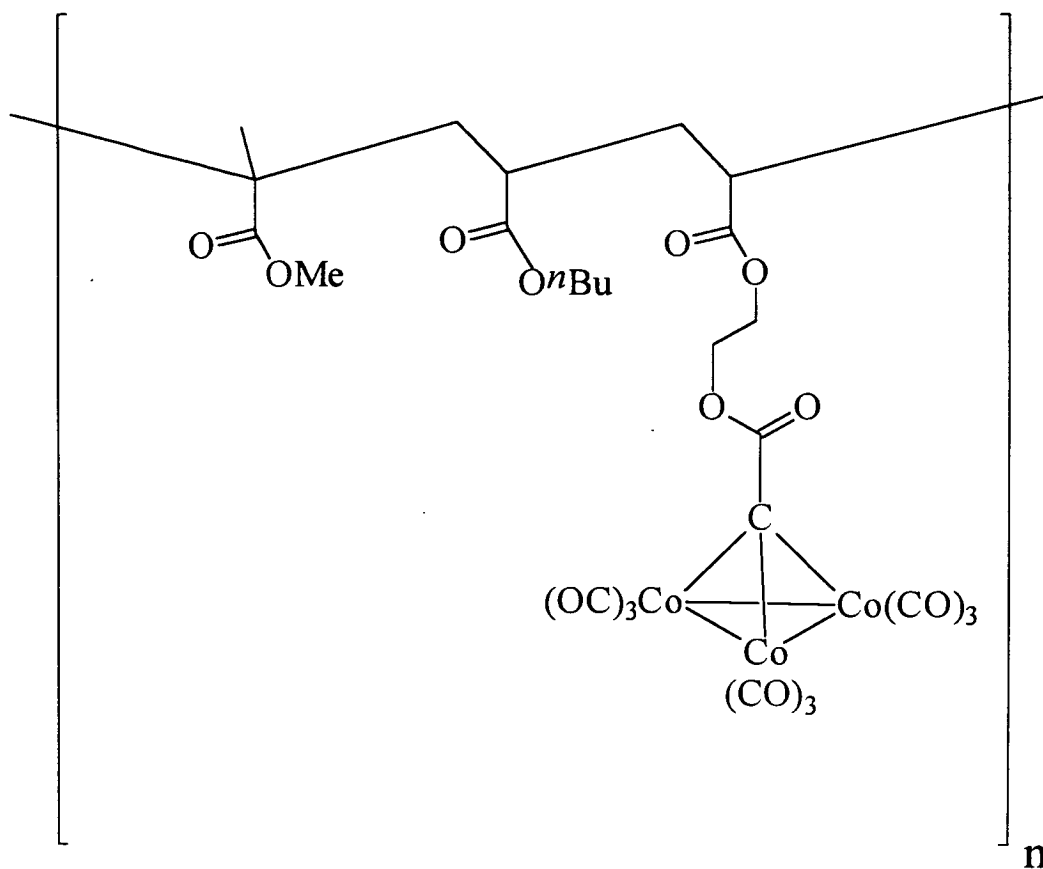
Figure 2.11 : Solution random copolymer (6) incorporating tricobalt clusters

The polymer was also extracted from the solution by precipitation. Upon addition of methanol to the polymer solution, a purple solid was obtained. GPC analysis for the precipitated species showed only the polymeric cobalt containing species present (Figure 2.12).
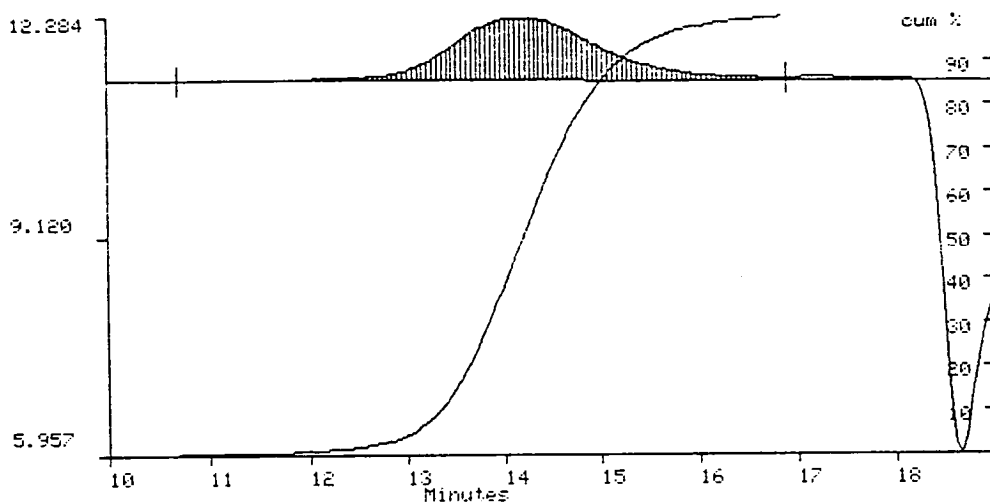
```
Molecular Weight Distribution Averages

Weight Average        40345      Number Average      15822
Z Average            150051      Dispersivity         2.550
Viscosity Average     40345      Intrinsic Viscosity  0.000
Z + 1 Average        589001      Peak Mol Weight      27937
Mz / Mw                3.719     Mz+1 / Mw           14.539
```

Figure 2.12: GPC trace for precipitated polymer

GPC/UV-VIS chromatography also confirmed the presence of only a cobalt containing polymer. As can be seen in Figure 2.13, only one peak is present at 230 and 300nm.

Figure 2.13: UV-VIS chromatogram of precipitated polymer
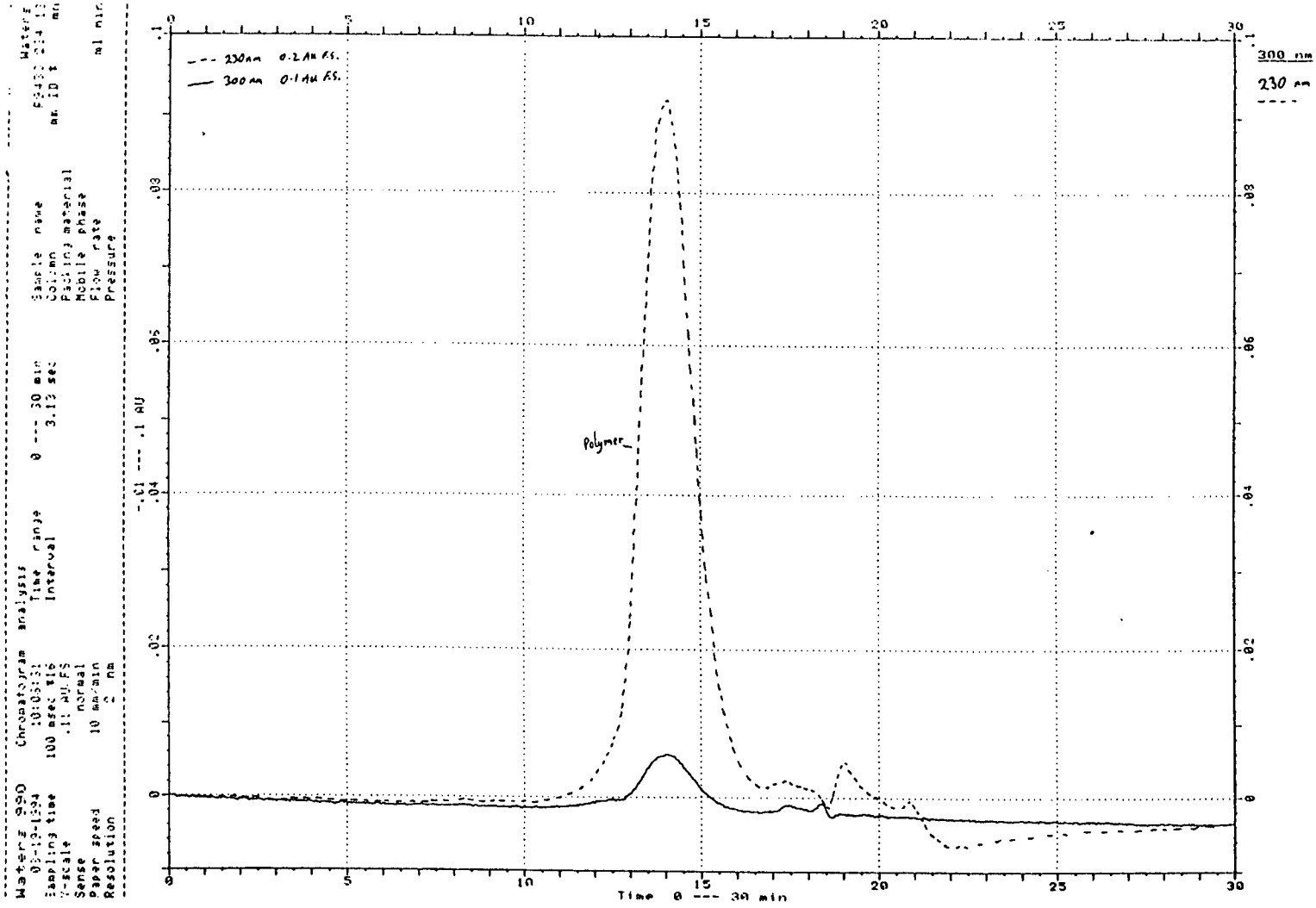
GPC analysis on the methanolic solution showed the absence of any polymeric species (Figure 2.14).
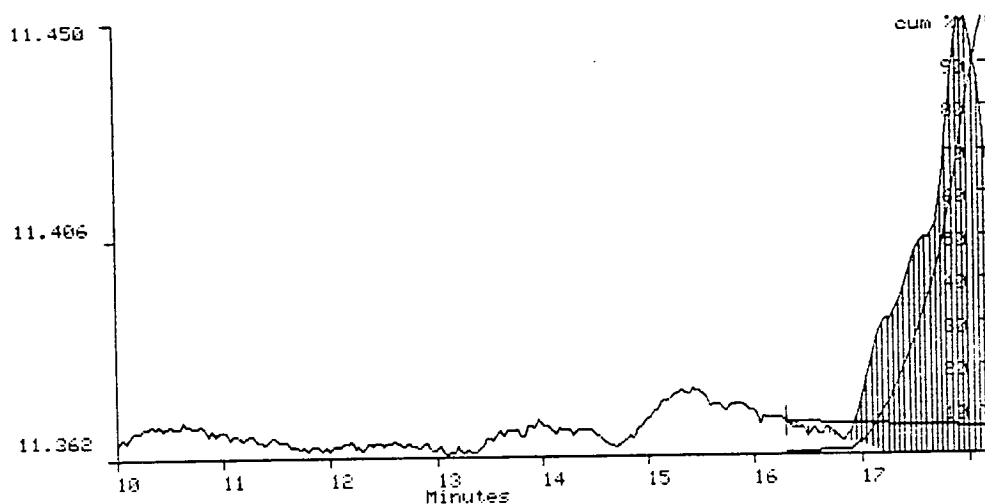
Molecular Weight Distribution Averages

Weight Average	431	Number Average	370
Z Average	527	Dispersivity	1.163
Viscosity Average	431	Intrinsic Viscosity	0.000
Z + 1 Average	681	Peak Mol Weight	301
Mz / Mw	1.224	Mz+1 / Mw	1.581

Figure 2.14: GPC trace for non precipitated species

The UV-VIS chromatogram in Figure 2.15, although noisy, does show the presence of a small amount of polymeric material. However, the bulk of the sample is mainly an unpolymerised cobalt species and solvent.

Figure 2.15: UV-VIS data for non precipitated species

71

The solution polymer was also spread as thin films on a glass substrate, and were quite stable under ambient conditions for some months.

Because of the lower temperature of reaction, the yield of polymer was considerably lower than would be expected. In this case 10.8% conversion from monomer to polymer, compared to a more usual figure in the region of 53%. (for a polymer produced at 120°C, incorporating 2-hydroxyethylacrylate instead of the cluster monomer.) Conversion yields are the percentage solids left (*i.e.* non volatile material, polymer) in the sample after evaporation of solvent and unreacted monomers has taken place in an oven. It was also thought that some breakdown of the cluster was promoting chain transfer (*vide supra*), which would lead to a lower yield of polymer.

It was initially hoped that chain transfer was being promoted by the intact cluster; however, polymerisation reactions under the same conditions in the presence of 320ppm cobalt (as methylidynetricobalt nonacarbonyl, $[(OC)_9Co_3(\mu_3\text{-}CCH)]$), showed no evidence of chain transfer. Hence, it was concluded that the reaction was either being modified by cluster breakdown products (i.e. ionic cobalt species) or, more probably, the lower reaction temperature was affecting the yield. Other initiators were tried in an attempt to improve the conversion- use of 1% *tert*-butyl ethyl perhexanoate as an initiator gave a conversion to polymer of only 2.6%. However, using an ammonium persulphate / ascorbic acid redox couple (1%) increased the percentage conversion to 21.7%.

2.7 Emulsion polymerisation

It was therefore decided to employ emulsion polymerisation in an attempt to increase the yield of polymer containing the cluster moiety. Emulsion polymerisation also produces much higher molecular weight polymeric species.

Using a water / surfactant solvent system, a seed shot of monomer and a seed shot of initiator was introduced to the reaction vessel, to produce an initial seed polymer which could then act as an initial building block for the bulk polymer. The initiator system employed was a redox couple consisting of *tert*-butyl hydroperoxide, ammonium persulphate and sodium metabisulphate. The presence of the seed polymer was confirmed by analysing the particle size distribution of the reaction mixture after heating the seed mixture to 60°C for 10 minutes. Once it had been confirmed that polymerisation was indeed occurring, the remaining monomer and initiator feedstocks were slowly added to the reaction vessel *via* an array of peristaltic pumps. It should be noted that during this polymerisation reaction, some homopolymerisation of the cobalt alkylidyne species was observed. An insoluble, purple solid was formed on the surface of some of the apparatus. No analysis of this solid was possible due to its insolubility, however it was virtually identical in form to the solid produced by AIBN initiated homopolymerisation of the monomer.

At the end of the polymerisation process, particle size analysis showed that the polymer particles were between 100 and 200 nm, with an average size of 120nm

GPC/UV-VIS of the resultant emulsion polymer (or latex) (7) was then undertaken. The sample was prepared by diluting the polymer emulsion with THF to a concentration of 0.5% and then filtering through a 0.45μm PTFE membrane. Figure 2.16 shows the molecular weight distribution from the GPC experiment, as detected by a refractive index detector.
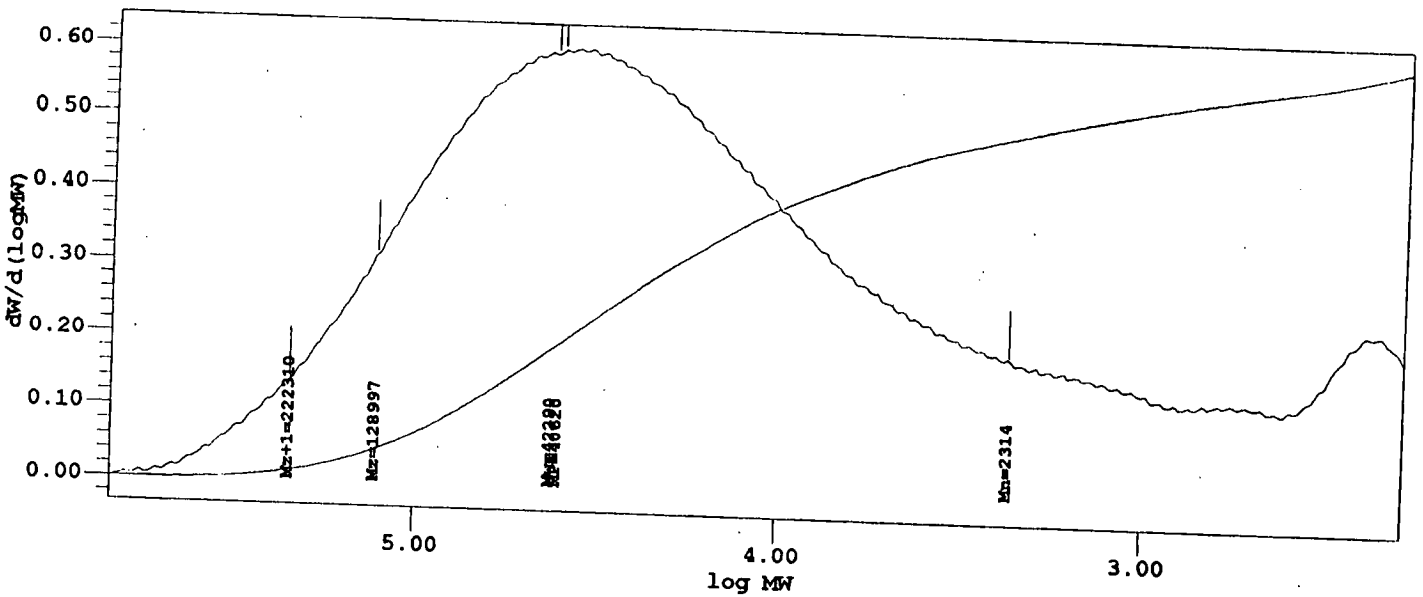
Figure 2.16 : GPC trace for emulsion polymer (7)

integration events

#	Channel Descr.	Baseline Start (min)	Baseline End (min)
1	Perkin Elmer	9.250	20.433
2	Perkin Elmer	9.250	20.433

Mol. Weight Averages

#	Mn	Mw	Mz	Mw/Mn
1	2314	42290	128997	18.27
2				

This signal can be compared, as before, to the UV-VIS signal as monitored at 230 and 300nm, reproduced in Figure 2.17.
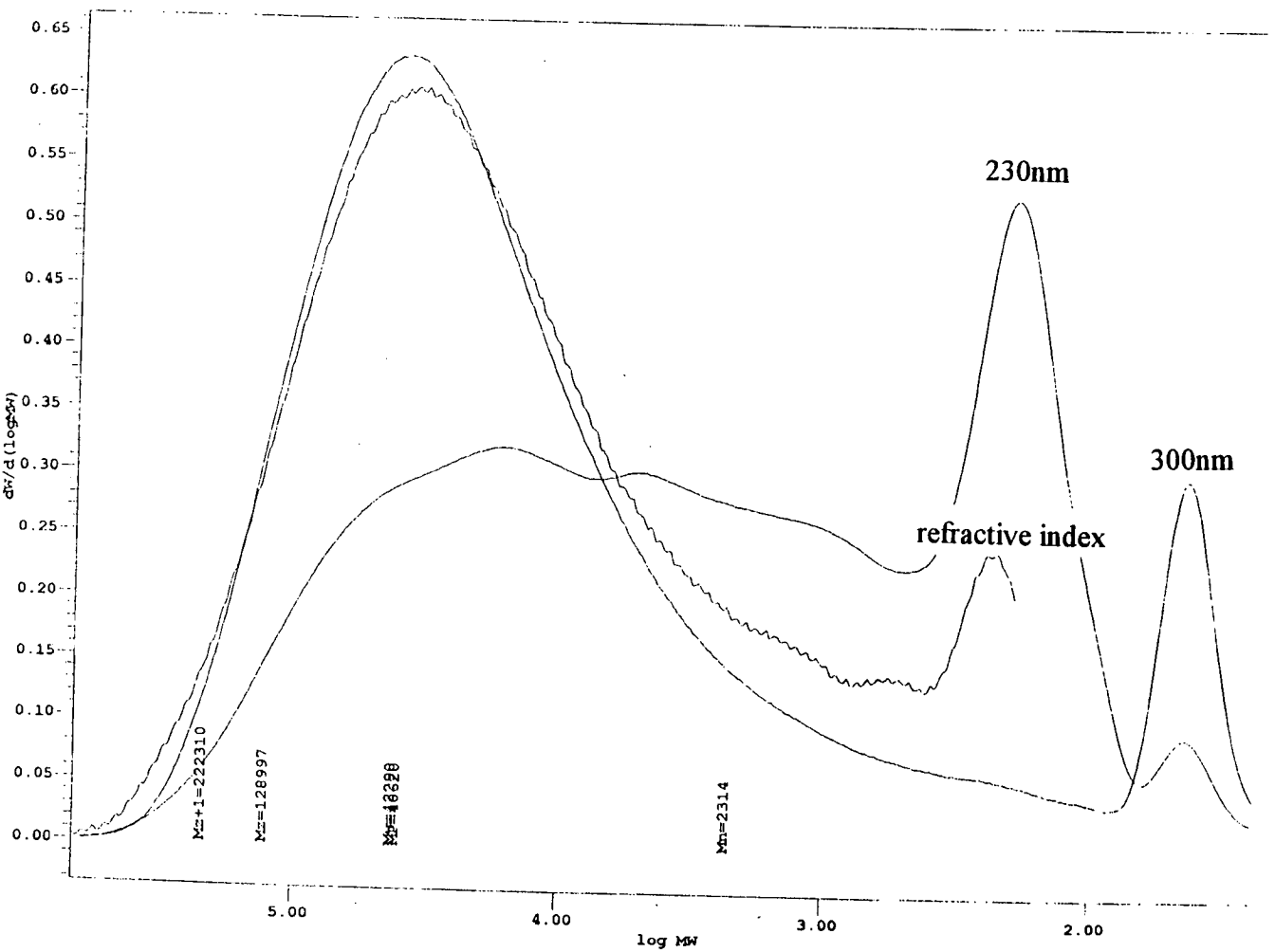
Figure 2.17: UV-VIS chromatogram for emulsion polymer (7)

Little difference can be seen between the distribution obtained at 300nm and that obtained from the refractive index. The conclusion drawn from these data is that if the cobalt alkylidyne is the only species present which absorbs at 300nm then this would indicate the inclusion of the cobalt alkylidyne into the polymer. The

chromatogram obtained at 230nm does show some differences to both the refractive index and the 300nm chromatogram. This is thought to be due to the presence of a higher degree of unsaturation in the lower half of the distribution[13]. It can be seen from the chromatograms that the molecular weight distribution varies from *ca.* 230,000 daltons to 2000 daltons, with a peak molecular weight of 42290 daltons, Therefore, as predicted, the emulsion polymer has a higher molecular weight than the solution polymer. The percentage yield was also greater, in this case 39.94% compared to 10.8% for the species prepared by solution polymerisation. Infrared spectroscopy of the latex also confirmed the presence of the cobalt cluster, with the characteristic v_{CO} signals in the terminal carbonyl region as for the initial monomeric cluster species.

The molecular weight data for the polymers prepared by solution and emulsion polymerisation is reproduced in Table 2.1.

	solution polymer (5)	pptd. polymer	emulsion polymer (6)
Weight average	28391	40345	42290
Z average	53070	150051	128997
Number average	11315	15822	2314
Peak mol. weight	24180	27997	40620

Table 2.1: Molecular weight data (in daltons) for acrylic copolymers containing the tricobalt alkylidyne nonacarbonyl unit

2.8: Catalytic evaluation of cluster species

The polymers synthesised were evaluated as potential catalysts for the cross linking reaction of alkyd polymers As highlighted in chapter one, autoxidation of a carbon carbon double bond results in the formation of a hydroperoxide. The

subsequent decompostion and radical coupling reactions produce a cross linked polymer network and hence a stable film containing saturated carbon species is formed from the unsaturated starting polymer. The initial autoxidation step and the decomposition of the hydroperoxide is catalysed by cobalt species, as previously noted. For these experiments to evaluate the catalytic activity (if any) of organocobalt cluster species, the same amount of catalyst (expressed in weight of cobalt metal) was used of each species. Currently, cobalt octoate is used, the amount employed being 0.05% Co metal per gram non volume polymer

To measure the time taken for the drying reaction (and hence the activity of the catalyst), two methods are currently employed by I.C.I. Paints.

2.8.1 BK Dry

A needle is dragged through the polymer film over a period of twenty two hours: When the polymer film is dry, the needle no longer leaves a mark on the film. The time taken for the film to dry can be read off the precalibrated scale. The BK Dry measures the time taken for complete film drying- the needle will leave a mark in the film unless the entire polymer film is dry, *i.e.* from the surface of the film through to the side of the film adhered to the substrate.

2.8.2 Sand Dry

A hopper filled with sand is drawn over the drying polymer film over a period of ten hours. Sand sticks to the un-dried (and therefore adhesive) polymer film, whereas the sand will not adhere to the dried film. Removing the excess sand by inverting the substrate "develops" the trace. The time taken for the film to dry can be seen from the precalibrated scale. The Sand Dry measures time taken for surface of film to dry- once the the surface of the film is dry, even if the bulk of the film is not dry, the sand will not adhere to the polymer film.

In both techniques the sample preparation is the same. The polymer to be dried and the catalyst are mixed well, before a film of known thickness is applied to a glass substrate by using a 100μm blockspreader.

The polymer to be dried was an alkyd condensation polymer of phthalic anhydride, pentaerythritol and soya bean oil. Unsaturation in the triglyceride's side chains provide the active sites for cross linking. The synthesis of the alkyd polymer is described in the experimental section (Chapter 5).

Several cluster species were evaluated using both the BK Dry and Sand Dry techniques: as control standard and benchmark, polymer samples were also monitored which contained (i) no cobalt species, and (ii) the standard catalyst used for this reaction, cobalt octoate. The results of experiments are summarised in table 2.2.

Cobalt species	%Co in species	Sand Dry / hours	BK Dry / hours
none	0	>10	>22
Co(octoate)	10[a]	2	7
$(CO)_9Co_3(\mu_3\text{-CH})$ (8)	40.01	>10	>22
$(CO)_9Co_3(\mu_3\text{-CCl})$ (1)	37.11	>10	>22
solution polymer supported cluster (5)	1.5[b]	>10	>22

a: as a solution of 10% Co (as Cobalt Octoate)

b: 5% cluster in polymer, monomer contains 30.27% Co;
      assuming 100% incorporation as polymer, polymer contains 1.5% Co

Table 2.2: Drying times for alkyd polymer crosslinking

As can be seen from Table 2.2, none of the cluster species catalysed the cross linking reaction- with all the cluster species recording the same result as for the sample with no added cobalt species. This is not surprising considering the proposed mechanism of the catalytic reaction. To catalyse the reaction the redox system in Scheme 2.18 has been proposed[1].

$$ROOH + Co^{2+} \longrightarrow RO^{\bullet} + OH^- + Co^{3+}$$

$$ROOH + Co^{3+} \longrightarrow ROO^{\bullet} + H^+ + Co^{2+}$$

Scheme 2.18: catalytic decomposition of hydroperoxide

The cobalt cluster species contain cobalt in oxidation state zero, and would therefore be unlikely to undergo the oxidation and reduction processes required to catalyse the hydroperoxide decomposition.

2.9: Chemical modification of polymer networks

As outlined in Chapter One, metal containing polymer systems can also be prepared by modification of an existing polymer network. Previous examples of such modifications have employed polymers with pendant phosphine[14, 15, 16] or cyclopentadienyl[17-24] groups. The metal species is then attached to the polymer backbone *via* the phosphine or cyclopentadienyl group. A previous study in this area by Patin[11] focused on using pendant groups which would react with dicobalt octacarbonyl to produce the trinuclear cluster *in situ* (Scheme 2.19).
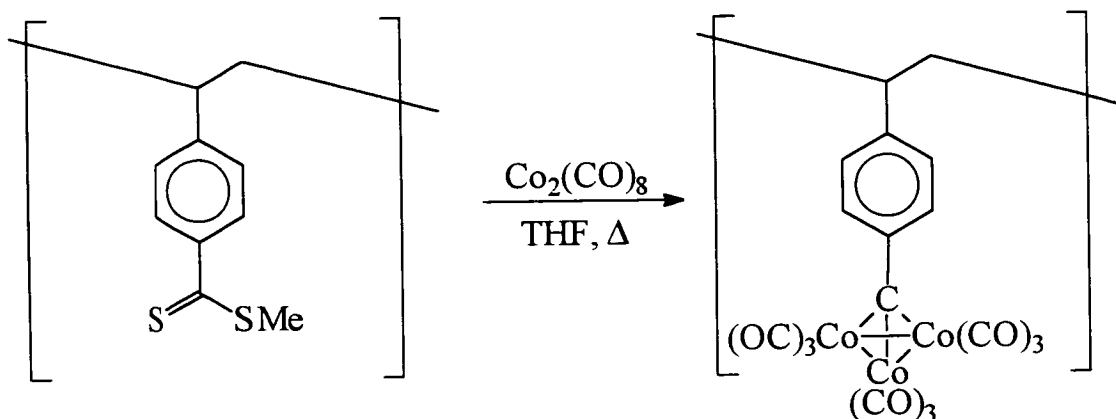
Scheme 2.19: polymer modification

The alternative to this method of synthesis is to attach the preformed trinuclear cluster species to the polymer. It was proposed that a polymer with a pendant nucleophilic function (10) would be able to combine with the electrophilic tricobalt decacarbonyl cation (11) and hence produce a polymer containing the cluster unit. This synthetic route would produce the same polymeric species as prepared by polymerising the organcluster monomer, and comparisons could thus be made between the two routes. Furthermore, by knowing the stoichiometry of the polymeric substrate, GPC data would indicate how many of the nucleophilic sites had been attacked, and the molecular profiles of unreacted and reacted polymer species would be easily compared. It was decided that a hydroxyl functionality would be most suitable to introduce as the pendant nucleophilic group.

Hence, a series of copolymers of methyl methacrylate and *n*-butyl acrylate which contained 5% of 2-hyroxyethyl acrylate were produced by free radical induced polymerisation of the monomers. By varying the relative amount of methyl methacrylate and *n*-butyl acrylate, the series of polymers produced had various glass transition temperatues, T_g. By adding chain transfer agents to some of the reaction mixtures, different molecular weight distributions were also prepared.

A sample of solution of polymer was then evaporated to dryness on a high vacuum line, to remove solvent and any unreacted monomers. This polymer was then

redissolved in dichloromethane, and then added *via* cannula to a suspension of $[(OC)_9Co_3(\mu_3\text{-}CCO)]^+$ PF_6^-, which had been freshly prepared by the addition of 60% HPF_6 in water, to a solution of $[(OC)_9Co_3(\mu_3\text{-}CCOOEt)]$ **(2)** in propionic anhydride. This affected an immediate colour change from brown to the ubiquitous purple colour associated with alkyl derivatives of the tricobalt alkylidyne cluster. After stirring overnight, any excess $[(OC)_9Co_3(\mu_3\text{-}CCO)]^+$ PF_6^- was destroyed by addition of methanol. The polymer was then analysed by GPC and the molecular weight distribution was compared to that of the unmodified polymer. The result of these experiments are shown in Table 2.3

$T_g/$ °C	Mn	Mn'	Mw	Mw'	Mz	Mz'	Mp	Mp'
-20 (10a)	3078	1615	5950	4418	9214	7376	6076	5416
20 (10b)	3450	2297	7072	6587	11139	11562	6860	6602
60 (10c)	3414	1402	9801	8871	19703	23727	8316	8871

Mn = number average, Mw = weight average,

Mz = Z average, Mp = peak molecular weight,

all molecular weights are expressed in daltons

Table 2.3: GPC Data for unmodified and modified (') polymers

These results are not as expected. As can be seen from the table, most of the modified polymer species are lighter in molecular weight than the unmodified species- the opposite of the expected result. The conclusion from these data is that the polymer is degrading upon exposure to some species in the reaction mixture. Most likely this is due to hydrolysis of the ester functionalities by HPF_6, as proposed in Scheme 2.20
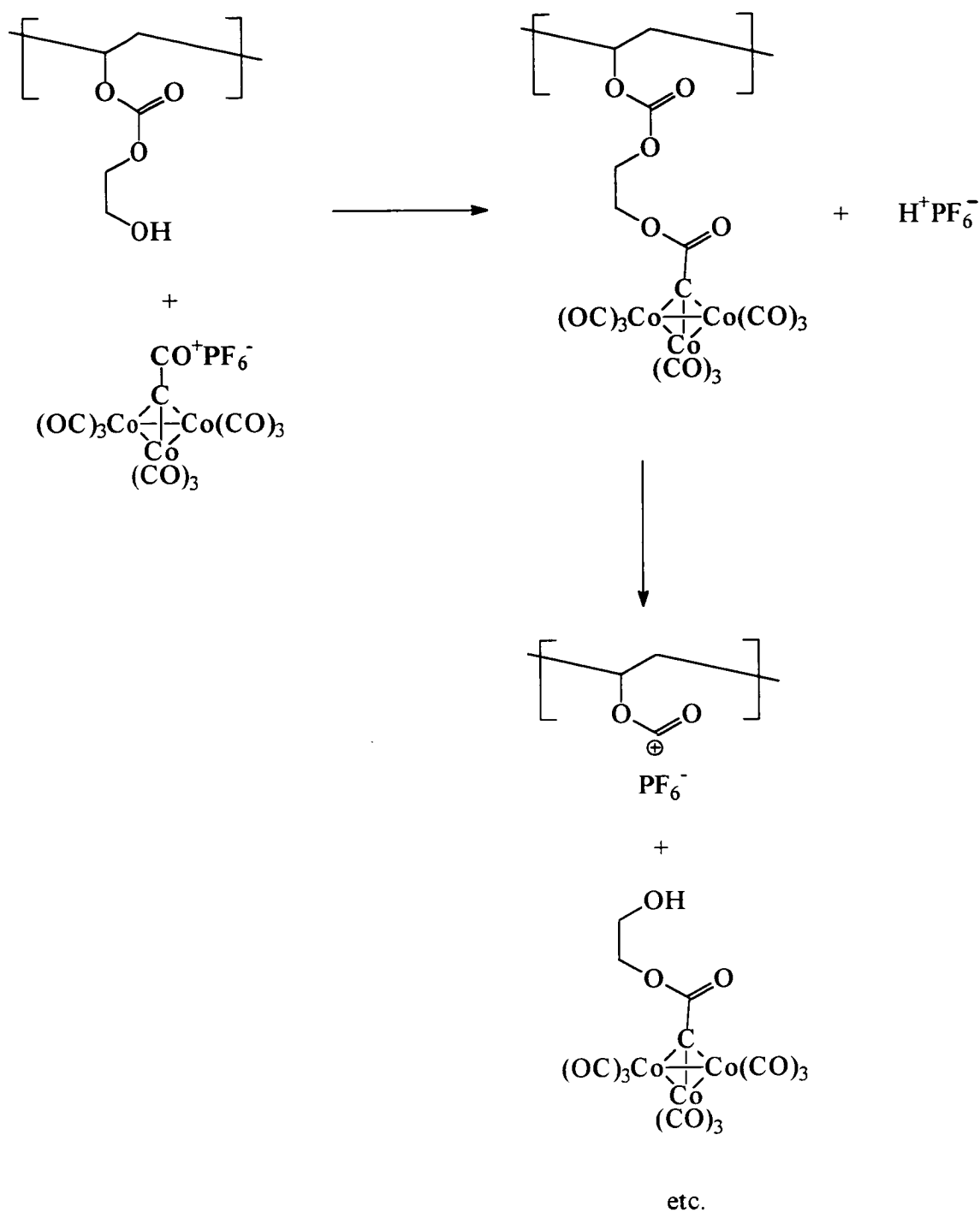
Scheme 2.20: Ester hydrolysis

As for the source of the HPF$_6$, there are 2 possibilities:

(1)   Not all of the HPF$_6$ has been flushed from the system prior to the addition of the polymer to the [(OC)$_9$Co$_3$(μ_3-CCO)]$^+$ PF$_6^-$ complex, or

(2)   The HPF$_6$ produced as a by-product of the reaction between the [(OC)$_9$Co$_3$(μ_3-CCO)]$^+$ PF$_6^-$ complex and the nucleophilic hydroxyl function is then hydrolysing the ester functionalities in the polymer, leading to polymer degradation and hence lighter molecular weight species.

2.10: Concluding remarks

Monomeric species containing the tricobalt nonacarbonyl alkylidyne cluster were sythesised and characterised. Polymers containing the tricobalt cluster unit were synthesised by both solution and dispersion polymerisation. The polymers prepared were characterised by GPC/UV-VIS spectroscopy and IR spectroscopy. GPC/UV-VIS provided molecular weight data, and proved that the cluster was attached covalently to the polymer support, whilst IR showed that the cluster unit was unchanged from that in the monomer.

The cluster containing polymers however, failed to catalyse the cross linking of unsaturated polymer species. This is thought to be due to the inability of the cluster to undergo redox reactions at ambient conditions. The current catalyst is a cobalt (II) / cobalt (III) species, whereas the cobalt in the alkylidyne cluster is cobalt (0).

Secondly, the cluster species investigated do not promote chain transfer of radicals, for the same reasons as outlined above.

Modification of nucleophilic groups on existing polymer networks by the tricobalt decacarbonyl cation led to polymer decomposition as a result of hydrolysis of the ester functionalities by hexafluorophosphoric acid.

2.11: References

1. P. J. Flory, *"Principles of polymer chemistry"*, Cornell University Press, 1953

2. K. J. Saunders, *"Organic Polymer Chemistry"*, Chapman and Hall, London, 1973

3. I. S. Morozova, V. G. Mairanovskii, B. R. Smirnov and L. M. Pushchaeva, *Dokl. Akad. Nauk SSSR*, 1981, **258** ,895

4. W. M. Bandaranayake and G. Pattenden, *J. C. S. Chem. Commun.* 1988, 1178

5. M. Kijima, K. Miyamori and T. Sato, *J. Org. Chem.*, 1987, **52**, 706

6. H. Gerrens, *Ber. Bunsenges. Physik. Chem.*, 1963, **67**, 741

7. D. Seyferth, C. S. Eschbach, G. H. Williams, P. L. K. Hung and Y. M. Cheng, *J. Organomet. Chem.*, 1974, **78**, C13

8. D. Seyferth, C. S. Eschbach, G. H. Williams and P. L. K. Hung, *J. Organomet. Chem.*, 1977, **134**, 67

9. D. Seyferth, J. E. Hallgren and C. L. Nivert, *Inorg. Chem.*, 1977, **16**, 758

10. T. Lis, J. Utko and P. Sobota, *Acta Crystallogr.*, *Section C*, **1993**, *49*, 2089

11. J. C. Gressier, G. Levesque, H. Patin and F. Varret, in *Metal Containing Polymeric Systems*, Eds. J. E. Sheats, C. E. Carraher Jr., and C. U. Pittman, Jr., Plenum, New York, 1984, 291

12. M. P. Stevens, *"Polymer Chemistry an Introduction"*, 2nd Edition, Oxford University Press, 1990, p. 61

13. Laurence Pollino, I. C. I. Paints, personal communication

14. R. H,. Grubbs, C. Gibbons, L. C. Kroll, W. D. Bonds and C. H. Brubaker Jr., *J. Am. Chem. Soc.*, 1973, **95**, 2373

15. B. H. Chang, R. H. Grubbs, and C. H. Brubaker Jr., *J. Organomet. Chem.*,1979, **172**, 81

16. P. Perkins and K. P. C. Vollhardt, *J. Am. Chem. Soc.*, 1979, **101**, 3985

17. M. Capka, P Svoboda, M. Corny and J. Hetflejs, *Tetrahedron. Lett.* 1971, 4787

18. R. H. Grubbs and L. C. Kroll, *J. Am. Chem. Soc.*, 1971, **93**, 3062

19.   R. H. Grubbs and E. M. Sweet, *Macromolecules*, 1975, **8**, 241

20.   C. U. Pittman, Jr. and L. R. Smith, *J. Am. Chem. Soc.*, 1975, **97**, 1749

21.   C. U. Pittman, Jr., L. R. Smith and R. M. Hanes, *J. Am. Chem. Soc.*, 1975, **97**, 1742

22.   C. U. Pittman, Jr., S. E. Jacobsen and H. Hiramota, *J. Am. Chem. Soc.*, 1975, **97**, 4774

23.   G. O. Evans, C. U. Pittman, Jr., R. McMillan, R. T. Beach and R. Jones, *J. Organomet. Chem.*, 1974, **67**, 295

24.   L. D. Rollman, *Inorg. Chim. Acta*, 1972, **6**, 137

Chapter 3

Synthesis and reactivity of hydroxy functionalised clusters

3.1 Introduction

Transition metal carbonyl clusters of osmium and ruthenium have been extensively studied by several groups over the last twenty five years. Within this research group, studies have concentrated mainly on multinuclear species which contain arene[1] and alkyne[2,3] ligands. However, in order to synthesise polymeric materials containing transition metal clusters, chemical functionality has to be introduced to the complex by modification of the bound ligand. Alternatively, the synthesis of a cluster with a functionalised ligand has to be developed. This functionality is necessary in order that the complex may undergo further reaction *via* the function introduced.

Recently, Lewis *et al* [4] showed how the arene ligand of a hexaruthenium transition metal cluster could be chemically modified (Scheme 3.1). This chemistry, however, remains largely undeveloped and will not be considered further.
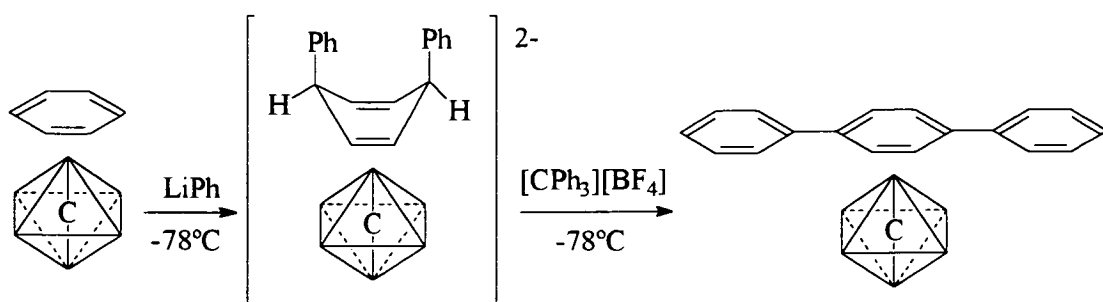
Scheme 3.1: Modification of cluster bound arenes

This leaves the second approach- attaching a functionalised ligand to the cluster framework. Additionally, the ligand has to be multi functional- the second functionality being necessary as a means to attach the ligand to the cluster. This, however, poses problems for the synthetic chemist, as many functionalities are more likely to react with the cluster during the synthesis, rather than remaining intact. The main problem is nucleophilic addition to the terminal carbonyl ligands to produce the relatively unstable anion $[Os_3(CO)_{11}(CONuc)]^-$. This anion may then undergo a variety of subsequent reactions, governed by the nature of the nucleophile.

Hence introduction of functionalised ligands is rare. However, Deeming[5, 6, 7] and coworkers have shown that hydroxy alkynes can be successfully attached to triosmium clusters *via* the alkyne π system, leaving the hydroxy function intact. This chapter is concerned with the formation of such hydroxy functionalised triosmium clusters, and their subsequent reactions.

3.2 Reaction of hydroxy alkynes with triosmium clusters

Deeming *et al* [5, 6, 7] showed that by heating an alkynol with $M_3(CO)_{12}$, (M = Os, Ru), the (μ_2: η^3) alkynol complexes, shown in Figure 3.1 could be produced, along with other reaction products. The retention of the OH function allows the possibility to exploit the chemistry of the cluster - alcohol.

| alkynol | $Os_3(CO)_{10}[\mu_3{:}\eta^2(alkynol)]$ |
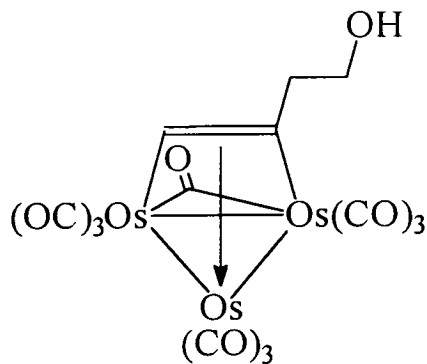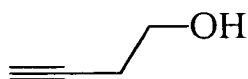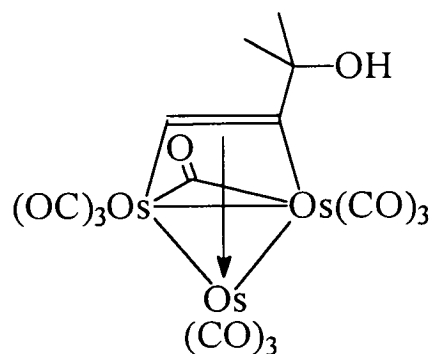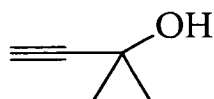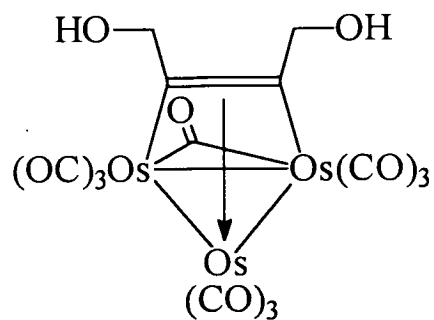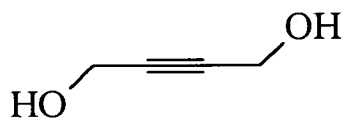
Figure 3.1: $(\mu_2{:}\eta^3)$ alkynol species from $Os_3(CO)_{12}$

We believed that the alkyne function would, as in previous reports [5, 6, 7], bind strongly to the cluster and donate 4 electrons, working against any possible oxygen atom coordination. Hence reaction of the activated trinuclear cluster triosmium decacarbonyl *bis*(acetonitrile) **(13)** with an excess of propargyl alcohol produced only alkyne and coupled alkyne products, as outlined in Scheme 3.2.
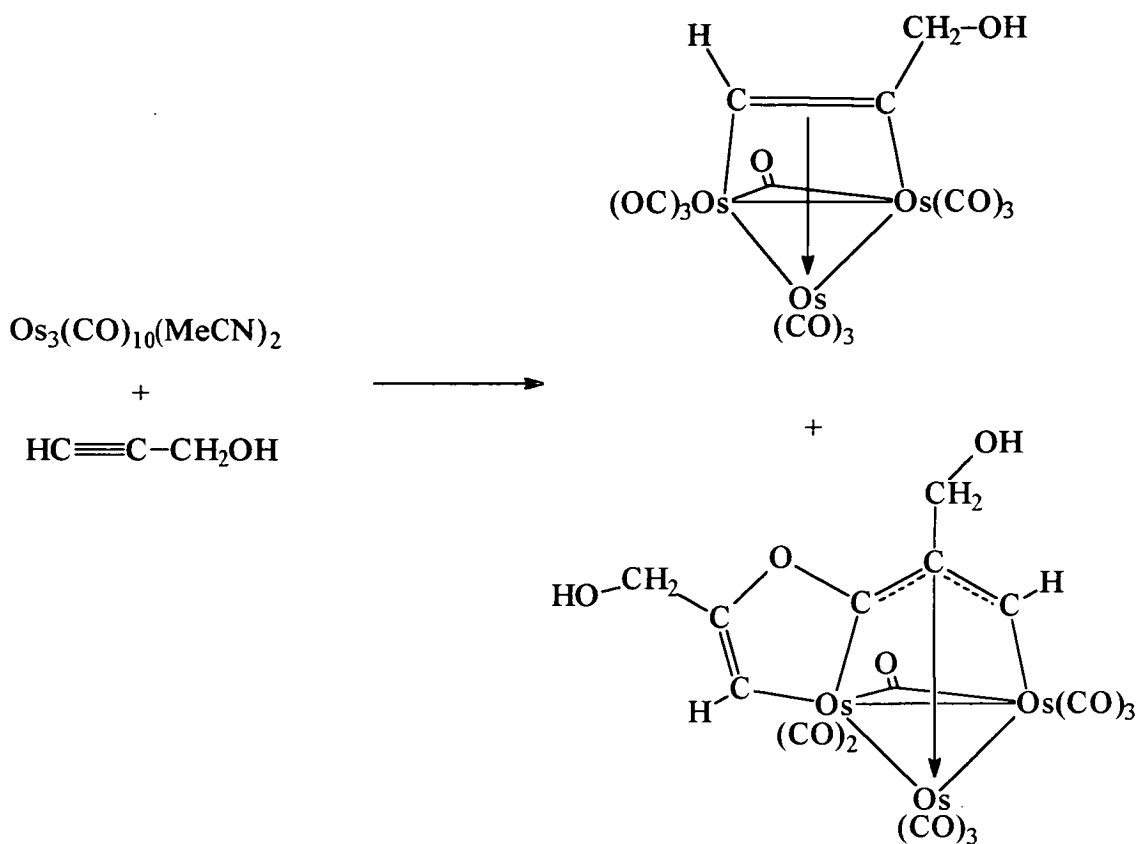
Scheme 3.2: Reaction of propargyl alcohol with $Os_3(CO)_{10}(MeCN)_2$

The structures are based on $v(CO)$ IR and ^1H NMR spectra which are quite characteristic for these known types of compounds[5] . The compound $[Os_3(CO)_8(\mu\text{-}CO)(\mu_3:\eta^2\text{-}(HC=CCH_2OH))]$ **(14)** adopts the usual bridging carbonyl structure ($v(CO)$ = $1864cm^{-1}$). The ^1H NMR shows a singlet at δ 9.28 ppm (s, 1H) due to the CH proton. The CH_2 protons gives rise to a doublet of doublets at δ 4.1 ppm (J = 13.7 Hz), and the hydroxy proton produces a broad singlet at δ 1.79 ppm. Due to relaxation effects, only the CH and CH_2 carbon atoms are observed in the ^{13}C spectrum, at δ 113.6 ppm (CH) and 77.3 ppm (CH_2).

Much more interesting, however, is the compound which eluted second from the column. Coupling of two propargyl ligands along with one carbon monoxide gives rise to the η^3-allyl compound, $Os_3(CO)_8(\mu\text{-}CO)[(HCCCH_2OH)_2CO]$, **(15)**, in

which the allylic ligand acts as a 5 electron donor, with a σ-Os-C bond at a side chain[8]. This novel ligand is undoubtedly the most interesting feature of this structure, and not only because of its potential for further reactivity. A crystal suitable for X ray diffraction was grown from dichloromethane / hexane solution in a freezer. Figure 3.2 shows the molecular geometry of this compound. It is composed from linkage of 2 propargyl units through a carbon and an oxygen atom [C(4) and O(2)] derived from the opening of a carbonyl C≡O bond.
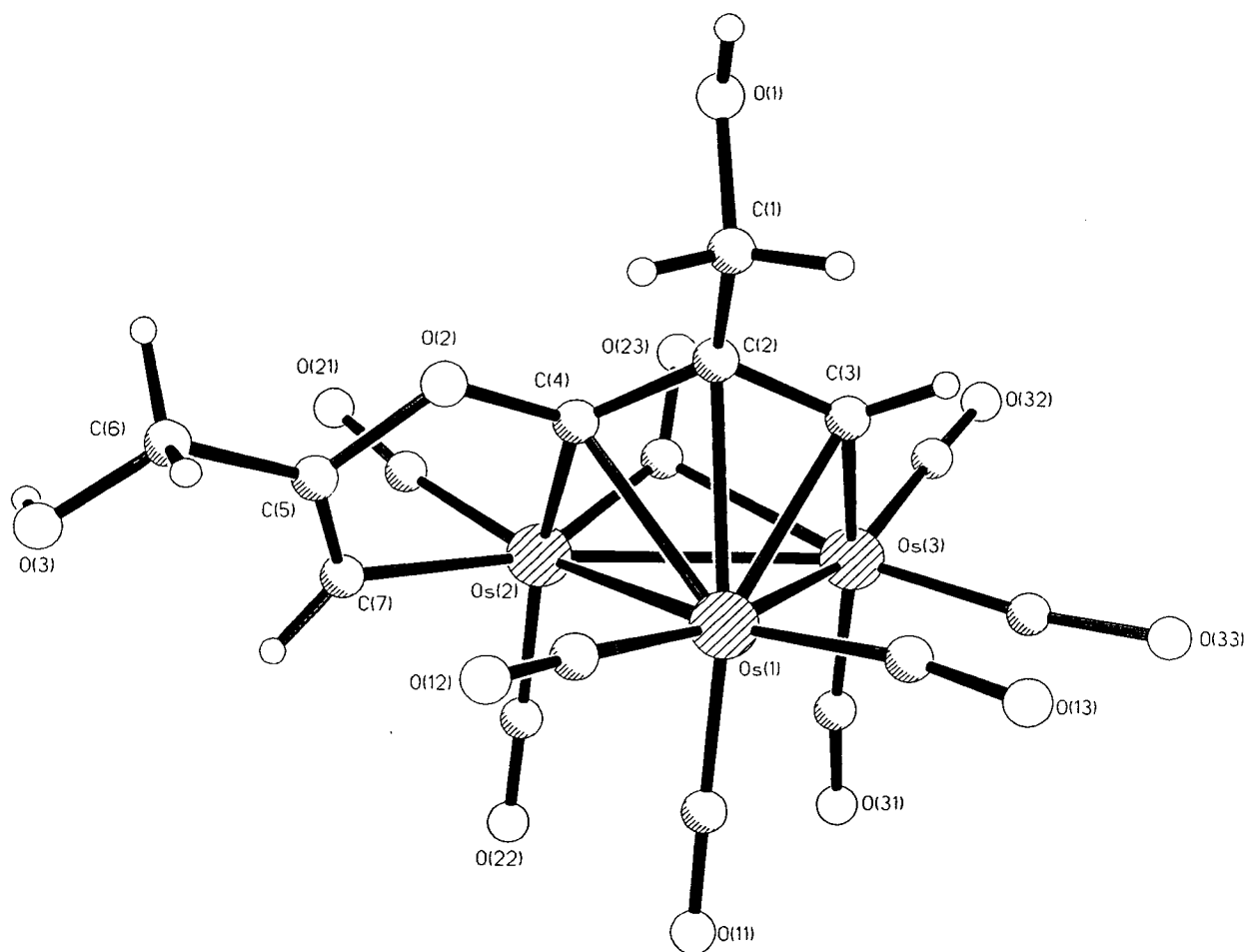

Figure 3.2: The molecular structure of $Os_3(CO)_8(\mu\text{-}CO)[(HCCCH_2OH)_2CO]$, (15)

Significant bond lengths(Å) and angles (°), for $Os_3(CO)_8(\mu\text{-}CO)[(HCCCH_2OH)_2CO]$:

Os(1)-C(3) 2.28(4), Os(1)-C(4) 2.32(4), Os(1)-C(2) 2.36(4), Os(1)-Os(3) 2.779(3), Os(1)-Os(2) 2.843(3), Os(2)-C(23) 1.86(3), Os(2)-C(4) 2.03(4), Os(2)-C(7) 2.07(4), Os(2)-Os(3) 2.902(2), Os(3)-C(3) 2.10(3), Os(3)-C(23) 2.24(3), O(23)-C(23) 1.31(5), O(1)-C(1) 1.41(4), O(2)-C(4) 1.40(5), O(2)-C(5) 1.43(5), O(3)-C(6) 1.38(5), C(1)-C(2) 1.53(5), C(2)-C(4) 1.41(6), C(2)-C(3) 1.41(5), C(5)-C(7) 1.28(5), C(5)-C(6) 1.53(5), C(3)-Os(1)-C(4) 62.5(14), C(3)-Os(1)-C(2) 35.3(12), C(4)-Os(1)-C(2) 35.0(14), C(3)-Os(1)-Os(3) 47.8(8), C(4)-Os(1)-Os(3) 81.1(9), C(2)-Os(1)-Os(3) 75.5(9), C(3)-Os(1)-Os(2) 81.0(9), C(4)-Os(1)-Os(2) 44.8(10), C(2)-Os(1)-Os(2) 73.3(9), Os(3)-Os(1)-Os(2) 62.16(7), C(23)-Os(2)-C(21) 81(2), C(23)-Os(2)-C(22) 100(2), C(23)-Os(2)-C(4) 94(2), C(4)-Os(2)-C(7) 76(2), C(23)-Os(2)-Os(1) 103.8(10), C(4)-Os(2)-Os(1) 53.8(11), C(7)-Os(2)-Os(1) 91.0(10), C(23)-Os(2)-Os(3) 50.5(10), C(4)-Os(2)-Os(3) 83.0(11), C(7)-Os(2)-Os(3) 148.8(10), Os(1)-Os(2)-Os(3) 57.85(6), C(3)-Os(3)-C(23) 90.8(12), C(3)-Os(3)-Os(1) 53.6(10), C(23)-Os(3)-Os(1) 96.2(8), C(3)-Os(3)-Os(2) 82.6(10), C(23)-Os(3)-Os(2) 40.0(9), Os(1)-Os(3)-Os(2) 60.00(7), O(1)-C(1)-C(2) 109(3), C(4)-C(2)-C(3) 116(4), C(4)-C(2)-C(1) 124(3), C(3)-C(2)-C(1) 120(3), C(4)-C(2)-Os(1) 71(2), C(3)-C(2)-Os(1) 70(2), C(1)-C(2)-Os(1) 120(2), C(2)-C(3)-Os(3) 128(3), C(2)-C(3)-Os(1) 75(2), Os(3)-C(3)-Os(1) 78.6(12), O(2)-C(4)-C(2) 113(3), O(2)-C(4)-Os(2) 117(3), C(2)-C(4)-Os(2) 130(3), O(2)-C(4)-Os(1) 116(2), C(2)-C(4)-Os(1) 74(2), Os(2)-C(4)-Os(1) 81.4(14), C(7)-C(5)-O(2) 118(4), C(7)-C(5)-C(6) 133(4), O(2)-C(5)-C(6) 109(3), O(3)-C(6)-C(5) 110(3), C(5)-C(7)-Os(2) 116(3)

This allylic mode of coordination has been reported previously for other tricuclear compounds of the iron triad. $Os_3(CO)_{10}(PhC_2H)_2$ was first reported in 1975 by Gambino et al [8], but not fully characterised until 1976 when Gervasio[9] reported the completed crystal structure. Both compounds have a distorted triosmium core and a semi bridging carbonyl. The core of the compound $Os_3(CO)_8(\mu\text{-}CO)[(HCCCH_2OH)_2CO]$ is shown in Figure 3.3. The values Os(2)-C(23) = 1.86(3), Os(3)-C(23) = 2.24(3) and C(23)-O(23) = 1.31(5) Å compare well with those reported for $Os_3(CO)_8(\mu\text{-}CO)(HC_2PhCOCPhCH)$ [9], and another grossly distorted CO bridged compound[10], $Fe_3(CO)_8(C_4H_8S)_2$, with tetrahydrothiophene as a ligand.
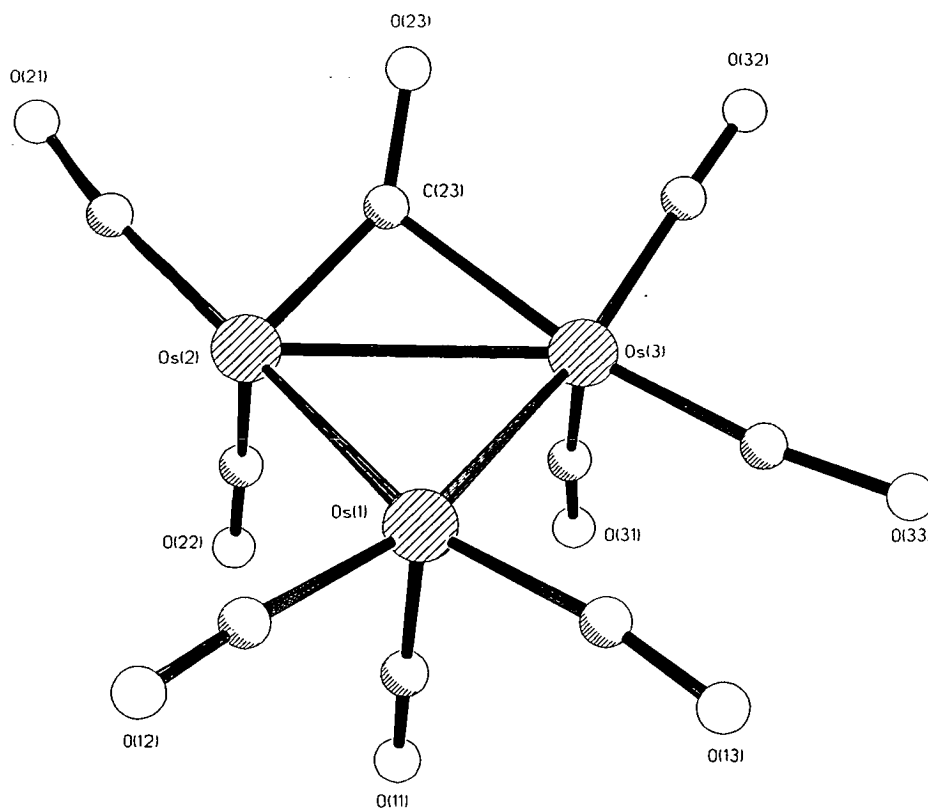
Figure 3.3: $Os_3(CO)_9$ core of compound $Os_3(CO)_8(\mu\text{-}CO)[(HC\equiv CCH_2OH)_2CO]$

Significant bond lengths (Å) and angles (°) detailed below:

Osmium - Osmium bond lengths and angles:
Os(1)-Os(2) 2.843(3), Os(2)-Os(3) 2.902(2), Os(1)-Os(3) 2.779(3)
Os(3)-Os(1)-Os(2) 62.16(7), Os(1)-Os(2)-Os(3) 57.85(6), Os(1)-Os(3)-Os(2)60.00(7)

Osmium - Carbon bond lengths:
Os(1)-C(11) 1.81(4), Os(1)-C(12) 1.86(4), Os(1)-C(13) 1.87(3)
Os(2)-C(21) 1.89(4), Os(2)-C(22) 1.92(5), Os(2)-C(23) 1.86(3)
Os(3)-C(31) 1.83(4), Os(3)-C(32) 1.88(4), Os(3)-C(23) 2.24(3), Os(3)-C(33) 1.80(5)

Carbonyl bond lengths and angles:
O(11)-C(11) 1.24(4), O(12)-C(12) 1.12(4), O(13)-C(13) 1.19(4), O(21)-C(21) 1.20(4), O(22)-C(22) 1.16(5), O(23)-C(23) 1.31(5), O(31)-C(31) 1.16(5), O(32)-C(32) 1.15(4), O(33)-C(33) 1.33(6), O(11)-C(11)-Os(1) 177(3), O(12)-C(12)-Os(1) 175(4), O(13)-C(13)-Os(1) 171(3), O(21)-C(21)-Os(2) 173(3), O(22)-C(22)-Os(2) 170(4), O(23)-C(23)-Os(2) 146(3), O(23)-C(23)-Os(3) 120(3), Os(2)-C(23)-Os(3) 89.5(13), O(31)-C(31)-Os(3) 174(4), O(32)-C(32)-Os(3) 179(3), O(33)-C(33)-Os(3) 172(5)

The infrared spectrum stretch of the semi bridging carbonyl also reflects this asymmetry, with a $\nu(CO)$ stretch of 1838 cm^{-1}.

The ^{13}C NMR spectrum of the allylic compound $Os_3(CO)_8(\mu\text{-}CO)[(HC{\equiv}CCH_2OH)_2CO]$ only showed, as expected, the signals due to the CH and CH_2 carbons of the ligand. This is due to the relaxation effects imparted on the quaternary carbons by the Osmium atoms. The ^1H spectrum, however, revealed much more information. Figure 3.4 shows the ^1H NMR spectrum at 200 MHz in d_6-DMSO, with an expansion of the region between δ 4.2 and 5.8 ppm shown in Figure 3.5.
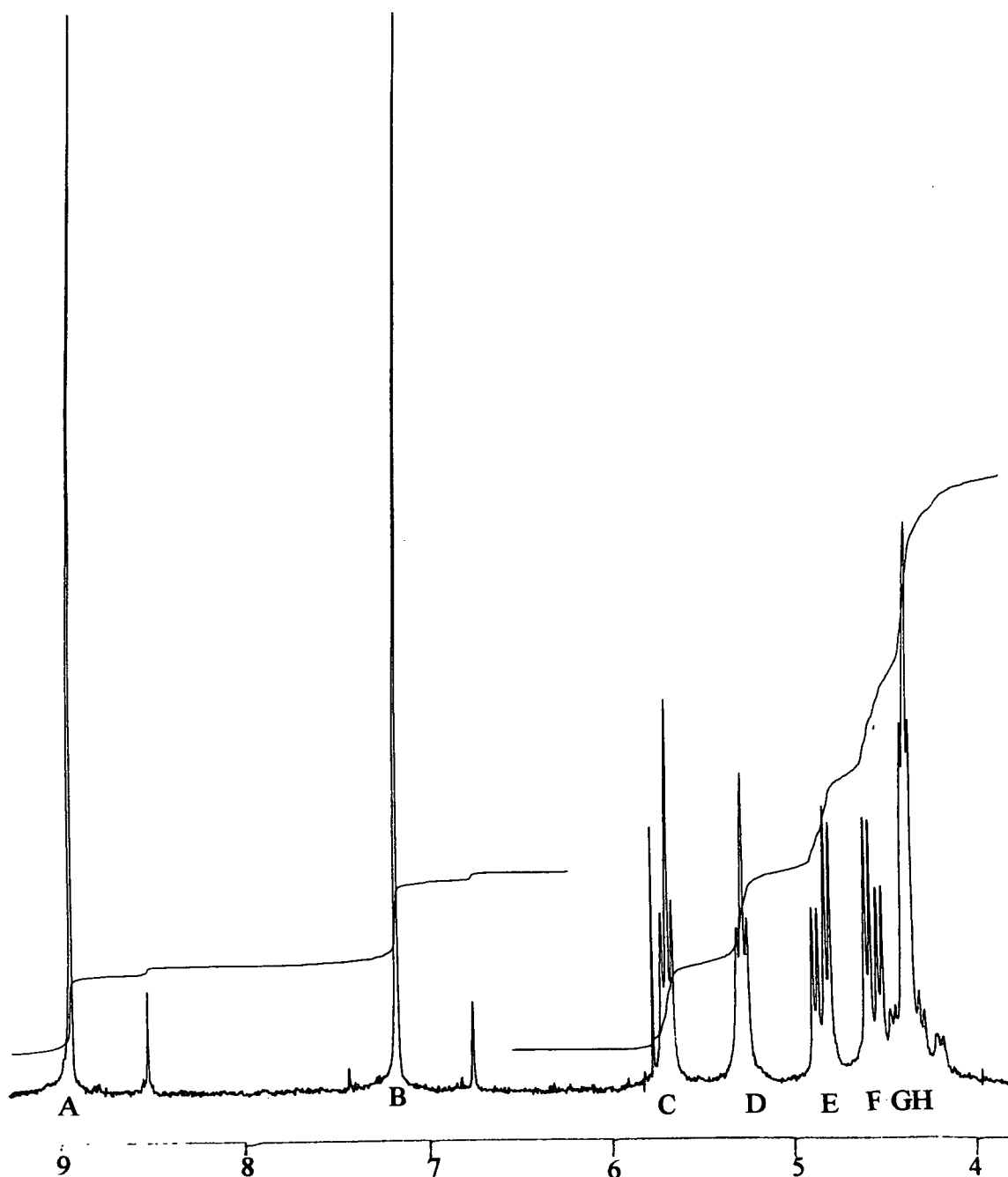
Figure 3.4: ^1H NMR spectrum of $Os_3(CO)_8(\mu\text{-}CO)[(HC{\equiv}CCH_2OH)_2CO]$
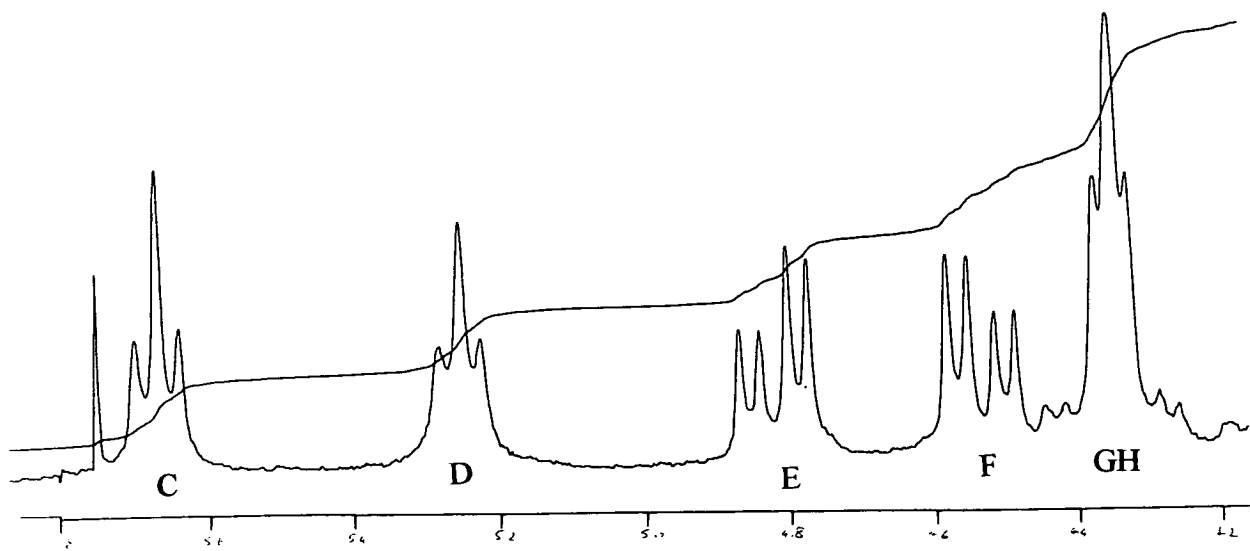
Figure 3.5: expansion of δ 4.0 to 5.8 ppm

The resonances due to the hydroxy protons (C and D) are clearly evident as triplets at δ 5.26 and 5.67 ppm. Due to exchange, probably with water dissolved in the solvent, these signals were not visible in a second sample prepared for study at 360 MHz (Figure 3.6). This had the added effect of simplifying the spectrum considerably; the signals referred to as G and H, which were two heavily overlapped doublets of doublets in figures 3.4 and 3.5, as the AB components of an ABX spin system, are now simplified due to the removal of the X component. Similarly, signals E and F are simplified.
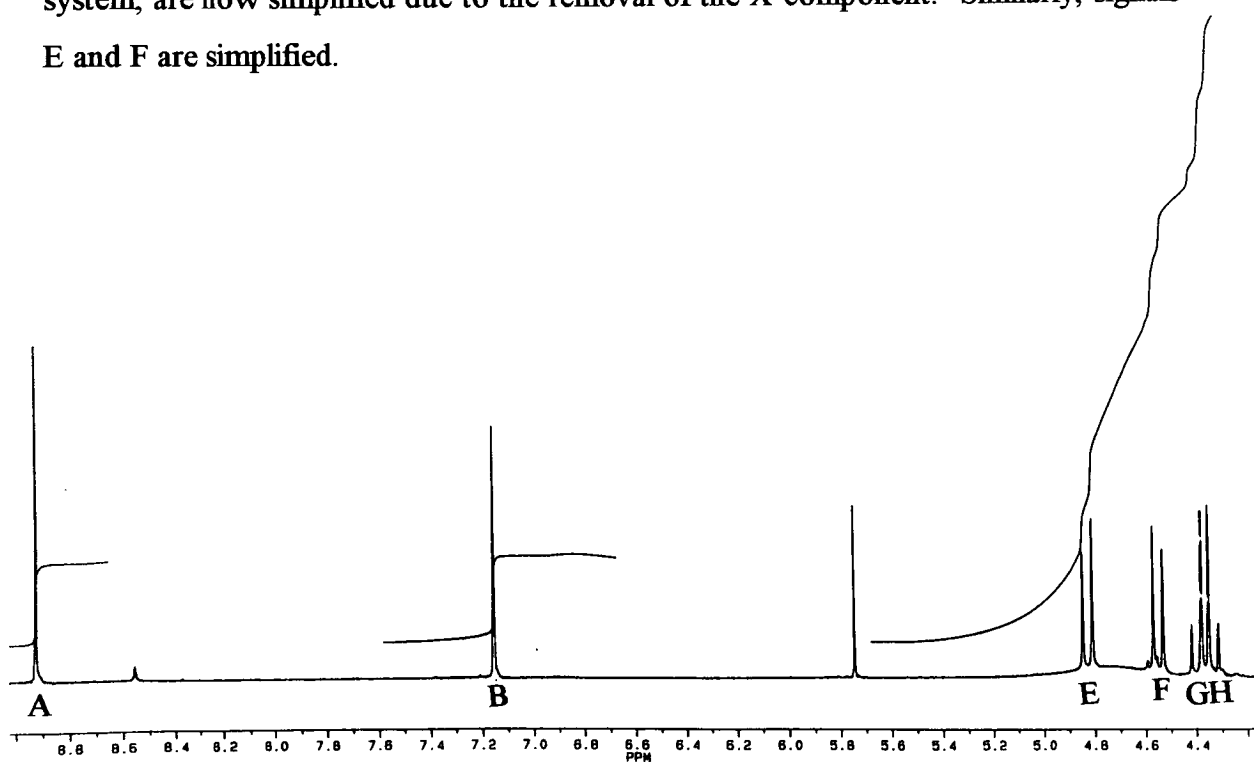
Figure 3.6: ¹H NMR spectrum at 360 MHz

Unfortunately, it was not possible to distinguish between the alkenic and the allylic systems in the spectra. However, on the basis of the coupling constant data, it is tentatively proposed that signals G and H are associated with signal D (J = 5.7 Hz), and that signals E and F are associated with signal C (J = 5.9 Hz).

NOe difference experiments provided more secure evidence for the relationships between the CH and CH_2 environments. The results obtained are reproduced in Figure 3.7.
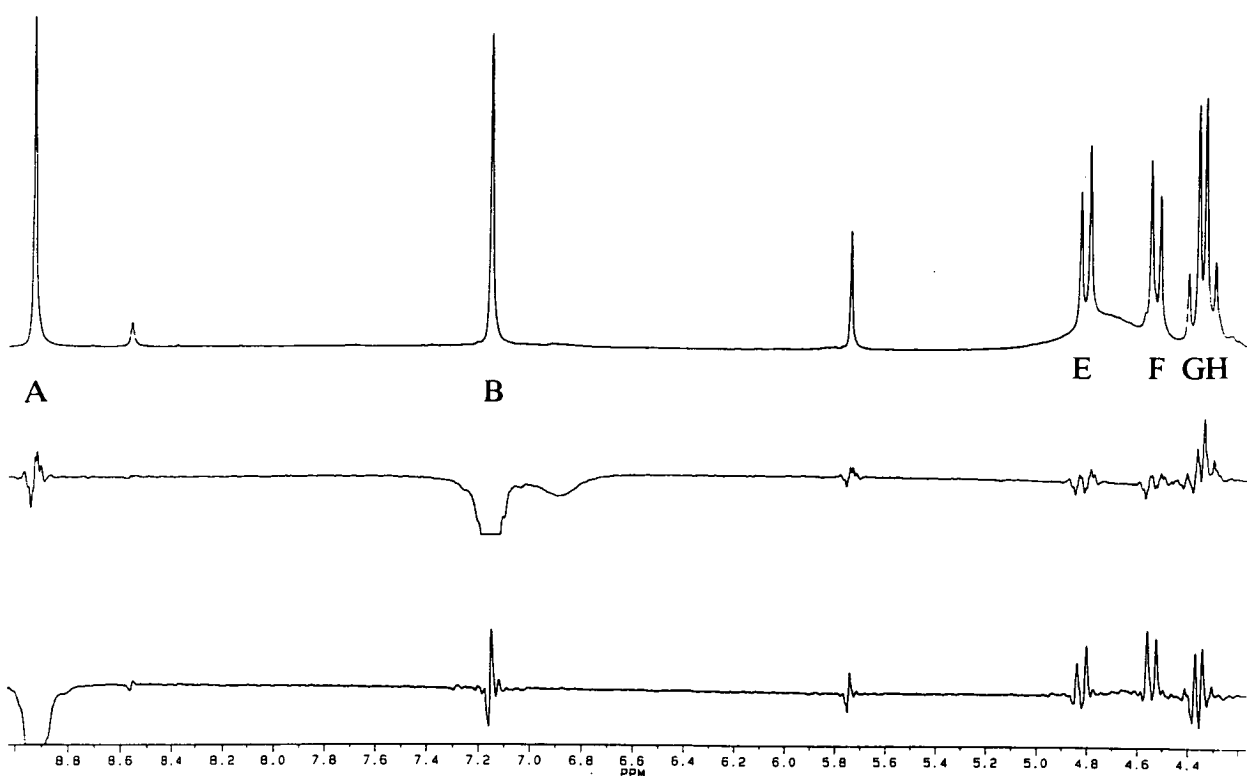
Figure 3.7: nOe difference spectra for $Os_3(CO)_8(\mu\text{-}CO)[(HC\equiv CCH_2OH)_2CO]$

Irradiation of signal B gave an approximately 2% enhancement in H. Likewise, irradiation at signal A gave rise to approximately 2% enhancement in signals E and F. Hence, one of the CH_2 protons which give rise to signals G and H is spatially close to the CH proton B. Similarly, the CH_2 protons responsible for signals E and F are spatially close to the CH proton responsible for signal A.

Hence the protons were assigned as shown below in Figure 3.8.
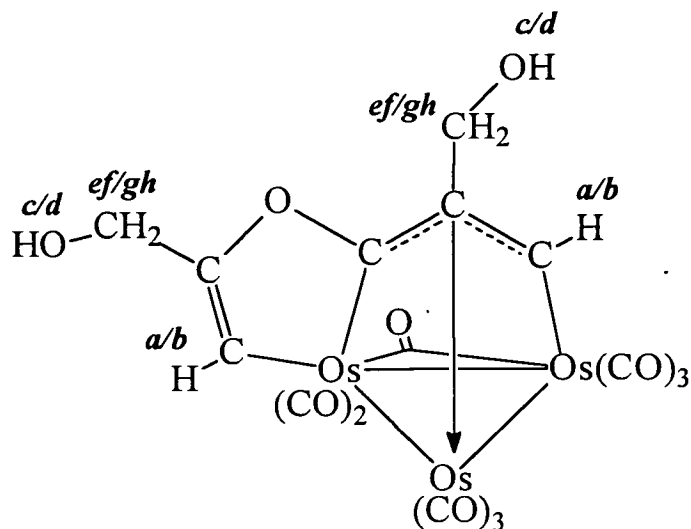
	δ ^{1}H/ppm	δ ^{13}C/ppm
a/b	7.14 (s, 1H, CH)	108.8 / 125.3
	8.93 (s, 1H, CH)	
c/d	5.26 (t, 1H, OH) J = 5.7 Hz	
	5.67 (t, 1H, OH) J = 5.9 Hz	
ef/gh	4.38 (q, 2H, CH$_2$)	58.11 / 63.19
	J= 13.9, 5.9 Hz	
	4.69 (q, 2H, CH$_2$)	
	J = 13.3, 5.7 Hz	

signals c and d were not observed in the 360 MHz spectrum due to exchange

Figure 3.8: NMR assignment for Os$_3$(CO)$_8$(μ-CO)[(HC≡CCH$_2$OH)$_2$CO]

96

3.3 Reaction of hydroxy functionalised clusters

Given the intact hydroxy groups of the complex $Os_3(CO)_8(\mu$-$CO)[(HCCCH_2OH)_2CO]$, it was envisaged that reaction with di-isocyanates would give rise, *via* addition polymersiation, to polyurethanes containing the triosmium cluster. Scheme 3.3 outlines the general reaction for the production of polyurethanes from the addition of diols to di-isocyanates.

$$HO-R-OH$$
$$+$$
$$O=C=N-R'-N=C=O$$

$$\longrightarrow$$
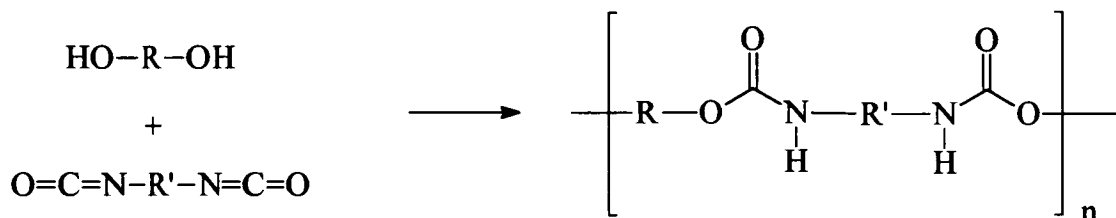
Scheme 3.3: Polyurethane synthesis

The addition polymerisation of hexamethylene di-isocyanate with a stirred solution of $Os_3(CO)_8(\mu$-$CO)[(HCCCH_2OH)_2CO]$ under nitrogen was attempted. Infrared spectroscopy was used to monitor the reaction: the isocyanate stretch ($v_{NCO} = 2275$ cm^{-1}) was seen to disappear whilst at the same time the amide stretch at $v_{CONH} = 1731$ cm^{-1} appeared. However, analysis of the resultant species by gel permeation chromatography showed that no polymeric species were present. Infrared and mass spectroscopy of the reaction mixture showed that the cluster unit was intact, ruling out the possibilty nucleophilic attack of the carbonyl ligands by the isocyanate. It is therefore concluded that the cluster diol failed to react with the di-isocyante, probably due to steric effects. Similar reactions with the cluster diols $Os_3(CO)_{10}(HOCH_2C\equiv CCH_2OH)$ and $Co_2(CO)_6(HOCH_2C\equiv CCH_2OH)$ also failed to produce polyurethanes, despite heating the reaction mixtures in solvents such as acetone and toluene. The appearance of the amide band is thought to be due to the reaction of the isocyanate with water vapor in the atmosphere when preparing the sample for infrared spectroscopy.

3.4 Concluding remarks

Reaction of propargyl alcohol and triosmium decacarbonyl *bis*(acetonitrile) (13) produced the $\mu_3:\eta^2$ compound $[Os_3(CO)_8(\mu\text{-}CO)(\mu_3:\eta^2\text{-}(HC=CCH_2OH)]$ (14), as well as the coupled alkyne product $Os_3(CO)_8(\mu\text{-}CO)[(HCCCH_2OH)_2CO]$ (15), which is produced from the coupling of 2 propargyl units with a carbonyl ligand. An X-ray study of this product showed that, in common with other trinuclear structures with allyl ligand systems, the triosmium core was distorted and that the bridging carbonyl ligand was bound asymmetrically. Unfortunately, reaction of this and other cluster diol species with hexamethylene di-isocyanate, failed to produce cluster containing polyamides. This was thought to be due to the large steric bulk of the metal carbonyl cores of the diol compounds. Increasing the distance between the cluster and the hydroxy functionality, by extending the CH_2 chain, would be one approach to investigate the possibility of making such polymeric species.

3.5 References

1. D. Braga, P. J. Dyson, F. Grepioni and B. F. G. Johnson, *Acc. Chem. Res.*, 1994, **94**, 1585

2. R. L. Mallors, PhD Thesis, The University of Edinburgh, 1995

3. J. L. Haggitt and B. F. G. Johnson, *J. Chem. Soc. Chem. Commun.*, 1995, 1263

4. T. Borchert, J. Lewis, H. Pritzkow, P. R. Raithby and H. Wadepohl, *J. Chem. Soc. Dalton Trans.*, 1995, 1061

5. S. Aime, S. Tiripicchio, M. Tiripicchio and A. J. Deeming, *Inorg. Chem.*, 1981, **20**, 2027

6. S. Aime and A. J. Deeming, *J. Chem. Soc. Dalton Trans.*, 1981, 828

7. S. Aime and A. J. Deeming, *J. Chem. Soc. Dalton Trans.*, 1983, 1807

8. O. Gambino, R. P. Ferrari, M. Chinone, and G. A. Vaglio, *Inorg. Chim. Acta*, 1975, **12**, 155

9. G. Gervasio, *J. Chem. Soc. Chem. Commun.*, 1976, 25

10. F. A. Cotton and J. M. Troup, *J. Am. Chem. Soc.*, 1974, **96**, 5070

Chapter 4

Tricobalt nonacarbonyl alkylidyne as a ligand

4.1 Introduction

Joining a transition metal cluster to a ligand functionality permits the construction of "clusters of clusters" and hence large metallic structures. This chapter is concerned with the coupling of the tricobalt nonacarbonyl acylium compound $[(OC)_9Co_3(\mu_3\text{-}CCO)^+]$ to clusters with ligands containing nucleophilic functionality.

Recently, the primary literature has contained several reports of transition metal cluster carboxylate compounds, where the carboxylate ligand is the tricobalt cluster acid $[(OC)_9Co_3(\mu_3\text{-}CCOOH)]$. The first such report was of the synthesis and characterisation of the (μ_4-oxo) tetracobalt(II) compound $OCo_4[OOCCCo_3(CO)_9]_6$, in 1991 by Schore and coworkers[1]. Subsequently, Fehlner and his research group published details of $[\mu_3\text{-}Co(CO)_3]Cd_3\{\mu\text{-}[(OC)_9Co_3(\mu_3\text{-}CCOO)]\}_3(THF)_3$ [2]. The syntheses and structures of $Zn[p\text{-}\{(OC)_9Co_3(\mu_3\text{-}CC_6H_4CH_2CH_2COO)]\cdot(C_6H_5CH_3)$ and $M_4O[(OC)_9Co_3(\mu_3\text{-}CCOO)]_6$ (M= Zn, Co) [3], $Mo_2\{\mu\text{-}[(OC)_9Co_3(\mu_3\text{-}CCOO)]_4$ $[(OC)_9Co_3(\mu_3\text{-}CCOOH)]_2$ and some related compounds [4], followed. In each case, a multinuclear metal centre is ligated to the tricobalt cluster, *via* the carboxylate functionality. This gives rise to species which have relatively large metallic content as well as aesthetically pleasing structures.

Robinson and his coworkers have also studied extensively the electrochemistry of the tricobalt alkylidyne cluster [5,6] and its derivatives, with particular attention to species with multiple redox sites, e.g. ferrocene [7] and indeed, other tricobalt alkylidyne clusters [8].

4.2 Synthesis of multicluster species

Our first attempt to marry two clusters was by reaction of triosmium decacarbonyl *bis*(acetonitrile)[9] with carboxylmethylidyne tricobalt nonacarbonyl, $(OC)_9Co_3(\mu_3\text{-}CCOOH)$[10], as outlined in Scheme 4.1.
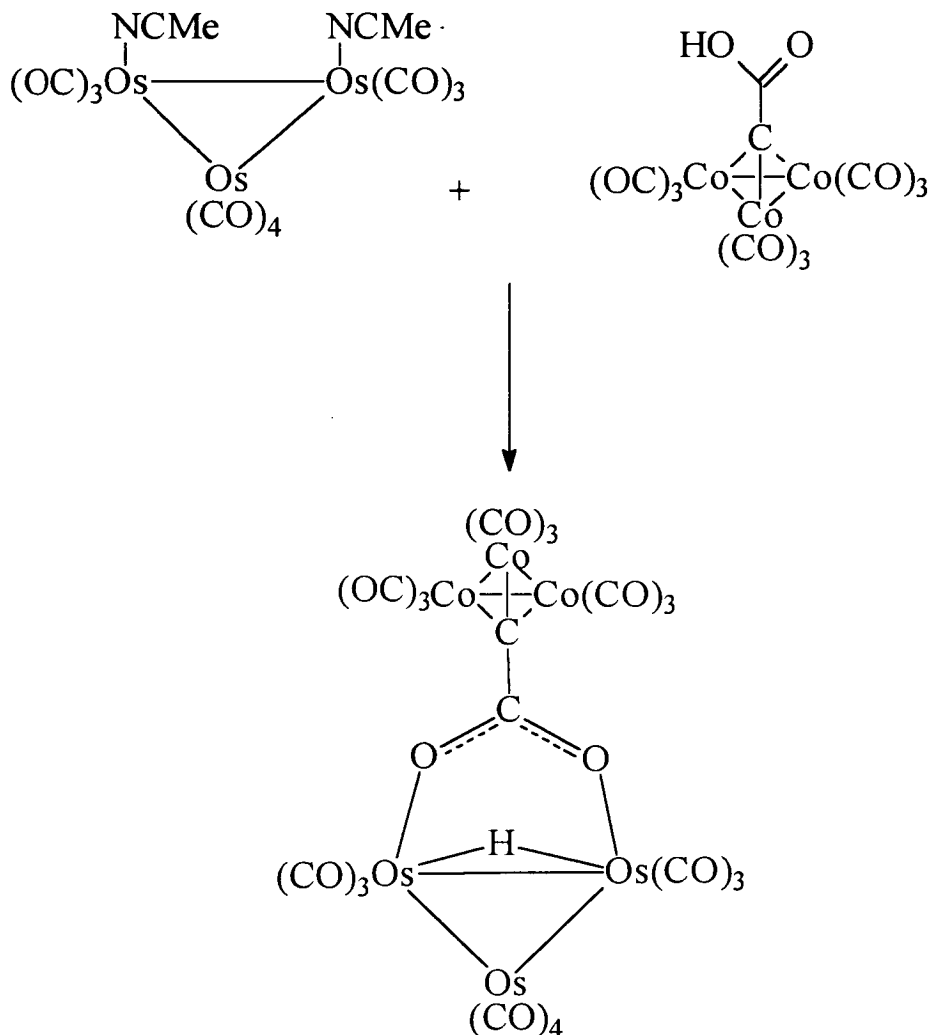
Scheme 4.1: Proposed synthetic route to $(\mu\text{-}H)Os_3(CO)_{10}[\mu\text{-}OOCCCo_3(CO)_9]$

Reaction in refluxing acetonitrile led to decomposition of the tricobalt cluster and the conversion of the triosmium decacarbonyl *bis*(acetonitrile) to triosmium dodecacarbonyl, by acquiring the carbonyl ligands from the tricobalt cluster. Reaction

at lower temperature (50°C) led to the same result. The activated cluster dihydrogen triosmium decacarbonyl was then used as the source of an activated triosmium cluster. No reaction occured at room temperature, even after extended period of time. Heating the reaction mixture to 60°C again led to decomposition of the tricobalt cluster and formation of triosmium dodecacarbonyl. Fehlner [3] has also reported problems with the spontaneous decomposition of $(OC)_9Co_3(\mu_3-CCOOH)$ in solution, a phenomenon which also helps explain the the unusual synthesis of $OCo_4[OOCCCo_3(CO)_9]_6$ from $[(OC)_9Co_3(\mu_3-CCO)^+]$ and water [1], where decomposition of the acid cluster presumably provides the source of the (μ_4-oxo) tetracobalt(II) core. Given that the $[(OC)_9Co_3(\mu_3-CCO)^+]$ species is formed via sacrificial decomposition of $(OC)_9Co_3(\mu_3-CCl)$, such instability in solution is not as unusual as it may at first seem.

A different approach to linking clusters was then developed. Similar experiments to those described above utilising the cluster amine $(OC)_9Co_3(\mu_3-CC_6H_4NH_2)$ (17) had also failed to produced coupled cluster products. However, it was thought that simple addition of the nucleophilic amine to the electrophilic acylium salt $[(OC)_9Co_3(\mu_3-CCO)^+]$ (PF_6^-) [11] (11) would thus produce a dicluster species linked by an amide bond. An extension of this reaction would be the possibility to investigate the electrochemical properties of any resulting multicluster species produced.

Synthesis of the derivative $(OC)_9Co_3(\mu_3-CC_6H_4NH_2)$, (17) from aniline[12], proceeded via the organomercury derivative [13], $ClHgC_6H_4NH_2$, (16) as outlined in scheme 4.2. Reaction of the organomercury species with methylidyne tricobalt nonacarbonyl produced the cluster species $(OC)_9Co_3(\mu_3-CC_6H_4NH_2)$ as a brown solid in 34% yield.

NH$_2$—C$_6$H$_5$ $\xrightarrow[\text{(ii) KCl}]{\text{(i) Hg(OAc)$_2$}}$ p-H$_2$N—C$_6$H$_4$—HgCl

p-H$_2$N—C$_6$H$_4$—HgCl $+$ (OC)$_3$Co—CoCo(CO)$_3$ (μ_3-CH)(CO)$_3$ $\xrightarrow{\text{THF, }\Delta}$ (OC)$_9$Co$_3$(μ_3-CC$_6$H$_4$NH$_2$)

Scheme 4.2: Synthesis of (OC)$_9$Co$_3$(μ_3-CC$_6$H$_4$NH$_2$)

The aniline derivative was found to be unstable in solution over extended periods of time. However, solution studies were still undertaken, with IR and NMR spectroscopy giving result consistent with the literature values [12].

As depicted in Scheme 4.3, a dichloromethane solution of p-anilinemethylidyne tricobalt nonacarbonyl (**17**) was added *via* syringe to a stoichiometric amount of freshly prepared methylidyne tricobalt decacarbonyl acylium hexafluorophosphate (**11**), slurried in dichloromethane. Upon addition of the nucleophile an exotherm was noted, although no colour change was evident due to the very dark brown colour of the aniline derivative.

NH$_2$

(OC)$_3$Co⟨⟩Co(CO)$_3$
Co
(CO)$_3$

+

CO$^+$ PF$_6^-$
C
(OC)$_3$Co⟨⟩Co(CO)$_3$
Co
(CO)$_3$

⟶

(CO)$_3$
C
(OC)$_3$Co⟨⟩Co(CO)$_3$
C
O═C—NH

C
(OC)$_3$Co⟨⟩Co(CO)$_3$
Co
(CO)$_3$

Scheme 4.3: Synthesis of [(CO)$_9$Co$_3$(μ_3-CCON(H)-p-C$_6$H$_4$(μ_3-C)Co$_3$(CO)$_9$], **(18)**

After stirring for 10 minutes, the solvent was removed *in vacuo* and separation of the reaction products was affected by thin layer chromatography on silica. Due to the very similar R$_f$ values of the reactants and products, care was needed when separating the three bands eluted. Two major bands and one minor band, all brown in colour, were isolated. The first band collected was identified by infrared, NMR and mass spectroscopy as unreacted amine. The second band closely followed this species, and was characterised as [(CO)$_9$Co$_3$(μ_3-CCON(H)-p-C$_6$H$_4$(μ_3-C)Co$_3$(CO)$_9$] **(18)**. The infrared spectrum of this resultant anilide linked dicluster showed a complex overlapping pattern in the terminal metal-carbonyl region, as expected for a compound containing two closely related clusters. FABMS gave the molecular weight as 1001 amu (the same as the value calculated), and showed the loss of 18 carbon monoxide ligands. The third minor band was tentatively formulated as the tertiary amide tricluster species [(CO)$_9$Co$_3$CC$_6$H$_4$N{CO(μ_3-C)Co$_3$(CO)$_9$}$_2$] **(19)** (Figure 4.1) on the basis of infrared and mass spectra recorded. The solution infrared spectrum is the same as for the dicluster species. However, more conclusive evidence was drawn from the FABMS spectrum which showed a molecular mass of 1470 amu, the calculated value being 1469 amu.
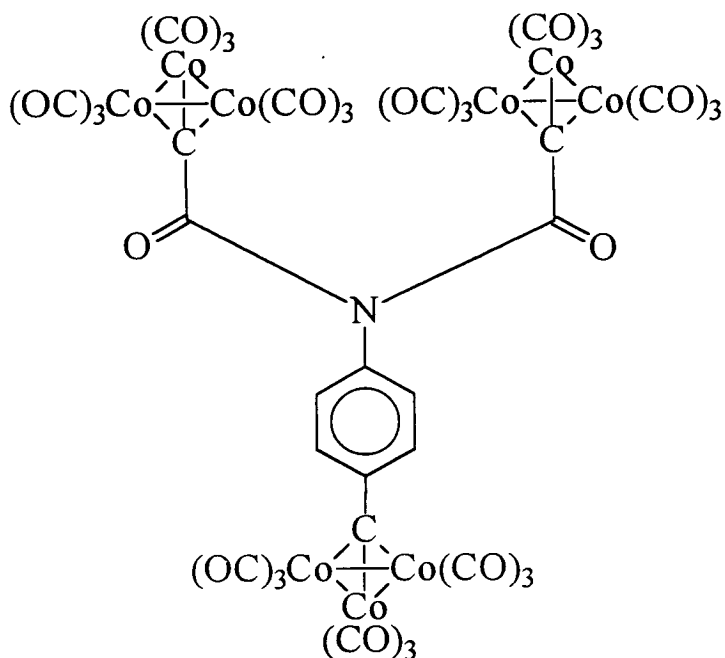
Figure 4.1: Amide linked tricluster species, (19)

Despite repeating the experiment using a vast excess of the $[(OC)_9Co_3(\mu_3\text{-}CCO)^+]$ (PF_6^-) reagent, only small amounts of this species were isolated.

The amide linked dicluster also proved to be more stable in solution than the parent amine, although less soluble. This decrease in solubility is not surprising, considering 35% (by weight) of the compound is metal. ^1H and ^{13}C NMR studies in d_6-acetone were undertaken, and the results are tabulated in Figure 4.2. Only one signal characteristic of the apical carbon was detected in the ^{13}C spectrum, and it is impossible to assign which of the cluster units it belongs to, or to be sure if it is in fact two signals with the same chemical shift.

Figure 4.2: NMR data for $[(CO)_9Co_3(\mu_3\text{-CCON(H)}\text{-}p\text{-}C_6H_4(\mu_3\text{-C})Co_3(CO)_9]$
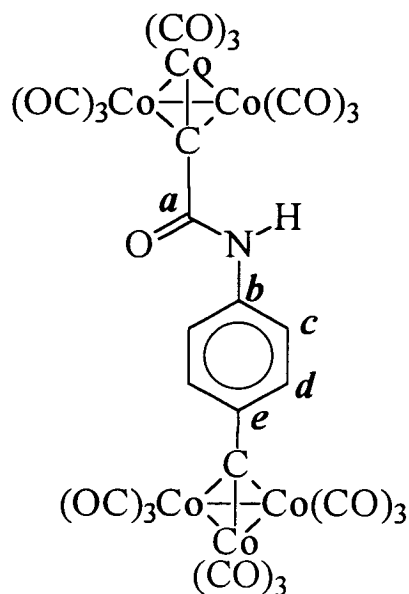
	δ^1H/ppm	$\delta^{13}C$/ppm
a	-	176
b	-	137.5
c/d	7.6, dd, 4H	129.5, 119.5
e		155.2
NH	7.8, bs,1H,	-
Co-C≡O	-	200
μ₃-CCo₃	-	199

A crystal of $[(CO)_9Co_3(\mu_3\text{-CCON(H)}\text{-}p\text{-}C_6H_4(\mu_3\text{-C})Co_3(CO)_9]$ suitable for X ray diffraction was grown from a dichloromethane / hexane solution in a freezer. The resultant structure is shown in Figure 4.3.
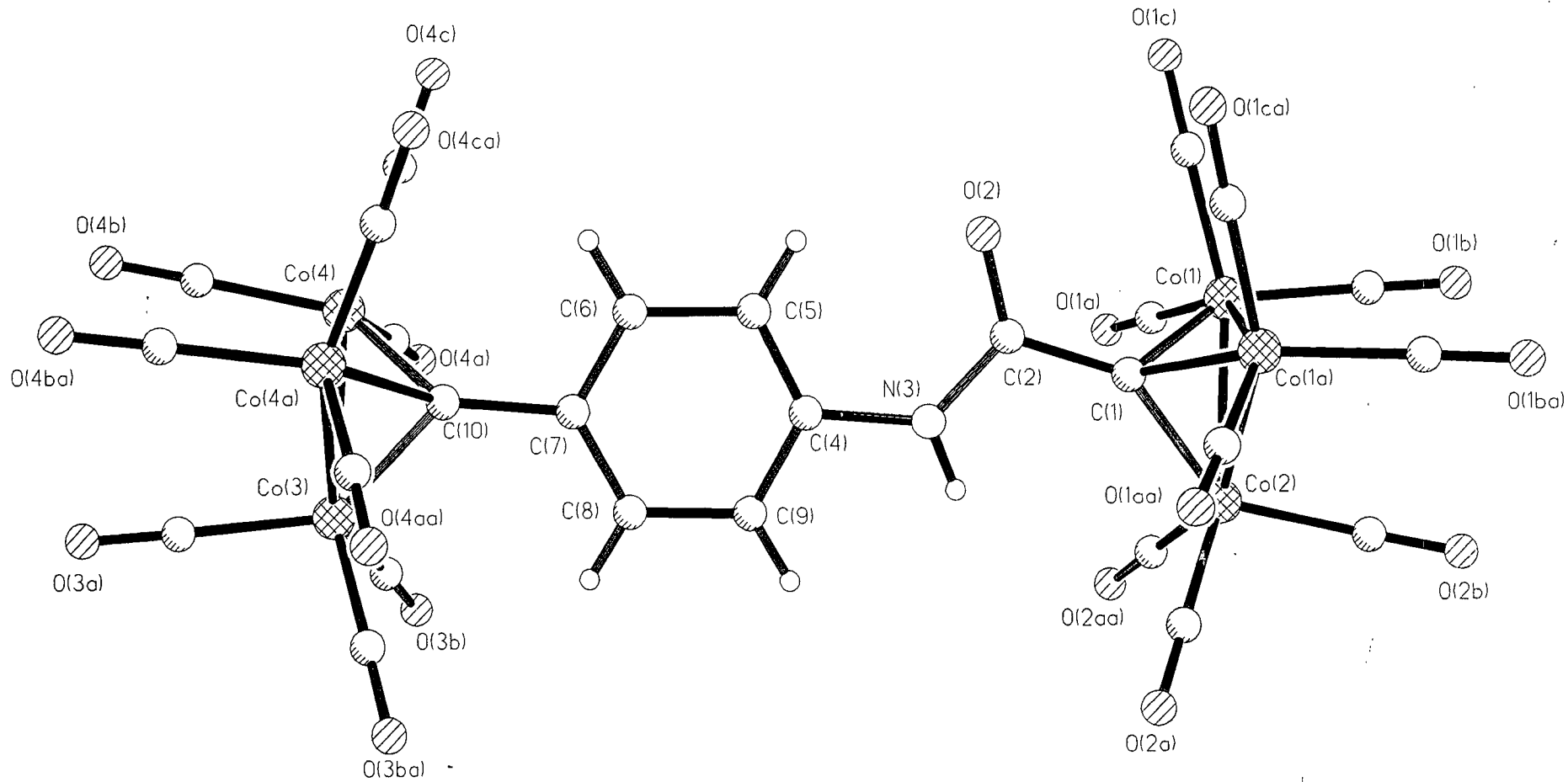
Figure 4.3: Molecular structure of [(CO)$_9$Co$_3$(μ_3-CCON(H)-p-C$_6$H$_4$(μ_3-C)Co$_3$(CO)$_9$], (18)

Significant bond lengths (Å) and angles (°) for $[(CO)_9Co_3(\mu_3\text{-CCON(H)-}p\text{-}C_6H_4(\mu_3\text{-C})Co_3(CO)_9]$:

Co(1)-C(1) 1.891(4), Co(1)-Co(2) 2.4602(10), Co(2)-C(1) 1.905(6), Co(3)-C(10) 1.895(6), Co(3)-Co(4) 2.4670(10), Co(4)-C(10) 1.916(5), C(2)-O(2) 1.225(9), C(2)-N(3) 1.356(8), C(2)-C(1) 1.506(9), N(3)-C(4) 1.451(9), C(4)-C(5) 1.346(10), C(4)-C(9) 1.372(9), C(5)-C(6) 1.443(10), C(6)-C(7) 1.359(9), C(7)-C(8) 1.371(10), C(7)-C(10) 1.522(10), C(8)-C(9) 1.420(10), C(1)-Co(1)-Co(2) 49.8(2), C(1)-Co(2)-Co(1) 49.37(13), C(10)-Co(3)-Co(4) 50.04(14), C(10)-Co(4)-Co(3) 49.3(2), O(2)-C(2)-N(3) 123.6(7), O(2)-C(2)-C(1) 121.9(6), N(3)-C(2)-C(1) 114.5(6), C(2)-N(3)-C(4) 127.9(6), C(5)-C(4)-C(9) 123.9(7), C(5)-C(4)-N(3) 121.3(6), C(9)-C(4)-N(3) 114.8(6), C(4)-C(5)-C(6) 116.9(7), C(7)-C(6)-C(5) 120.5(7), C(6)-C(7)-C(8) 121.0(7), C(6)-C(7)-C(10) 115.9(7), C(8)-C(7)-C(10) 123.1(6), C(7)-C(8)-C(9) 119.4(7), C(4)-C(9)-C(8) 118.3(7), C(2)-C(1)-Co(1) 124.4(3), C(2)-C(1)-Co(2) 143.9(5), Co(1)-C(1)-Co(2) 80.8(2), C(7)-C(10)-Co(3) 129.8(5), C(7)-C(10)-Co(4) 132.8(2), Co(3)-C(10)-Co(4) 80.7(2),

The structure shows two cluster units bound *para* to each other through the aniline system, one cluster being bound from the apical cluster carbon to the aromatic ring, the second cluster bound to the system *via* an amide functionality. Figure 4.4 shows a space filling diagram of the molecule, the carbonyl ligands are omitted for clarity.
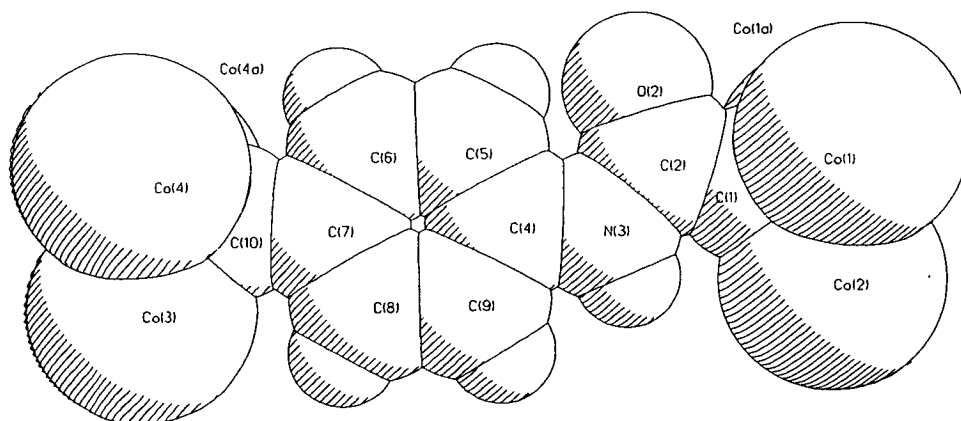
Figure 4.4: Space filling diagram of

$[(CO)_9Co_3(\mu_3\text{-CCON(H)-}p\text{-}C_6H_4(\mu_3\text{-C})Co_3(CO)_9]$

There is a plane of symmetry through the plane of the aromatic ring, as can be seen from the projection in Figure 4.5. The carbonyl ligands have been omitted for clarity.
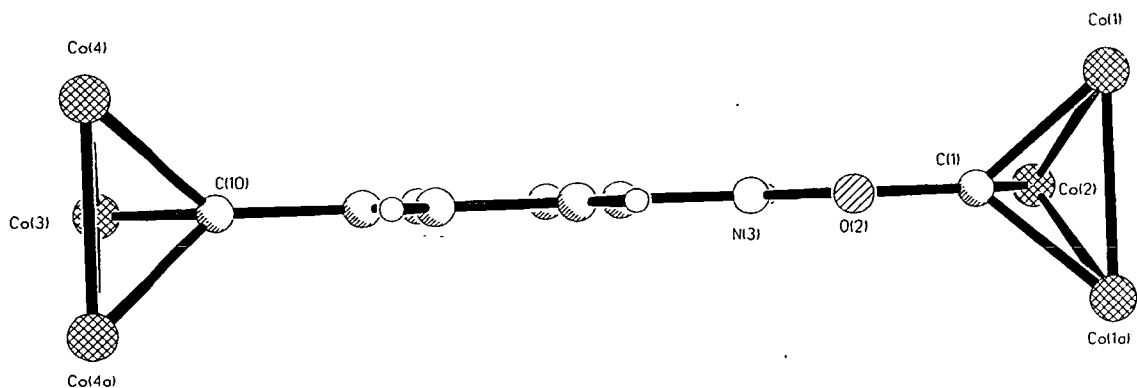
Figure 4.5: Side projection of $[(CO)_9Co_3(\mu_3\text{-}CCON(H)\text{-}p\text{-}C_6H_4(\mu_3\text{-}C)Co_3(CO)_9]$

Figure 4.6 shows this view as a space filling diagram. Again, the carbonyl ligands have been omitted for clarity.
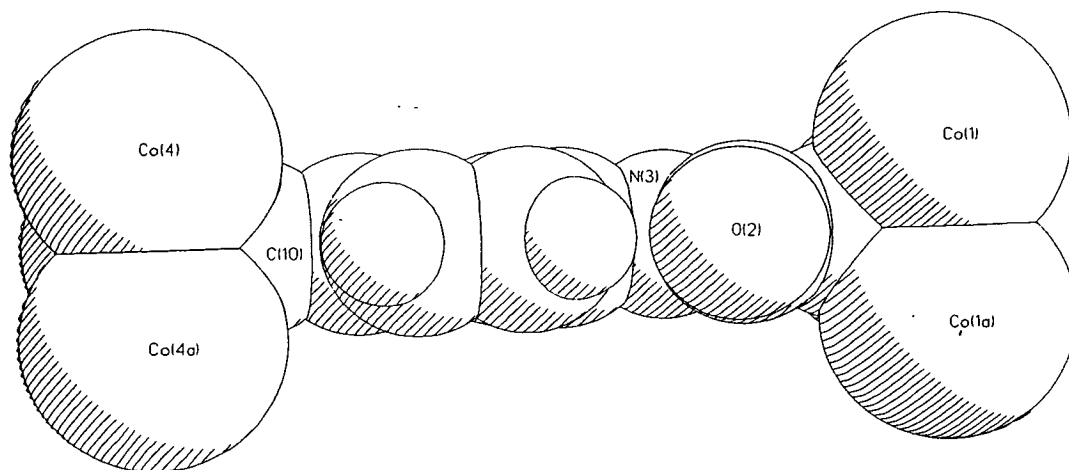
Figure 4.6: Space filling diagram (side view) of
$[(CO)_9Co_3(\mu_3\text{-}CCON(H)\text{-}p\text{-}C_6H_4(\mu_3\text{-}C)Co_3(CO)_9]$

4.2.1 Electrochemistry of the amide linked dicluster

An electrochemical study of the amide linked dicluster was undertaken. Cyclic voltammetry of [(CO)$_9$Co$_3$(μ_3-CCON(H)-p-C$_6$H$_4$(μ_3-C)Co$_3$(CO)$_9$], in dichloromethane / 0.5M [TBA][BF$_4$], at room temperature showed two reversible reductions and an irreversible oxidation, as shown in Figure 4.7.
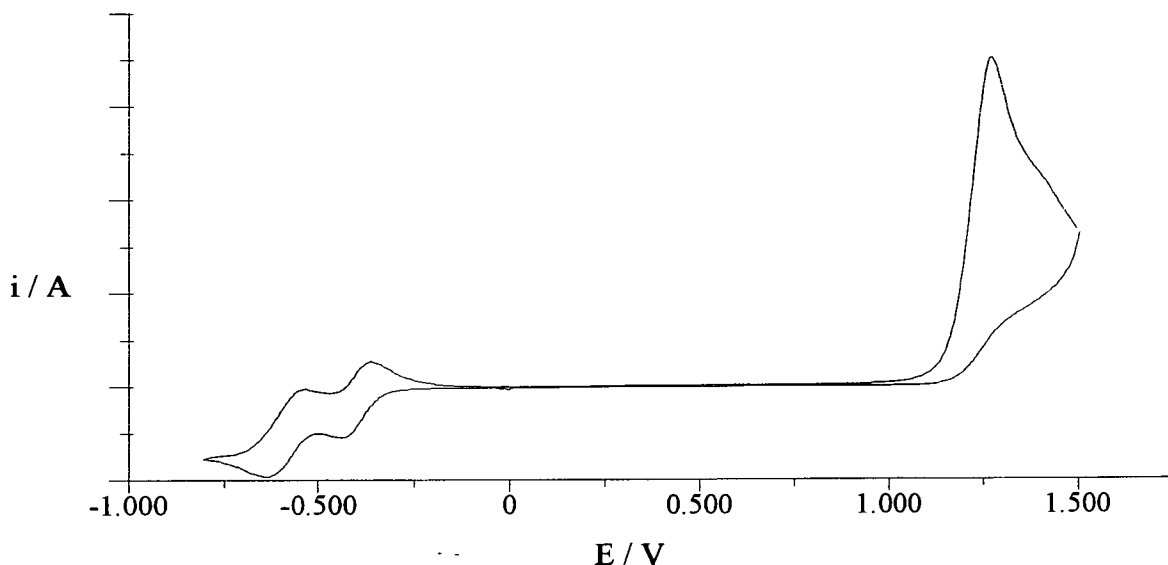
Figure 4.7: CV of [(CO)$_9$Co$_3$(μ_3-CCON(H)-p-C$_6$H$_4$(μ_3-C)Co$_3$(CO)$_9$] in CH$_2$Cl$_2$ /0.5 M [TBA][BF$_4$] at room temperature (vs. Ag/AgCl).

Figure 4.8 shows an expansion of the two reversible reductions.
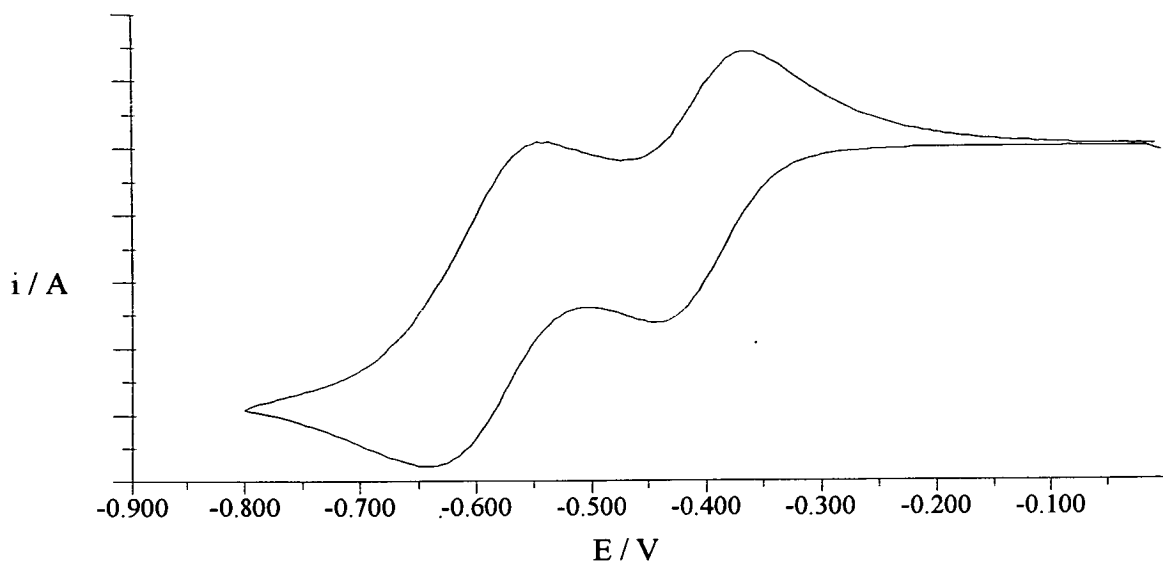
Figure 4.8: Reversible reductions of

$[(CO)_9Co_3(\mu_3\text{-}CCON(H)\text{-}p\text{-}C_6H_4(\mu_3\text{-}C)Co_3(CO)_9]$

in CH_2Cl_2 /0.5 M [TBA][BF$_4$] at room temperature (vs. Ag/AgCl).

The two reversible reductions (one for each cluster unit) were found to be of 1 electron each, by addition of a molar equivalent of ferrocene. Coulometry of the complex was attempted, but was unsuccessful due to decomposition of the complex. The four electron oxidation is irreversible at all temperatures studied (-30 to 25°C), and leads to decomposition of the complex and coating of the working electrode.

The reduction at $E_{1/2}$ = -0.406 V can be assigned to the cluster unit bound to the carbonyl group of the amide link. This is because the $[(CO)_9Co_3(\mu_3\text{-}CC=O)]$ unit is a better electron withdrawing group than the $[p\text{-}C_6H_4(\mu_3\text{-}C)Co_3(CO)_9]$ unit, which shows reversible reduction at $E_{1/2}$ = -0.584 V. The value of $E_{1/2}$ for the amide bound cluster is very similar to that observed in the ferrocene derivative $[(CO)_9Co_3(\mu_3\text{-}C(CO)NHFc)]$ by Robinson [7], at -0.41 V.

4.3 Attempted coupling of other cluster species

Following the successful coupling of the two cluster units, it was decided to pursue this avenue of research and to try and couple clusters of different metals. Several other clusters with a required nucleophilic functionality were in hand, as part of the studies reported in chapter 3. It was therefore hoped that reaction of the compound $[(OC)_9Co_3(\mu_3\text{-}CCO)^+]$ (PF_6^-) with hydroxy functionalised clusters would produce multicluster species linked by the resultant ester functionality. This idea is not wholly without precedent, as many nucleophiles have been reacted with the tricobalt decacarbonyl cation, including but-2-yne diol, which was then further reacted with dicobalt octacarbonyl to form the tricluster species outlined in Scheme 4.4 [11].
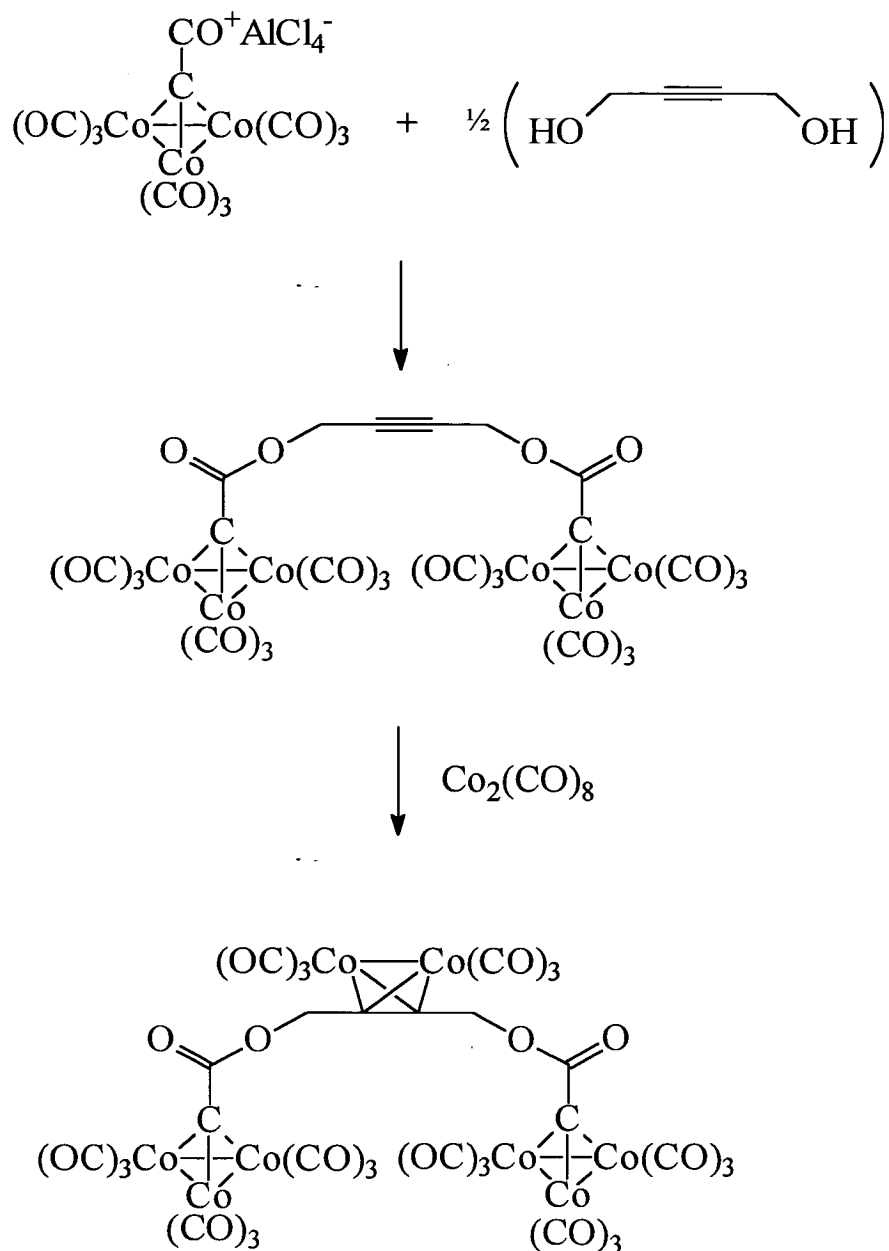
Scheme 4.4: Synthesis of tricluster species

Hence reaction of $[(OC)_9Co_3(\mu_3\text{-}CCO)^+]$ (PF_6^-) with the dicobalt hexacarbonyl capped alkyne $(HOCH_2C)_2Co_2(CO)_6$ also produced the known tricluster species $[(OC)_9Co_3(\mu_3\text{-}CCOOCH_2C)]_2Co_2(CO)_6$ [11]. This experiment was intended to prove that a cluster could be attached to a ligand with another cluster very close to the site of attachment of the $[(OC)_9Co_3(\mu_3\text{-}CCO)]$ moiety. However, similar reactions with

functionalised triosmium clusters failed to yield multicluster products. The first reaction attempted is outlined in Scheme 4.5.
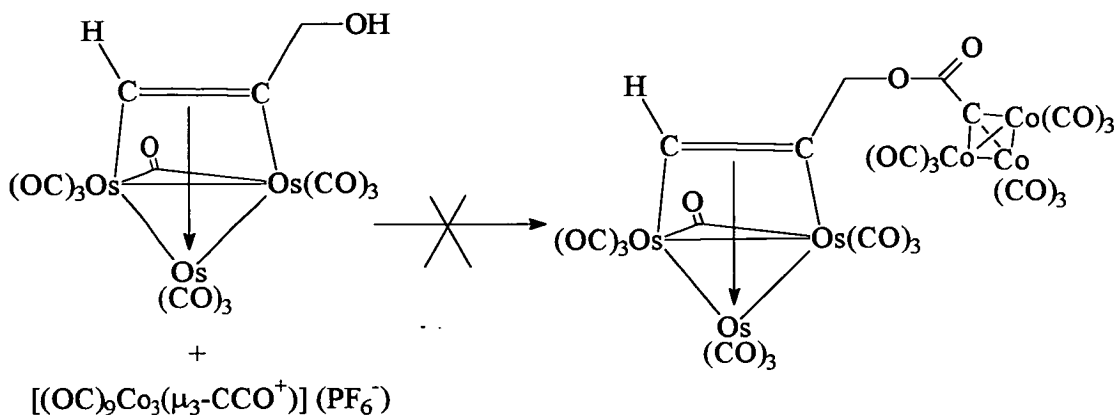
Scheme 4.5: Attempted reaction with $Os_3(CO)_9(\mu\text{-}CO)(\mu_2\text{-}\eta^3\text{-}HC{\equiv}CCH_2OH)$

Addition of the triosmium decacarbonyl ($\mu\text{-}\eta^3$- propargyl alcohol) cluster yielded mainly the cluster acid, $(OC)_9Co_3(\mu_3\text{-}CCOOH)$, a small amount of triosmium dodecacarbonyl, and a large amount of decomposition products from the triosmium clusterwhich were ionic in nature and were confined to the baseline of the chromatographic plate.

The analagous reaction was attempted with the triosmium decacarbonyl (μ_2-η^3- but-2-yne-diol) species, as outlined in Scheme 4.6.
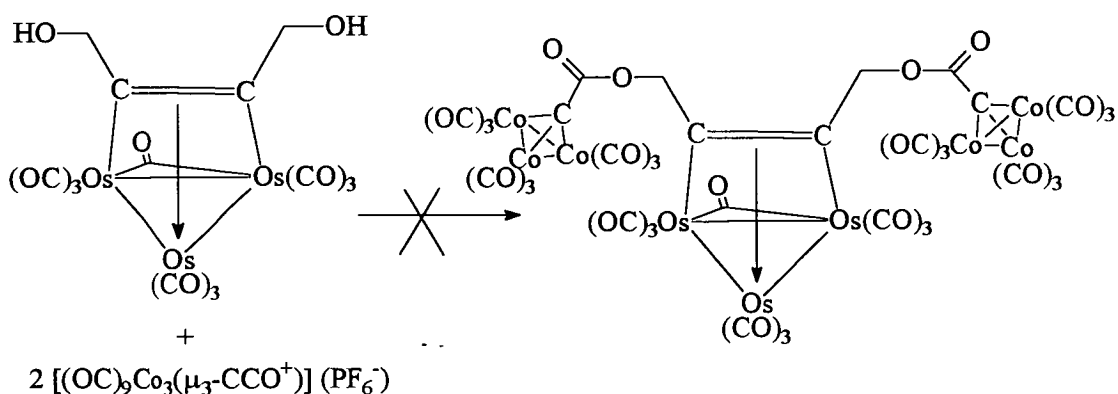
Scheme 4.6: Attempted coupling to $Os_3(CO)_9(\mu\text{-}CO)(\mu_2\text{-}\eta^3\text{-}(CCH_2OH)_2)$

114

This reaction is also analagous to the successful reaction between [(OC)$_9$Co$_3$(μ_3-CCO)$^+$] (PF$_6^-$) and the dicobalt hexacarbonyl species, [Co$_2$(CO)$_6$(HOCH$_2$C)$_2$] (*vide supra*). Therefore it would appear that the greater steric bulk of the triosmium cluster, compared to that of the dicobalt cluster, is preventing any successful coupling of the triosmium and tricobalt species. One possible method of surmounting this problem would be to increase the length of the CH$_2$ chain between the triosmium cluster and the ligand OH functionality. However, this would also produce problems regarding characterisation- increasing the length of the CH$_2$ chain would lower the melting point of the complex, and also increase the chance of disorder in any resulting crystalline species. A further problem is that of intramolecular nucleophilic attack: if the CH$_2$ chain were long and flexible enough, the hydroxyl group may then be able to attack the alkyne functionalised end of the ligand, leading to cyclisation [14] *via* isomerisation.

One final attempt was made, utilising the allyl cluster diol [Os$_3$(CO)$_8$(μ-CO){(HOCH$_2$C$_2$H)$_2$(CO)}], as outlined in scheme 4.7. As before, the identified products of the reaction were the carboxymethylidyne tricobalt nonacarbonyl, some triosmium dodecacarbonyl, and a large amount of ionic breakdown products.
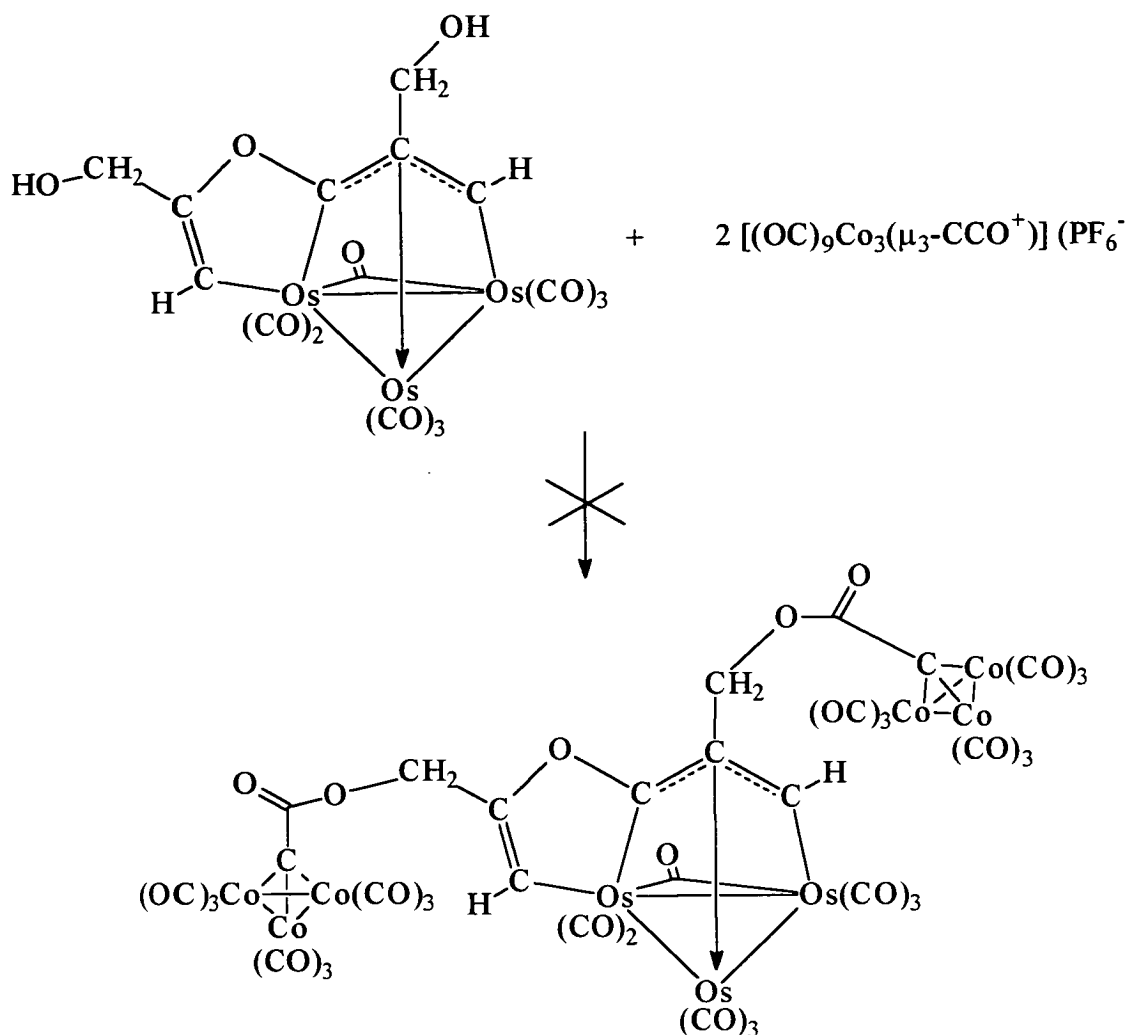
Scheme 4.7: Attempted reaction with $[Os_3(CO)_8(\mu\text{-}CO)\{(HOCH_2C_2H)_2(CO)\}]$

4.4 Concluding remarks

Whilst reaction of carboxymethylidyne tricobalt nonacarbonyl with activated triosmium clusters failed to yield multicluster products, some success was achieved by using the tricobalt decacarbonyl cation as a ligand source. Hence, reaction of $[(OC)_9Co_3(\mu_3\text{-}CCO)^+]$ (PF_6^-) with $(OC)_9Co_3(\mu_3\text{-}CC_6H_4NH_2)$ yielded the dicluster species $[(CO)_9Co_3(\mu_3\text{-}CCON(H)\text{-}p\text{-}C_6H_4(\mu_3\text{-}C)Co_3(CO)_9]$. This novel compound was characterised by infrared, FABMS, ^1H and ^{13}C NMR, as well as by X ray crytsallography and cyclic voltammetry. Some evidence also suggested the synthesis of the tricluster tertiary amide species $[(CO)_9Co_3CC_6H_4N\{CO(\mu_3\text{-}C)Co_3(CO)_9\}_2]$.

Reaction of $[(OC)_9Co_3(\mu_3\text{-}CCO)^+]$ (PF_6^-) with the dicobalt hexacarbonyl species, $[Co_2(CO)_6(HOCH_2C)_2]$ produced the known compound $[(OC)_9Co_3(\mu_3\text{-}CCOOCH_2C)]_2Co_2(CO)_6$ [11]. However, reactions between $[(OC)_9Co_3(\mu_3\text{-}CCO)^+]$ (PF_6^-) and the functionalised triosmium clusters $[Os_3(CO)_{10}(HC\equiv CCH_2OH)]$, $[Os_3(CO)_{10}(HOCCH_2C\equiv CCH_2OH)]$ and $[Os_3(CO)_9\{(HOCH_2C\equiv CH)_2CO\}]$, failed to yield any multicluster products. This is thought to be due to the increased steric bulk of the triosmium species in comparison to that of the dicobalt cluster unit. Further studies, using CH_2 units to increase the distance from the triosmium cluster and the ligand OH function are needed.

4.5 References

1.   R. L. Sturgeon, M. M. Olmstead and N. E. Schore, *Organometallics*, 1991, **10**, 1649

2.   W. Cen, K. J. Haller and T. P. Fehlner, *Organometallics*, 1992, **11**, 3499

3.   W. Cen, K. J. Haller and T. P. Fehlner, *Inorg. Chem.*, 1993, **32**, 995

4.   W. Cen, P. Lindenfeld and T. P. Fehlner, *J. Am. Chem. Soc.*, 1992, **114**, 5451

5.   B. M. Peake, B. H. Robinson, J. Simpson and D. J. Watson, *Inorg. Chem.*, 1977, **16**, 405

6.   B. M. Peake, B. H. Robinson, J. Simpson and D. J. Watson, *Inorg. Chem.*, 1977, **16**, 410

7.   B. H. Robinson, J. Simpson and M. E. Trounson, *Aust. J. Chem.*, 1986, **39**, 1435

8.   G. H. Worth, B. H. Robinson and J. Simpson, *Organometallics*, 1992, **11**, 3863

9.   J. N. Nicholls and M. D. Vargas, *Inorg. Synth.*, 1989, **26**, 289

10.   J. E. Hallgren, C. S. Eschbach and D. Seyferth, *J. Am. Chem. Soc.*, 1972, **94**, 2547

11.   D. Seyferth, J. E. Hallgren and C. S. Eschbach, *J. Am. Chem. Soc.*, 1974, **96**, 1730

12.   D. Seyferth, J. E. Hallgren, R. J. Spohn, G. H. Williams and P. L. K. Hung, *J. Organomet. Chem.*, 1974, **65**, 99

13.   J. Barluenga, A. M. Bayon, J. Perez-Preito and G. Asensio, *Tetrahedon*, 1984, **40**, 5053

14.   S. Aime and A. J. Deeming, *J. Chem. Soc. Dalton Trans.*, 1983, 1807

Chapter 5.

Experimental

5.1 General experimental procedures and instrumentation

5.1.1   Synthesis

All experiments were carried out under an atmosphere of nitrogen, using freshly distilled solvents, unless otherwise stated.   Materials were obtained from commercial suppliers and used without further purification, with the exception of trimethylamine N-oxide, which was purchased as the dihydrate and dried by a Dean and Stark distillation overnight in benzene.   The dried trimethylamine N-oxide was sublimed *in vacuo* immediately prior to use.   Subsequent work-up of reaction products was achieved with laboratory-grade solvents without precautions to exclude air.   Reactions were monitored by thin-layer chromatography (TLC) on 5x20 cm Polygram Sil G/UV$_{254}$ supplied by Camlab.

5.1.2   Separations

All separations were achieved chromatographically on silica.   Column chromatography was carried out using an appropriately sized glass column packed with Silica gel 60 ASTM, 230-400 mesh (0.040-0.063 mm) supplied by Merck. Columns were eluted with solvent mixtures prepared from laboratory grade solvents. Preparative thin layer chromatography was carried out using plates supplied by Merck with a layer of Merck Kieselgel 60 F$_{254}$.

5.1.3 Infrared spectroscopy

Infrared spectra were recorded on a Perkin Elmer 1600 series FTIR spectrometer, calibrated with carbon monoxide, in CH_2Cl_2 (unless stated otherwise) using 0.1 mm path length NaCl cells.

5.1.4 Mass spectroscopy

Positive fast atom-bombardment mass spectra (FABMS) were obtained using a Kratos MS 50TC spectrometer, employing CsI as a calibrant. 3-Nitrobenzyl alcohol was used as a matrix.

5.1.5 NMR spectroscopy

Nuclear magnetic Resonance (NMR) spectra were recorded using a Bruker WP 200SY spectrometer for ^{1}H and ^{13}C NMR, referenced to an internal $SiMe_4$ standard. In some instances, ^{1}H NMR spectra were recorded by the author on a Jeol PMX60 instrument, referenced to an external $SiMe_4$ standard.

5.1.6 Single crystal X ray diffraction analysis

Diffraction data were collected on a Stoë Stadi 4-circle diffractometer. An Oxford Cryosystems device was used for low temperature data collection.[1] The appropriate crystal data, data collection and structure refinement parameters are presented in the text, and full crystallographic listings are given in the appropriate experimental section. All refinements were carried out using the crystallographic program SHELXL 93 [2], and all figures were produced using SHELXTL PC [3].

5.1.7 Gel permeation chromatography

Gel Permeation Chromatography was performed on a PL Gel Mix C column, calibrated against a broad calibration polystyrene standard, from 500 to 4×10^6 daltons. The unit was controlled by a Perkin Elmer Series 2 HPLC Pump and a Perkin Elmer ISS100 autosampler. Refractive Index detection was achieved with an Erma ERC 7510 Refractive Index Detector. UV-VIS detection was performed with Waters 990 and Waters 994 Photodiode Arrays. Data processing was performed using Waters Millenium Software v2.0 and Waters Revision 4 Software.

5.1.8 Particle size analysis

Particle size analysis was performed using a Malvern Autosampler.

5.1.9 Electrochemistry

Cyclic voltammetry was carried out using an Autolab with a PGSTAT 20 potentiostat, using GPES 4.2 software. A three electrode system was used, with platinum microdisc working electrode, platinum working electrode and Ag/AgCl reference. Experiments were conducted in degassed 0.5 M dichloromethane solution of TBA BF$_4$.

5.2   Experimental details for chapter 2

5.2.1   Preparation of Chloromethylidynetricobalt nonacarbonyl [4], [(CO)$_9$Co$_3$(μ_3-CCl)] (1).

Dicobalt octacarbonyl (9.03 g, 26.9 mmol) was dissolved in carbon tetrachloride (400 cm^3). The mixture was stirred at 60°C for a period of 24 hours. Spot tlc indicated almost complete consumption of brown starting material and formation of a purple product. Water (200 cm^3) was added and the lower organic

layer was separated and dried over anhydrous magnesium sulphate for 30 minutes. The product was filtered through a coarse glass frit with suction, absorbed onto silica and the solvent removed *in vacuo*. The residue was separated by column chromatography on silica using hexane as eluent. The product was characterised spectroscopically as [(CO)$_9$Co$_3$(μ_3-CCl)] (1) (purple solid, 6.045 g, yield = 47%).

Spectroscopic data for [(CO)$_9$Co$_3$(μ_3-CCl)] (1):
IR (hexane): ν(CO) 2109(w), 2062(vs), 2046(s) and 2029(w) cm^{-1}.
FABMS: M = 476 (calc: 476.5), plus sequential loss of CO.

5.2.2 Preparation of Carbonylethoxymethylidynetricobalt nonacarbonyl[5], [(CO)$_9$Co$_3$(μ_3-CCO$_2$C$_2$H$_5$)] (2).

Chloromethylidyne tricobalt nonacarbonyl, [(CO)$_9$Co$_3$(μ_3-CCl)], (1) (6.045 g, 12.6 mmol) was dissolved in dichloromethane (600 cm^3) at room temperature. Aluminium trichloride (5.07 g, 38 mmol, 3.1 mol equivalent) was added and the mixture was stirred for 30 mins during which time the solution turned brown. At this point tlc indicated that none of the purple chloromethylidynetricobalt nonacarbonyl remained, only a single brown spot (R$_f$ = 0) was observed indicating the presence of the methylidynetricobalt decacarbonyl cation. To the brown solution, excess ethanol (200 cm^3) was added giving an instantaneous purple colour to the solution. The mixture was stirred for 1 hour. The solvent was removed *in vacuo* and the residue purified by column chromatography on silica using a mixture of hexane-dichloromethane (1:1, v/v) as eluent. The product was characterised spectroscopically as [(CO)$_9$Co$_3$(μ_3-CCO$_2$C$_2$H$_5$)] (2), (purple solid, 5.132 g, yield = 79%).

Spectroscopic data for [(CO)$_9$Co$_3$(μ_3-CCO$_2$C$_2$H$_5$)] (2):
IR (CH$_2$Cl$_2$): ν(CO) 2110(m), 2065(vs), 2040(s), 2020(w) and 1990(vw) cm^{-1}.
FABMS: M = 515 (calc. = 514) with initial fragmentation showing loss of nine CO ligands.
NMR (200 MHz, acetone D$_6$) : δ^1H/ppm = 4.36 (dd, 2H), 2.05 (t, 3H). δ^{13}C/ppm = 204.6 (Co(CO)), 198.5 (μ_3-C), 60.5(CH$_2$), 12.9(CH$_3$)

5.2.3 Preparation of allyloxycarbonylmethylidyne tricobalt nonacarbonyl [(CO)₉Co₃(μ₃-CCOOCH2CH=CH2)], (3).

Chloromethylidyne tricobalt nonacarbonyl, [(CO)₉Co₃(μ₃-CCl)], (1) (0.58 g, 1.22 mmol) was dissolved in dichloromethane (25 cm³) at room temperature. Aluminium trichloride (0.49 g, 3.68 mmol, 3.0 molar equivalents) was added and the mixture was stirred for 30 mins during which time the solution changed from purple to brown. Spot tlc indicated that none of the chloromethylidynetricobalt nonacarbonyl remained, only a single brown spot (R$_f$= 0) was observed indicating the presence of the methylidynetricobalt decacarbonyl cation. To the brown solution an excess (5 ml) of allyl alcohol was added dropwise *via* syringe, producing an instantaneous purple colour to the solution. The mixture was stirred for 1 hour, after which time tlc indicated complete consumption of the brown tricobalt methylidyne decacarbonyl species, and the appearance of a purple product. The solvent was removed *in vacuo* and the residue purified by column chromatography on silica using a solution of hexane-dichloromethane (1:1, v/v) as eluent, to yield 0.43 g purple solid. (yield = 67%) The product was characterised spectroscopically as allyloxycarbonylmethylidyne tricobalt nonacarbonyl, [(CO)₉Co₃(μ₃-CCOOCH₂CH=CH₂)].

A crystal suitable for X ray diffraction was grown by vacuum sublimation.

Spectroscopic data for [(CO)₉Co₃(μ₃-CCOOCH₂CH=CH₂)] (3):
IR (CH₂Cl₂) : ν(CO) = 2104 (m), 2064 (vs), 2046 (vs), 1681 (m) cm⁻¹.
NMR (200MHz, CDCl₃): δ¹H = 5.93-6.12 (m,1H), 5.26 (dd, 1H, J$_{cis}$ = 18.8 Hz, J$_{gem}$ = 1.27 Hz), 5.37 (dd, 1H, J$_{trans}$ = 10.3 Hz, J$_{gem}$ = 1.27 Hz), 4.77 - 4.81 (m,2H).
FABMS: M+3 = 527, plus sequential loss of 9 CO ligands.
Crystal data: C$_{14}$H$_5$Co$_3$O$_{11}$, M = 525.97, triclinic, space group P-1. a = 7.879(5), b = 8.719(6), c = 15.182(9)Å, α = 73.48(5), β = 78.87(5), γ = 67.51(5)°, U = 919.7Å³, D$_{calc}$ = 1.899 gcm⁻³, Z = 2, dark red crystal 0.23 x 0.15 x 0.08 mm, T = 150.0(1)K. R1 = 0.0258 [reflections with F > 4σ(F)]. wR2 = 0.0575, for 3054 independent reflections, corrected for absorption and 259 parameters.

5.2.4 Preparation of propargyloxycarbonylmethylidyne tricobalt nonacarbonyl [(CO)$_9$Co$_3$(μ_3-CCOOCH$_2$C≡CH)], (4).

To a dichloromethane solution (30 ml) of 0.60 g (1.26 mmol) chloromethylidyne tricobalt nonacarbonyl (1) was added 0.5 g (3.75 mmol) aluminium trichloride. The mixture was stirred until a brown solution had formed, and tlc showed the absence of any purple starting material and the presence of only one species of $R_f = 0$ (indicating the formation of [(CO)$_9$Co$_3$(μ_3-CCO)]$^+$ [AlCl$_4$]$^-$). Excess propargyl alcohol (4 ml) was added dropwise and the solution turned purple immediately. The reaction mixture was stirred for a further 30 minutes. Spot tlc showed the presence of only one product, a purple species of $R_f = 0.8$. Solvent was removed in vacuo and the product purified by column chromatography on silica. This realised 0.20 g (30%) of a purple solid, which was found to decompose rapidly after isolation to form an insoluble brown solid.

Spectroscopic data for [(CO)$_9$Co$_3$(μ_3-CCOOCH$_2$C≡CH)] (4):
IR :(CH$_2$Cl$_2$) : ν(CO) = 2110 (w), 2095 (w), 2065 (vs), 2046 (vs), 1681 (w).
NMR (60MHz, CDCl$_3$): δ ^{1}H (ppm) = 2.5 (m, 1H), 5.0 (d, 2H)

5.2.5 Preparation of ethoxyacrylylmethylidyne tricobalt nonacarbonyl [(CO)$_9$Co$_3$(μ_3-CCOOCH$_2$CH$_2$OCOCH=CH$_2$)], (5).

Chloromethylidyne tricobalt nonacarbonyl (1) (0.50 g, 1.05 mmol) was dissolved in 60 ml dichloromethane. Aluminium trichloride (0.42 g, 3.16 mmol, *ca.* 3 molar equivalents) was added and the reaction mixture was stirred at room temperature until tlc showed only one species of $R_f = 0$ present. Excess 2-hydroxyethylacrylate was added dropwise with stirring. The addition of the nucleophile affected an instananeous colour change from brown to purple. The mixture was stirred for a further 30 minutes before being filtered through celite. The solvent was removed *in vacuo*, and the product purified by column chromatography on silica with gradient elution, starting with hexane and finishing with acetone. The main product isolated was 0.48 g of a purple oil (yield = 78%) which was characterised spectroscopically as [(CO)$_9$Co$_3$(μ_3-CCOOCH$_2$CH$_2$OCOCH=CH$_2$)].

Spectroscopic data for [(CO)₉Co₃(μ₃-CCOOCH₂CH₂OCOCH=CH₂)], (5):

IR(CH₂Cl₂) : ν(CO) = 2109(m), 2062(vs), 2046(vs), 1724(m), 1681(m) cm-1.

NMR (200MHz, CDCl₃) : δ¹H/ppm: 6.38 (dd, 1H, J$_{trans}$ = 10.4, J$_{gem}$ = 1.6 Hz), 6.05 (dd, 1H, J$_{cis}$ = 17.2, J$_{trans}$ = 10.4Hz), 5.80 (dd, 1H, J$_{cis}$ = 17.2, J$_{gem}$= 1.6Hz), 4.54 (m, 2H), 4.44 (m, 2H), δ¹³C/ppm: 199.0 (CoC≡O), 178.5 (μ₃-C), 170.0 (C=O), 165.8 (C=O), 130.9 (CH₂), 128.2 (CH), 63.5 (CH₂), 62.6 (CH₂),

FABMS: m+3 = 587, sequential loss of 9 CO ligands

5.2.6 Preparation of polymer (6) containing the tricobalt nonacarbonyl species: solution polymerisation of ethoxyacrylylmethylidyne tricobalt nonacarbonyl (5).

A 2 litre reaction flask fitted with a reflux condensor, overhead stirrer, thermocouple, nitrogen bubbler and two feed inlets was charged with 180 g methoxy-2-propanol and flushed with nitrogen. The feedstocks were (i) 10 g (*i.e.* 5% w/w) azo[*bis*(ethylnitrile)] in 20 g 1-methoxy-2-propanol, and (ii) 10 g ethoxyacrylylmethylidyne tricobalt nonacarbonyl (5), 118 g methyl methacrylate and 72 g *n*-butyl acrylate. The reaction flask and charge were heated to 60°C, and the feedstocks added simultaneously over a period of 2 hours at a constant rate of addition *via* peristaltic pump. The reaction mixture was then allowed to cool to ambient temperature under a flow of nitrogen. Room temperature evaporation of the volatile components showed that the resultant solution contained 10.84% polymer. Spot tlc indicated complete consumption of monomer, and IR spectroscopy showed the presence of terminal metal carbonyl groups. GPC chromatography showed that the polymer had a molecular weight average of 28,391 daltons, with a peak molecular weight of 24,180 daltons. UV-VIS of the polymer species eluted from the GPC column confirmed the presence of the cluster unit by monitoring the signals obtained at 230 and 300 nm.

Spectroscopic data for solution polymer (6):

IR (polymer film): ν(CO) = 2111(w), 2064(vs), 2047(m) cm⁻¹.

GPC (daltons) : weight average: 28391, peak molecular weight : 24180

UV-VIS : monitoring the UV-VIS signal at 300 and 230nm confirmed the presence of the cobalt cluster in the eluting polymer species.

Solids : 10.84%

5.2.7 Preparation of polymer (7) containing the tricobalt nonacarbonyl species: emulsion polymerisation of ethoxyacrylylmethylidyne tricobalt nonacarbonyl (5).

A 3 litre reaction vessel equipped with overhead stirrer, reflux condenser, nitrogen bubbler, thermocouple and two feedstock inlets was charged with 482 g deionised water, 7.6 g surfactant and 0.88 g borax. The temperature of the aqueous charge was raised to 60°C and the apparatus flushed with nitrogen and stirred for 30 minutes. A seed shot of monomers, comprising of 23.6 g methyl methacrylate, 14.4 g n-butyl acrylate and 2 g ethoxyacrylylmethylidyne tricobalt nonacarbonyl (5) was added and stirred for 10 minutes. A primary seed shot of initiator, consisting of 0.16 g t-butyl hydroperoxide in 11.74 g water, was added. After 10 minutes stirring, the secondary seed shot of initiator (0.16 g sodium metabisulphite in 4.64 g water) was added. After 20 minutes, the particle size of the seed polymer was checked to confirm that polymerisation was taking place. A monomer feed comprising of 18 g ethoxyacrylylmethylidyne tricobalt nonacarbonyl (5), 212.4 g methyl methacrylate and 129.6 g n-butyl acrylate was added to the seed polymer suspension over a period of 3 hours. Simultaneously and at the same rate of addition, the initiator feed of 0.87 g sodium metabisulphite in 25.23 g water was added to the reaction. After the addition of the feedstocks the reaction mixture was allowed to cool to ambient temperature before being filtered. A final particle size analysis was performed to confirm polymerisation. The presence of terminal metal carbonyl species was confirmed by IR and UV-VIS spectroscopy.

Spectroscopic data for emulsion polymer (7):
IR (polymer film): $\nu(CO) = 2111(w), 2064(vs), 2046(m)$ cm^{-1}.
Particle Size : average particle size : 135.9 nm
GPC (daltons) : weight average : 42290, peak molecular weight : 40620
UV-VIS : monitoring the UV-VIS signal at 300 and 230nm confirmed the presence of the cobalt cluster in the eluting polymer samples.
Solids : 39.94%

5.2.8 Preparation of Methylidynetricobalt nonacarbonyl [6]

[(CO)₉Co₃(μ₃-CH)], (8).

Dicobalt octacarbonyl (17 g, 49.7 mmol) was dissolved in a solution of THF (500 cm³) and tribromomethane (3 cm³, ca. 7 g, 5/9 mol equivalent). The mixture was stirred under reflux at 50°C for 12 hours. Spot tlc indicated complete consumption of the brown starting material. Ethyl acetate was added (100 cm³) and the solution filtered through celite with subsequent washes of ethyl acetate. The solvent was removed *in vacuo* and the residue purified by column chromatography on silica using dichloromethane as eluent. The single product was characterised as [(CO)₉Co₃(μ₃-CH)] 4 (purple, 5.23 g, yield = 24%).

Spectroscopic data for [(CO)₉Co₃(μ₃-CH)], (8):
IR (CH₂Cl₂) : ν(CO) 2105(m), 2060(vs), 2045(s), 2025(w) cm⁻¹.
FABMS: m-1 = 441, plus sequential loss of carbonyl ligands

5.2.9 Preparation of alkyd polymer (9)

A three litre round bottom flask, fitted with a Dean and Stark trap, reflux condenser, overhead stirrer, thermocouple and dropping funnel was charged with 1100 g soya bean oil and 0.55 g lithium hydroxide monohydrate. The flask and contents were heated to 110°C, at which time 273 g pentaerythritol in 27.55 g xylene was added and melted into the reaction mixture. The temperature of the reaction mixture was raised to 240°C to affect the transetherification reaction. After 2 hours the solution had changed appearance from cloudy to clear. At this point 453 g phthalic anhydride was washed into the flask with 23 g xylene and the reaction mixture allowed to reflux to·remove the water produced by the condensation polymerisation. The water was collected in the Dean and Stark trap and removed periodically; the volume of water removed being replaced by xylene. After refluxing for 3 hours the solution was allowed to cool to ambient temperature.

Spectroscopic data for alkyd polymer (9):
GPC (daltons) : weight average : 58419
Solids : 61.05%

5.2.10 Catalytic evaluation of cluster species

For each sample to be tested, to a solution of 20g of alkyd polymer (comprising of 61% solids) was added the species to be assessed, at a level of 0.05% Co. Hence 5 samples were prepared as detailed in Table 5.1:

species	% Co in species	mass added/g
none	0	0
Cobalt octoate	10	0.061
[(CO)$_9$Co$_3$(μ_3-CH)]	40.0	0.015
[(CO)$_9$Co$_3$(μ_3-CCl)]	37.1	0.017
solution polymer	1.5	0.41

Table 5.1 : Samples for catalytic evaluation

After thorough mixing, each sample was applied to a glass substrate. A 100μm blockspreader was used to deposit the film and thus ensure films of equal thickness were evaluated.

5.2.10.1   BK Dry

Simultaneously, each sample was assesed by allowing a motor driven needle to drag through the sample for a period of 22 hours. The alkyd polymer was considered to be cross linked (or dried) at such time as when the needle no longer made an imprint on the polymer film. The results for the BK dry are shown in Table 5.2. In this experiment, a drying time of 22 hours is the maximum measurable. The current catalyst for this reaction is cobalt octoate.

species	Time to dry/hours
none	>22
Cobalt octoate	7
[(CO)$_9$Co$_3$(μ_3-CH)]	>22
[(CO)$_9$Co$_3$(μ_3-CCl)]	>22
solution polymer	>22

Table 5.2 : BK dry times for cobalt species

5.2.10.2 Sand dry

A motorised hopper filled with sand was slowly dragged over the 100µm thick polymer samples over a period of 10 hours. Sand deposited on each sample would adhere to the sample if the catalytic cross linking reaction had not occurred, and *vice versa*. The results for the sand dry are shown in Table 5.3.

species	Time to dry/hours
none	>10
Cobalt octoate	2
[(CO)$_9$Co$_3$(μ_3-CH)]	>10
[(CO)$_9$Co$_3$(μ_3-CCl)]	>10
solution polymer	>10

Table 5.3 : Sand dry times for cobalt species

5.2.11 Preparation of acrylic polymers containing pendant hydroxy groups: compounds (10a), (10b) and (10c).

In a typical experiment, a 3 litre reaction flask fitted with a reflux condenser, thermocouple, nitrogen bubbler and two feed inlets, was charged with 180 g 1-methoxy-2-propanol. The flask and charged were heated to reflux and the monomer and initiator feedstocks fed into the flask over a two hour period. The feedstock

profiles are detailed below in Table 5.4. The flask and contents were then cooled to ambient temperature. Table 5.5 details the GPC data for the polymers produced.

Tg/°C	initiator/g	HEA/g	MMA/g	BA/g
-20	10	10	63	127
20	10	10	118	72
60	10	10	160	30

Table 5.4: Feedstock profiles for HEA containing polymers

Tg/°C	Mn/daltons	Mw/daltons	Mz/daltons	Mp/daltons
-20	3708	5950	9214	6076
20	3450	7072	11139	6860
60	3414	9801	19703	8316

Table 5.5: GPC data for HEA containing polymers

Tg = -20°C : (**10a**), Tg = 20°C : (**10b**), Tg = 60°C : (**10c**)

5.2.12 Preparation of tricobaltmethylidyne decacarbonyl hexafluorophosphate [7] (11)

0.525 g (1.02 mmol) carbonylethoxymethylidyne tricobalt nonacarbonyl, $[(CO)_9Co_3(\mu_3\text{-}CCO_2C_2H_5)]$ (**2**), was dissolved in 10 ml propionic anhydride. An excess (1 ml) of 65% HPF_6 in H_2O was added by pipette in a single addition. A black precipitate of $[(CO)_9Co_3(\mu_3\text{-}CCO)]^+$ PF_6^- (**11**) formed immediately, which was isolated by removing the solvent *via* filter cannula under positive nitrogen pressure. The black precipitate was washed 3 times with freshly distilled dichloromethane, the solvent being removed after each washing *via* filter cannula under positive nitrogen pressure. The black precipitate was then suspended in dichloromethane prior to addition of the nucleophilic species.

5.2.13 Reaction of acrylic polymers with tricobaltmethylidyne decacarbonyl hexafluorophosphate. Preparation of polymers (12a), (12b) and (12c).

An acrylic copolymer containing 2-hydroxyethylacrylate was produced as described in section 5.2.10, and was then evaporated to dryness *in vacuo* on a high vacuum line. The isolated polymer was then redissolved in dichloromethane and the solvent again removed *in vacuo*. This process was repeated a further 2 times, to ensure complete removal of the nucleophilic solvent 1-methoxy-2-propanol. The polymer was redissolved in dichloromethane in preparation for addition to the tricobaltmethylidyne decacarbonyl hexafluorophosphate salt.

In a typical reaction, tricobaltmethylidyne decacarbonyl hexafluorophosphate, $[(CO)_9Co_3(\mu_3\text{-}CCO)]^+$ PF_6^- (11), was prepared as described in section 5.2.12. Immediately after suspending the tricobalt species in dichloromethane, a solution of polymer in dichloromethane was added *via* cannula. An immediate purple colour was imparted to the solution, which was then left to stir under nitrogen overnight. Methanol was added to the solution via syringe to destroy any unreacted tricobaltmethylidyne decacarbonyl hexafluorophosphate. The solvents were then removed *in vacuo*. IR spectroscopy confirmed the presence of the tricobalt cluster. GPC analysis of modified and unmodified polymer species was then undertaken. The GPC data showed that in each case, the modified polmer species was *lighter* than the unmodified species, as the results in Table 5.6 show, below.

$T_g/$ °C	Mn	Mn'	Mw	Mw'	Mz	Mz'	Mp	Mp'
-20	3078	1615	5950	4418	9214	7376	6076	5416
20	3450	2297	7072	6587	11139	11562	6860	6602
60	3414	1402	9801	8871	19703	23727	8316	8871

Mn = number average, Mw = weight average,

Mz = Z average, Mp = peak molecular weight,

all molecular weights are expressed in daltons

Table 5.6: Comparison of unmodified and modified polymeric species

5.3 Experimental details for chapter 3

5.3.1 Preparation of triosmium decacarbonyl *bis*(acetonitrile) [8], (13).

Triosmium dodecacarbonyl (0.5 g, 0.55 mmol) was refluxed with stirring in acetonitrile (750 cm^3) for 1 hour. The solution was allowed to cool to room temperature. A solution of freshly sublimed trimethylamine N-oxide (100 mg, 1.31 mmol, 2.2 equivalents) in acetonitrile (200 cm^3) was added to the stirred suspension over a period of 4 hours *via* pressure equalised dropping funnel. The mixture was stirred for 24 hours, filtered through silica and the solvent was removed *in vacuo*. The product was characterised spectroscopically as [Os$_3$(CO)$_{10}$(NCMe)$_2$] **(13)** (brown-yellow solid, 412 mg, yield = 80%).

Spectroscopic data for Os$_3$(CO)$_{10}$(MeCN)$_2$ (13) :
IR (CH$_2$Cl$_2$): ν(CO) = 2079(w), 2025(sh), 2021(vs), 1983(m) and 1960(w) cm^{-1}

5.3.2 Reaction of triosmium decacarbonyl *bis*(acetonitrile) with propargyl alcohol

500 mg of freshly prepared triosmium decacarbonyl *bis*(acetonitrile) **(13)** was dissolved in 100 ml dichloromethane and 5 ml acetonitrile. Excess propargyl alcohol (2 ml) was added *via* syringe, and the reaction mixture stirred under nitrogen for 2

hours, during which time the solution changed colour from yellow to orange and spot tlc showed the presence of 3 products. The solvents were removed *in vacuo* and the residue absorbed onto silica. The reaction products were separated by column chromatography on silica with gradient elution starting with hexane and finishing with acetone. Two major products were isolated, in order of elution:

(i) $Os_3(CO)_9(\mu\text{-CO})(\mu_3\text{-}\eta^2\text{-HCC}\equiv CH_2OH)$ **(14)**

(ii) $Os_3(CO)_8(\mu\text{-CO})(HOCH_2C=CCHOCCHCCH_2)$,

       ie $[Os_3(CO)_8(\mu\text{-CO})\{(HOCH_2C_2H)_2(CO)\}]$, **(15)**

Spectroscopic data for (14) :
IR (CH_2Cl_2): $\nu(CO) = 2102(w), 2062(vs), 2021(s), 1967(sh)$ cm^{-1}.
FABMS : m = 910 (calc. 912), with sequential loss of CO.
NMR: δ^1H/ppm: 9.27 (s, 1H), 3.83-4.36 (m, 2H), 1.79 (s, 1H). $\delta^{13}C$/ppm : 113.6, 77.3

Spectroscopic data for (15) :
IR (CH_2Cl_2): $\nu(CO) = 2098(m), 2059(vs), 2023(s), 1990(w), 1838(m)$ cm^{-1}.
FABMS : m=962 (calc. 962) and sequential loss of CO.
NMR : δ^1H/ppm : 8.93 (s, 1H, CH), 7.14 (s, 1H, CH), 5.67 (t, 1H, OH), 5.26 (t, 1H, OH), 4.69 (q, 2H, CH$_2$), 4.38 (q, 2H, CH$_2$). $\delta^{13}C$/ppm : 125.3 (CH), 108.8 (CH), 63.19 (CH$_2$), 58.11 (CH$_2$).

A crystal of **(15)** suitable for X ray diffraction was grown from a dichloromethane/hexane solution in a freezer.

Crystal data: $C_{16}H_8O_{12}Os_3$, M=962.82, monoclinic, space group P2$_1$, $a = 8.384(7)$, $b = 15.200(7)$, $c = 15.825(9)$ Å, $\beta = 95.17(6)$, U = 2009(2) Å^3, Z = 4, D$_{calc}$ = 3.184 Mg/m^3, F(000) = 1712, crystal size 0.80x 0.19x 0.15 mm, T=150 K, $2.58 < \theta < 22.61°$, R1 = 3.95% [based on reflections with F > 4σ(F)]. wR2 = 0.1068, for 2618 independent reflections, corrected for absorption and 279 parameters.

5.4 Experimental details for chapter 4

5.4.1 Preparation of methylidyne tricobalt nonacarbonyl

As per section 5.2.8.

5.4.2 Preparation of *para*-chloromercuryaniline [9]

[*p*-NH$_2$C$_6$H$_4$HgCl], (16).

WARNING - Toxic mercury derivatives

A solution of mercury (II) acetate (32 g, 0.1 mol) in hot water (100 cm^3) was added to a stirred solution of aniline (19 g, 0.2 mol, 2 mol equivalents) in methanol (100 cm^3). A creamy yellow precipitate was observed immediately and the mixture was stirred for 24 hours. The solution was filtered through a coarse glass frit, washed with hexane and the resultant solid dried under vacuum (cream solid, 37.50 g, 106 mmol, p-acetoxydiethylaniline). The cream coloured solid produced was dissolved in dimethylsulphoxide (100 cm^3). A solution of potassium chloride (12.4 g, 0.214 mol, 2 mol equivalents) in water (50 cm^3) was added dropwise and stirred for 24 hours. The cream coloured precipitate produced was filtered through a frit, washed with hexane and dried under vacuum . The single product was characterised as [*p*-NH$_2$C$_6$H$_4$HgCl], (16), (cream solid, 19.34 g, yield = 29%).

Spectroscopic data for [p-NH2C6H4HgCl], (16)

NMR (d$_6$-DMSO): δ^1H/ppm : 6.96 (d, 2H, ArH), 6.53 (d, 2H, ArH), 5.06 (br s, 2H, NH$_2$). δ^{13}C/ppm : 148.8 (C, J$_{H-Hg}$ =221 Hz), 137.2 (2 x CH, J$_{H-Hg}$ =70Hz), 130.2 (C), 114.42 (2 x CH, J$_{H-Hg}$ = 110 Hz)

5.4.3 Preparation of *para*-anilinemethylidynetricobalt nonacarbonyl [10]

[(CO)$_9$Co$_3${μ$_3$-C[(*p*-C$_6$H$_4$NH$_2$)]}], (17).

Methylidynetricobalt nonacarbonyl (5.23 g, 12 mmol) and *para*-chloromercuryaniline (16) (7.89 g, 24 mmol, 3/2 mol equivalents) were added to THF (900 ml) which was heated at reflux for 24 hours. Spot tlc indicated complete consumption of starting material. The mixture was allowed to cool to room temperature, the product was filtered through celite and washed with

dichloromethane. The solvent was removed *in vacuo* and the residue purified by column chromatography on silica using a solution of hexane-dichloromethane (1:1, v/v) as eluent. The product was characterised spectroscopically as $[(CO)_9Co_3(\mu_3\text{-}C(p\text{-}C_6H_4NH_2))]$, (17), (bronze solid, 2.12g, yield = 34%).

Spectroscopic data for $[(CO)_9Co_3\{\mu_3\text{-}C[(p\text{-}C_6H_4NH_2)]\}]$ (17):
IR (CH_2Cl_2): $v(CO)$ 2097.9(m), 2049.4(vs), 2034.2(s) and 2015.0(w) cm^{-1}.
FABMS : m+1 = 534 plus sequential loss of CO.
NMR (acetone-D$_6$): δ^1H/ppm : 2.53 (broad singlet, NH$_2$), 6.53 (dd).
$\delta^{13}C$/ppm : 204.6 (q), 199.8 (q), 148.2 (q), 147.4 (q), 129.5 (2 x CH), 112.3 (2 x CH)

5.4.4 Reaction of $[(CO)_9Co_3(\mu_3\text{-}CCO^+)][PF_6^-]$ (11) with

$[(CO)_9Co_3(\mu_3\text{-}C)(p\text{-}C_6H_4NH_2)]$ (17);

Synthesis of $[(CO)_9Co_3(\mu_3\text{-}CCON(H)\text{-}p\text{-}C6H4(\mu_3\text{-}CCo_3(CO)_9]$, (18)

The acylium hexafluorophosphate salt (11) was prepared from 0.5 mmol of carboxymethylidynetricobalt nonacarbonyl as described above and was slurried with dichloromethane (5 cm^3). The suspension was treated with *p*-anilinemethylidynetricobalt nonacarbonyl (17) (250 mg, 0.47 mmol, *ca.* 1 molar equivalent) added *via* cannula. The solution was stirred and the apparatus was allowed to cool for 5-10 mins. The reaction was evaluated by spot tlc. The solvent was removed *in vacuo* and the residue was separated by tlc on silica using a solution of hexane-dicloromethane (3:1, v/v) as eluent. The major product was characterised spectroscopically as $[(CO)_9Co_3CCONHC_6H_4CCo_3(CO)_9]$ (18) (brown, 301 mg, yield = 64%).

Spectroscopic data for $[(CO)_9Co_3(\mu_3\text{-}CCON(H)\text{-}p\text{-}C6H4(\mu_3\text{-}CCo_3(CO)_9]$ (18):
IR (CH_2Cl_2): $v(CO)$ = 2111(w), 2101(w), 2065(vs), 2053(sh) and 2038(sh) cm^{-1}.
NMR (acetone-D$_6$) : δ^1H/ppm : 7.6 (m, 4 H), 7.8 (bs, 1 H). δ13C/ppm : 200.2 (CoC≡O), 198.9 (μ_3-C), 176.3 (C=O), 155.2 (C), 137.5 (C), 129.5 (2 x CH), 119.5 (2 x CH).
FABMS : m = 1001 (calc. 1001) with initial fragmentation showing loss of 18 carbon monoxide ligands.

A dark red crystal of **(18)** suitable for X ray diffraction was grown from dichloromethane/hexane solution at -30 °C.

Crystal data : $C_{27} H_5 N O_{19} Co_6$. M =1000.9, monoclinic, space group P2$_1$/m, $a =$ 8.443(2), b = 10.582(2), c = 18.998(4) Å, β = 95.61(3)°, U = 1689.2(6) Å^3, Z = 2, D_{calc} = 1.968 Mg/m^3, T = 150.0(1) K, F(000) = 976, crystal size 0.74 x 0.19 x 0.12 mm, 2.55 < θ < 22.51°, R1 = 2.97% [based on reflections with F > 4σ(F)]. wR2 = 7.01, for 2360 independent reflections, corrected for absorption and 285 parameters.

A minor product was also suggested to be $[(CO)_9Co_3CC_6H_4N\{COCCo_3(CO)_9\}_2]$ **(19)** (brown, trace). However, a similar reaction of $[(CO)_9Co_3(\mu_3\text{-}C)(p\text{-}C_6H_4NH_2)]$ **(17)** with excess $[(CO)_9Co_3(\mu_3\text{-}CCO^+)][PF_6^-]$ **(11)** failed to yield the expected tertiary amide in appreciable quantity. **FABMS** : m +1 = 1470 (calc. 1469).

5.5 References

1.   J. Cosier, A.M. Glazer, *J. Appl. Crystallogr.*, 1986, **19**, 105.

2.   G.M. Sheldrick, SHELXL 93, Program for crystal structure refinement, University of Göttingen, Germany, 1993.

3.   G.M. Sheldrick, SHELXTL PC, University of Göttingen and Siemens Analytical X-ray Instruments, Madison, 1990.

4.   G. Bor, L. Markó and B. Markó, *Chem. Ber.*, 1962, **95**, 333

5.   D. Seyferth, G. H. Williams, and C. L. Nivert, *Inorg. Chem.*, 1977, **16**, 758

6.   D. Seyferth, J. E. Hallgren and P. L. King, *J. Organomet. Chem.*, 1974, **50**, 265

7.   D. Seyferth, J. E. Hallgren and C. S. Eschbach, *J. Am. Chem. Soc.*, 1974, **96**, 1730

8.   J. N. Nicholls and M. D. Vargas, *Inorg. Synth.*, 1989, **26**, 289

9.   J. Barluenga, A. M. Bayon, J. Perez-Preito and G. Asensio, *Tetrahedon*, 1984, **40**, 5053

10. D. Seyferth, J. E. Hallgren, R. J. Spohn, G. H. Williams and P. L. K. Hung, *J. Organomet. Chem.*, 1974, **65**, 99